Charles University

Second Faculty of Medicine

Doctoral study program: Human Physiology and Pathophysiology

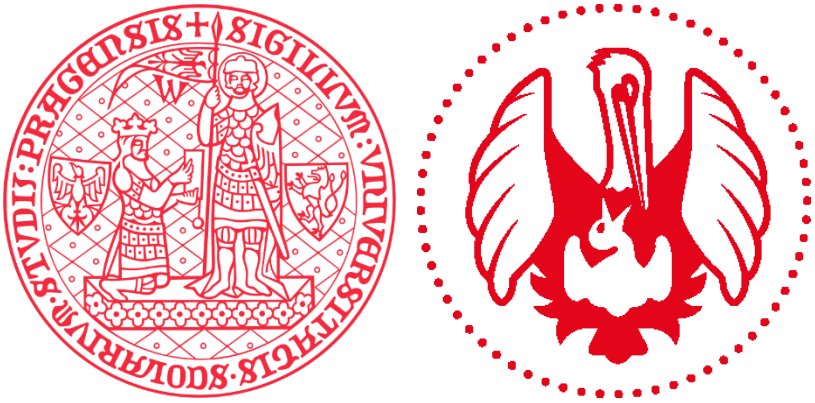

Mgr. Júlia Tomšů (née Pajorová)

Interactions of Skin and Stem Cells with Polymer Nanofibers for Construction of Skin Substitutes

Interakce kožních a kmenových buněk s nanovlákennými polymery pro konstrukci kožních náhrad

Dissertation Thesis

Supervisor: doc. MUDr. Lucie Bačáková, CSc.

Praha, 2022

Declaration:

I declare hereby that I made this dissertation thesis by myself and that I mentioned and cited properly all the sources and literature. At the same time, I declare that this thesis was not used to obtain another or the same title.

I agree with permanent deposition of an electronic version of my thesis in the system database of interuniversity project Thesis.cz for a permanent control of similarities of theses.

Prohlášení:

Prohlašuji, že jsem závěrečnou práci zpracovala samostatně a že jsem řádně uvedla a citovala všechny použité prameny a literaturu. Současně prohlašuji, že práce nebyla využita k získání jiného nebo stejného titulu.

Souhlasím s trvalým uložením elektronické verze mé práce v databázi systému meziuniverzitního projektu Theses.cz za účelem soustavné kontroly podobnosti kvalifikačních prací.

V Praze, dne 15.02.2022

Mgr. Júlia Tomšů (née Pajorová)
Podpis

Acknowledgements:

First of all, I would like to thank my supervisor doc. MUDr. Lucie Bačáková, CSc. who gave me the opportunity to work in her well-equipped laboratory and enthusiastically guided me during my doctoral studies. She has always been open-minded to new ideas and provided me with unique and valuable opportunities to participate in various domestic and international projects and present my results at leading scientific conferences related to skin tissue engineering.

Furthermore, I would like to acknowledge the colleagues from our department for wonderful collaboration and teaching me new laboratory skills and techniques. I would particularly like to single out my friends and colleagues Markéta Bačáková, Martina Trávníčková and Antonín Brož, for their close collaboration and willingness to help me with experiments and studies.

I am also very thankful to our external collaborators; in particular the colleagues from Technical University in Liberec for preparation the nanofibrous membranes, the colleagues from Biomedical Center in Pilsen (Charles University) for providing the know-how related to collagen hydrogel preparation, and the colleagues from Tampere University in Finland, namely Prof. Pasi Kallio and Dr. Anne Skogberg, for the amazing opportunity to work in their lab and to prepare the nanocellulose coatings.

In addition, I have had an enormous support from all of my friends and family members, including our dog Rumík, throughout my studies.

Finally, my work was supported by the Grant Agency of Charles University (GAUK, project No. 756218), by the Grant Agency of the Czech Republic (grants No. 17-02448S, 17-00885S and No. 20-01641S) and by the Ministry of Education, Youth and Sports of the Czech Republic (confocal imaging and image analysis support).

Abstrakt

Kůže je nejrozsáhlejší orgán lidského těla, který hraje významnou roli v udržování homeostázy, a proto rozsáhlá kožní poranění můžou způsobit vážné zdravotní komplikace. Užití auto-, alo- i xeno-transplantátů doprovázejí komplikace v podobě nedostatku náhradní tkáně a jejího odhojování. Proto se vytvoření artificiální kožní náhrady v laboratorních podmínkách zdá být jedním ze slibných způsobů hojení rozsáhlých ran. Tato práce je v první části zaměřena na zhotovení dvouvrstvé prevaskularizované kožní náhrady sestávající z kolagenového hydrogelu podloženého biodegradabilní nanovlákennou membránou. Druhá část této práce se pak zabývá odlišnou strategií, tedy vývojem dočasného krytu ran na bázi celulózy. Pro výzkum byly využity lidské kožní fibroblasty a keratinocyty, kmenové buňky tukové tkáně a endotelové buňky.

Pro zlepšení adheze a růstu buněk byl povrch syntetických nanovlákenných membrán potažen vrstvami adhezních proteinů. Bylo zjištěno, že lidské fibroblasty a tukové kmenové buňky upřednostňují fibrinové nanovrstvy, zejména homogenní síť z fibrinu na povrchu podkladové membrány. Keratinocyty pak lépe adherují a také stratifikují na kolagenových podkladech. Tyto poznatky motivovaly další vývoj dvouvrstvých konstruktů, kde dermální fibroblasty migrovaly z nanovlákenných membrán potažených fibrinem do kolagenového gelu a na povrchu gelu pak byly kultivovány epidermální keratinocyty. Na rozdíl od zalévání buněk do gelu zde docházelo k postupné degradaci a následné syntéze kolagenu během migrace buněk. Buňky tak byly schopné kolonizovat gel v celém jeho objemu bez jeho znatelné kontrakce. Tento nový přístup byl rovněž využit pro prevaskularizaci dvouvrstvého konstruktu, ve kterém migrující kmenové buňky tukové tkáně podporovaly formování tubulárních struktur z endotelových buněk zalitých v gelu.

Druhá část této práce byla zaměřena na celulózové materiály jakožto slibné přírodní krytí kožních ran. Za účelem zlepšení adheze a proliferace buněk byly celulózové textilie pokryty dvěma typy fibrinových nanovrstev nebo vrstvou z kladně nebo záporně nabitých celulózových nanovláken. Výsledky ukázaly, že negativně nabitá celulózová nanovlákna na rozdíl od pozitivně nabitých nanovláken zlepšovala růst fibroblastů a kmenových buněk tukové tkáně. Tento výsledek však závisel na typu buněk a na složení vrstvy proteinů ze séra kultivačního média, ovlivňujících adhezi buněk na materiál. Dále bylo zjištěno, že síť z fibrinu, která se utvořila na povrchu celulózové textilie, lépe podporovala adhezi a růst fibroblastů než fibrin obalující jen jednotlivá vlákna textilie.

Klíčová slova

Nanovlákenná membrána, fibrinová nanovrstva, kolagenový hydrogel, fibroblasty, keratinocyty, tukové kmenové buňky, endotelové buňky, prevaskularizace, dvouvrstevný kožní konstrukt, celulózová nanovlákna, krytí ran, kožní náhrada

Abstract

The skin is the largest organ of a human body with a crucial role in the maintenance of homeostasis; therefore any extensive skin injury leads to severe complications. Since the application of auto-, allo- and xeno-grafts is accompanied by severe problems like the source limitation and the graft rejection, a bioengineered skin substitute seems to be one of the promising healing approach. This work is focused mainly on the construction of a pre-vascularized skin substitute consisting of a collagen hydrogel reinforced by a biodegradable nanofibrous membrane. Another strategy described in this work is the development of temporary cellulose-based wound dressings. For both research strategies, various cell types were utilized, i.e. normal human dermal fibroblasts (NHDFs), human keratinocytes (hKs), adipose tissue-derived stem cells (ADSCs) and human umbilical vein endothelial cells (HUVECs).

In order to enhance the cell adhesion and growth, the synthetic nanofibrous membranes were improved by protein nanocoatings. It was found out that NHDFs and ADSCs preferred fibrin nanocoatings, mainly thin fibrin homogeneous mesh on the surface of the membrane. Keratinocytes rather adhered and stratified on collagen substrates. These observations further motivated the construction of the bi-layered construct, where the NHDFs migrated from the fibrin-coated nanofibrous membrane into the collagen hydrogel, and the epidermal hKs were cultivated on the surface of collagen. Unlike to the direct cell embedding into the gel, the gradual degradation and synthesis of the collagen by the migrating cells allowed them to colonize the entire volume of the collagen hydrogel without any considerable shrinkage. This novel approach was also utilized for pre-vascularization of the bi-layered construct in which the migrating ADSCs supported the formation of a tubular structures from the HUVECs embedded in the collagen.

Another research area of this work is focused on a cellulose-based material as a promising nature-derived wound dressing. The cellulose meshes were coated with negatively and positively charged cellulose nanofibrils (CNFs) or with two types of fibrin nanocoatings to increase the cell attachment and proliferation. The results showed that the negatively charged CNFs, in contrast to the positively charged CNFs, enhanced the growth of NHDFs and ADSCs. However, it depended on a particular cell type and on the composition of the cell adhesion-mediating proteins. It has been also detected that the fibrin mesh on the surface of the cellulose mesh supported the adhesion and growth of NHDFs better than just the fibrin coating.

Keywords

Nanofibrous membrane, fibrin nanocoatings, collagen hydrogel, fibroblasts, keratinocytes, adipose-derived stem cells, endothelial cells, pre-vascularization, bi-layered skin construct, cellulose nanofibrils, wound dressing, skin substitute

Abbreviations

2D, 3D	two-dimensional, three-dimensional
AA	2-phospho-L-ascorbic acid trisodium salt
ACTB	β-actin
ADSCs	adipose tissue-derived stem cells
AFM	atomic force microscopy
ANOVA	analysis of variance
bFGF (FGF2)	basic fibroblast growth factor
BSA	bovine serum albumin
c+aCNFs	combination of anionic and cationic cellulose nanofibrils
$CaCl_2$	calcium chloride
cCNFs, aCNFs	cationic cellulose nanofibrils, anionic cellulose nanofibrils
CD	cluster of differentiation
CKs	cytokeratines
CNFs	cellulose nanofibrils
CO_2	carbon dioxide
COO^-	carboxyl
Ct values	cycle threshold values
DAPI	4',6-diamidin-2-fenylindol
DGEA	Asp-Gly-Glu-Ala sequence
dH_2O	deionized water
DMEM	Dulbecco's Modified Eagle's Medium
dsADSCs	adipose-derived stem cells isolated from discarded burned skin
ECM	extracellular matrix
ECs, EPCs	endothelial cells, endothelial progenitor cells
EDC	epidermal differentiation complex

EDTA	ethylenediaminetetraacetic acid
EGF	epidermal growth factor
EGM-2	endothelial cell growth medium 2
EPTMAC	2,3-epoxypropyl trimethylammonium chloride
F12 medium	Ham's Nutrient Mixture F12 medium
FBS	fetal bovine serum
FDA	food and drug administration
Fn	fibronectin
H form, P form	homogeneous form, porous form
HaCaT	aneuploid immortal keratinocyte cell line
HB-EGF	heparin-binding epidermal growth factor
HCl	hydrogen chloride
HDMS	hexamethyldisilazane
hKs	primary human keratinocytes
HUVECs	human umbilical vein endothelial cells
IGF	insulin-like growth factor
IL	interleukin
KDAF	keratinocyte-derived anti-fibrogenic factor
KGM	keratinocyte growth medium
MMP	matrix metalloproteinase
mRNA	messenger RNA
MSCs	mesenchymal stem cells
MTS	CellTiter 96® Aqueous One Solution Cell Proliferation Assay
$N(CH_3)_3^+$	trimethylammonium
NaCl	sodium chloride
NHDFs	normal human dermal fibroblasts

PBS	phosphate-buffered saline
PBT	polybutylene terephthalate
PCL	polycaprolactone
PCR	polymerase chain reaction
PDGF	platelet-derived growth factor
PEG	polyethylene glycol
PEO	polyethylene oxide
PGA	polyglycolic acid
PIPES	piperazine-N,N′-bis(2-ethanesulfonic acid)
PLA, PLLA	polylactic acid, poly-L-lactic acid
PLGA	polylactic-*co*-glycolic acid
PS	polystyrene
Ra	roughness average
RGD	arginylglycylaspartic acid
SD	standard deviation
SEM	scanning electron microscopy
SVF	stromal vascular fraction
TEMPO	2,2,6,6-tetramethylpiperidinyloxy oxidation
TGase	transglutaminases
TGF	transforming growth factors
TNF	tumor necrosis factor
Tris	tris(hydroxymethyl)aminomethane
TRITC	tetramethylrhodamine isothiocynate
UV	ultraviolet
VEGF	vascular endothelial growth factor

Contents

1 Introduction

The skin is the main barrier protecting the internal organs of the body against external environmental effects, and consequently it contributes to the overall immunity of the body. Therefore, any loss of the skin integrity can cause health problems or even death in case of large or chronic wounds. The skin self-repairing process is sufficient for small defects, but deep and extensive dermal injuries have to be treated with skin dressings or substitutes. Wound dressings have been used for many centuries, but one of the first three-dimensional cell cultivating systems was devised by Bell in the late 1970s (Bell *et al.* 1979). This system based on fibroblasts embedded in a collagen gel has been upgraded for many years. Moreover, it has become the main building block of various skin substitutes. Commonly used skin substitutes can improve the process of healing. However, currently available constructs are not sufficient and their exogenous or allogenic origin can cause an immunological response and rejection. Therefore, the novel treatment approaches are focused on development of autologous bio-artificial skin equivalents, which should mimic all functions of the native skin.

1.1 Anatomy and Physiology of the Skin

The skin is by far the largest organ of the human body, which covers about 1.5 – 1.8 m^2 of the body surface of an average young adult, and weights around one-sixth of the total adult body weight. The thickness of the skin varies according to the area of the body, but the thinnest skin is on a lower eyelid (0.5 mm) and the thickest skin is on a foot sole (15 mm). The skin is the most exposed organ of the human body to external agents, and therefore it plays an important role in mechanical, energetic, metabolic and immunological functions of the body. From the point of view of tissue engineering, the most important function of the skin is its ability to continuously self-remodel and regenerate due to permanent loss of tissue. Skin tissue can be anatomically divided into three layers: epidermis, dermis and hypodermis (Gunter *et al.* 2016).

Epidermis is the upper multi-layered part of the skin consisting mainly of keratinocytes which differentiate into squamous epithelium and migrate through several strata: *stratum corneum*, *stratum lucidum*, *stratum granulosum*, *stratum spinosum* and *stratum basale* (Fig.1 and 2) (Savoji *et al.* 2018). *Stratum corneum* is the most upper layer with cornified cells (corneocytes) in a lipid matrix (free fatty acid, cholesterol and ceramides), which constitutes the main barrier and protects lower layers against absorption of unwanted agents and water

loss (Flaten *et al.* 2015; Groen *et al.* 2011). *Stratum basale* is the starting point for keratinocyte migration and outward stratification through *stratum spinosum*, *granulosum* and *lucidum* to *stratum corneum*. Dead cells in *stratum corneum* are permanently shed from the surface by proteolysis of corneodesmosomes (Costanzo *et al.* 2015; Haftek 2015).

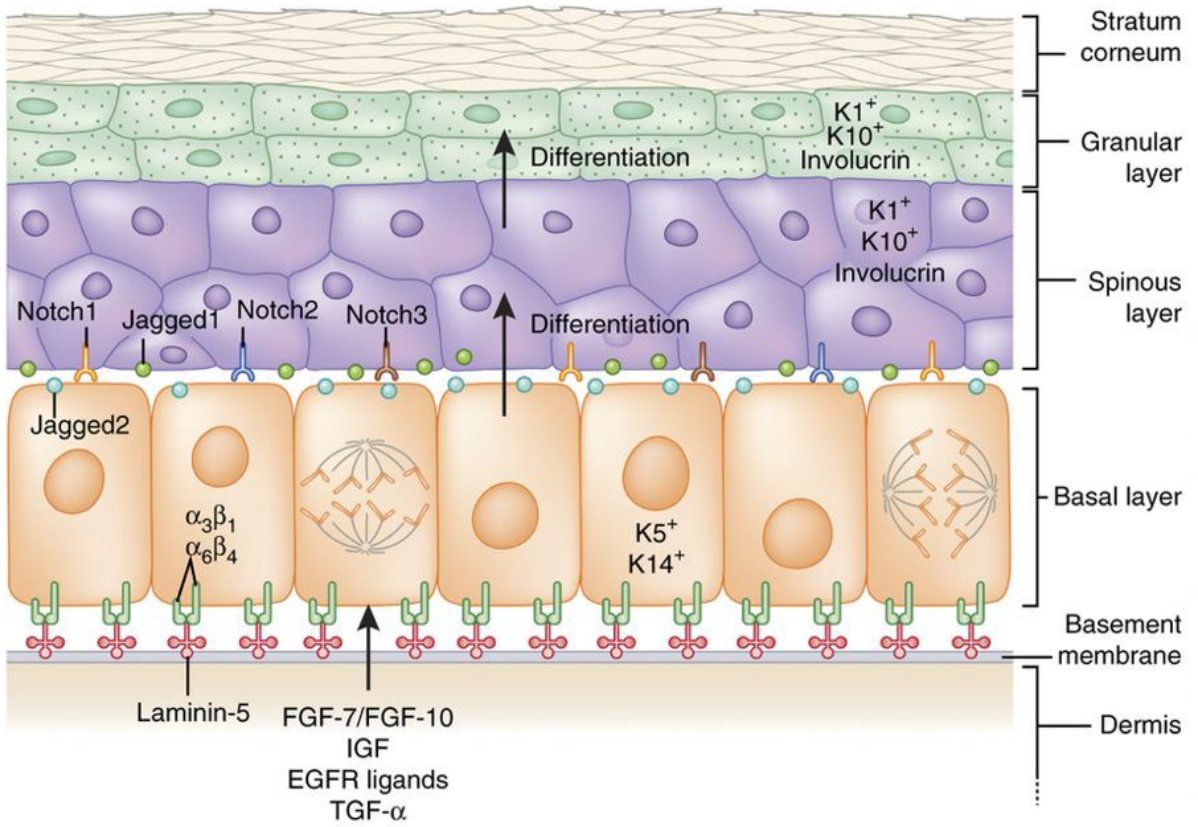

Figure 1. *Stratified interfollicular epidermis: signaling and stratification (Hsu et al. 2014).*

Specific gene expression of cytokeratins (CKs) reflects each stage of migration and differentiation of keratinocytes. CKs are intermediate filaments, which are encoded by 54 conserved genes (37 for human epithelial CKs) and are folded to proteins of type I and type II (28 genes for type I, 26 for type II). Genes for CKs are downregulated and upregulated in the pairwise manner depending on the type of tissue and a differentiation state (Wang *et al.* 2016; Ter Horst *et al.* 2018). Epithelial CKs have many functions, e.g. maintenance of mechanical integrity, regulation of cell migration and influence of growth. They support the cell integrity, which leads to the resistance of tissue against mechanical stress. The functions of CKs are regulated by CK-associated proteins and by posttranslational modifications (Ramms *et al.* 2013). Keratinocytes in the basal layer are the cells with high mitotic activity and express predominantly CK5 (type II, large, basic), CK14 (type I, small, acidic) and small amount of CK15 (type I, small, acidic) (Wang *et al.* 2016; Lloyd *et al.* 1995; Ter Horst *et al.* 2018). At

the beginning of differentiation, the cells stop dividing and start expressing CK1 (type II, large, basic), CK10 (type I, relatively large, acidic) and Caspase-14. In *stratum granulosum*, the cells accumulate keratohyalin granules, become flatter and increase the expression of "epidermal differentiation complex" (EDC). EDC is a cluster of genes encoding proteins appearing in a late differentiation phase – profilaggrin, involucrin and loricrin (Costanzo *et al.* 2015; Henry *et al.* 2012). Keratinocytes lack their nucleus and desquamate cellular organelles between granular and cornified layer. This physiological process is caused by increasing intracellular Ca^{2+} and activating transglutaminases (TGase). Cellular proteins are crosslinked by TGase and form a cornified envelope under the surface of a cell. Corneocytes are composed only of CKs supporting mechanical strength of the skin (Candi *et al.* 2005; Costanzo *et al.* 2015). CK9 (type I, intermediate size, acidic) is expressed in stress-bearing interfollicular epidermis to enhance mechanical resilience (Kumar and Jagannathan 2018). The paired expression of CK6 (type II, large, basic), CK16 and CK17 (both type I, large, acidic) are typical for palmoplantar glabrous skin or they appear during an injury and chronical hyperproliferative diseases (Stark *et al.* 1987; Lessard and Coulombe 2012). The expression of CK19 (type I, smallest, acidic) was found in a wide range of epithelia, e.g. many simple epithelial tissues, diverse stratified epithelia, and moreover in cultured keratinocytes (Moll *et al.* 2008; Wang *et al.* 2016). The expression of CKs in hair follicles is more complex than in the interfollicular epidermis. The inner root sheath expresses CK1 and CK 10, while the outer root sheath expresses CK5 and CK14 in the outer layer, and CK6, CK16 and CK17 in the inner layer. The associated sebaceous gland expresses CK5 and CK14 (Chu and Weiss 2002). Full skin self-renewing process lasts on average 4 weeks. Cell migration from basal layers to *stratum corneum* takes around 2 weeks, and two additional weeks are necessary for cell crossing through *stratum corneum*.

Keratinocytes represent approximately 95% of the epidermis, but there are also melanocytes, Langerhans cells, i.e. dendritic cells of the skin, and Merkel cells, i.e. tactile cells serving as mechanoreceptors (Gunter *et al.* 2016). The epidermis and dermis layers are separated by a highly specialized dynamic structure that is called the basement membrane. Although the membrane physically separates two different types of cells, still it enables the communication between them by mechanical changes and chemical signaling (Jayadev and Sherwood 2017). Furthermore, the epidermis has no direct connection to the circulation of blood, therefore the nutrition of the cells is provided via diffusion from dermis. Both keratinocytes and fibroblasts are involved in the formation of basement membrane and the production of biomolecules, such as laminin, collagen types IV, VII and XVIII, nidogen,

entactin, proteoglycans and perlecan (Nishiyama *et al.* 2000; Poschl *et al.* 2004; Varkey *et al.* 2014).

Dermis is the connective tissue between epidermis and hypodermis, which provides mainly mechanical support for the skin (Fig 2.). Mechanical and elastic properties are mediated by fibroblasts, which produce extracellular matrix (ECM) molecules, e.g. collagen type I, elastin and fibronectin. The thickness of the dermis is around 1 – 2 mm. The dermis can be further divided into papillary and reticular dermis. The upper papillary layer is composed of loosely arranged collagen fibers, while the reticular layer has dense collagen fibers. The superficial papillary dermis and the epidermis are overlaid while the basement membrane between them mediates their mutual interactions (Jayadev and Sherwood 2017). Other structural components of the dermis are hair follicles, sweat glands, sebaceous glands, nerve endings and blood vessels (Fig. 2). One of the most important functions of the dermis is thermoregulation, which is mediated by two parallel vascular networks running through the dermis to the surface of the skin – superficial and deep plexus (Fig. 2). These two networks are connected by vertical vessels, which supply nutrition and regulate temperature (Gunter *et al.* 2016). The vessel network is also important for the regeneration after the transplantation of split-thickness skin grafts. The vessels in the skin grafts are reconnected with underlying blood vessels within 24 hours after transplantation by a process called inosculation (Converse *et al.* 1975).

Hypodermis is considered to be the main insulating layer with lots of adipocytes. This layer serves as energy storage for the body and participates in thermoregulation (Savoji *et al.* 2018). For tissue engineers, the hypodermis is an important source of adult mesenchymal adipose-derived stem cells that can be obtained by liposuction (Fig 2) (Bacakova *et al.* 2018a).

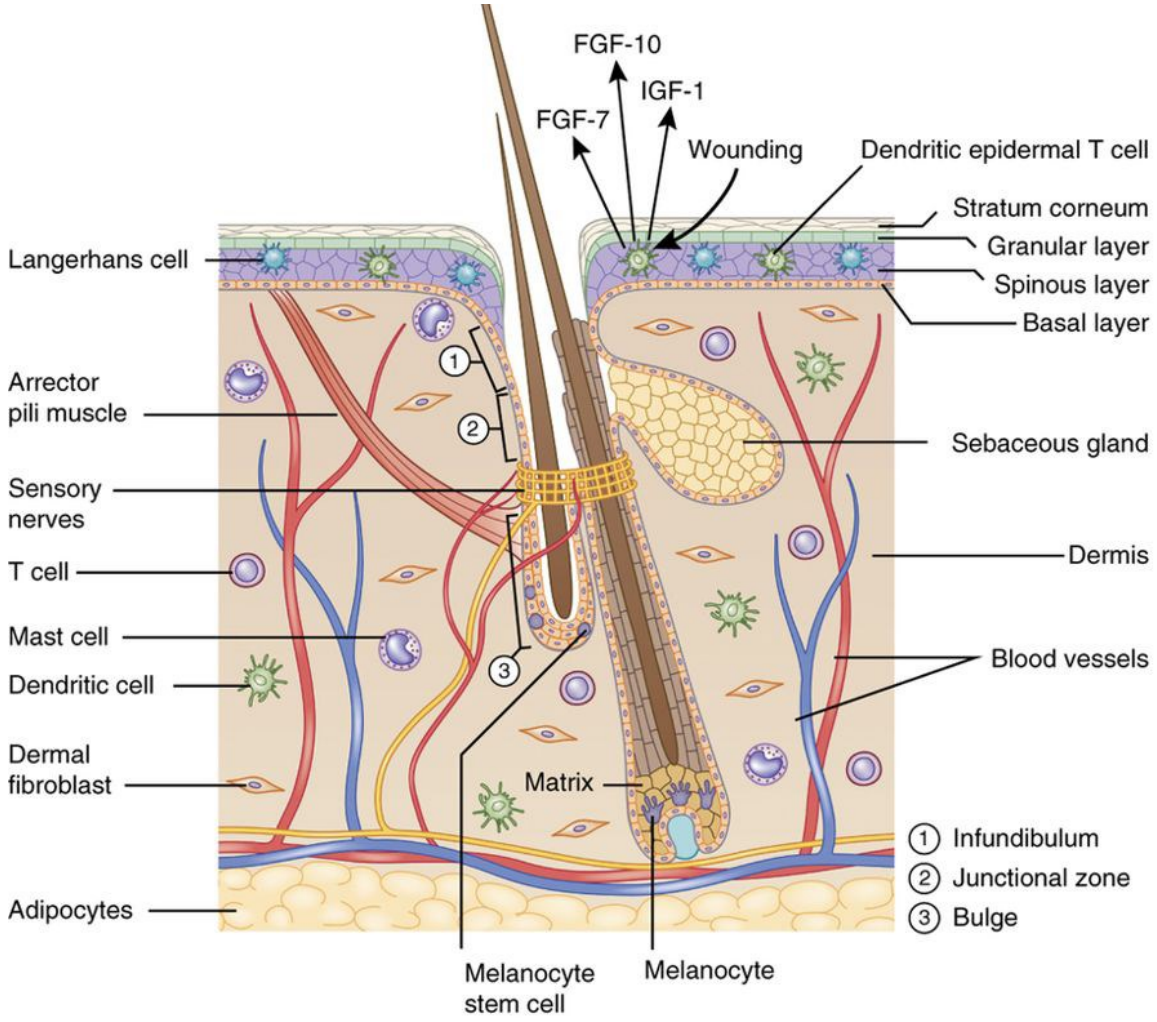

Figure 2. *Structure of the skin: epidermis, dermis, hypodermis (Hsu et al. 2014).*

1.2 Physiology and Pathophysiology of Wound Healing

The skin is the most exposed organ of a human body to exogenous noxes which can lead to several physical or chemical traumas. Skin wounds can be also caused by genetic irregularities or surgical procedures. The skin wounds can be divided into four categories based on the depth of damage and correlating with the grade of burns – epidermal, superficial dermal, deep dermal and sub dermal (full-thickness) (Savoji *et al.* 2018; Gunter *et al.* 2016). While skin wounds caused by autoimmune diseases, for example toxic epidermal necrolysis or epidermolysis bullosa, mostly affect epidermis or a dermo-epidermal junction, the skin burns can destroy all skin layers. Regenerative capacity of the skin depends on the total amount of undamaged dermis and epidermis, on the ability of a local tissue to regenerate, and on the capability to recruit stem cells from resources, e.g. bone marrow, adipose tissue or uninjured surrounding tissue (Gunter *et al.* 2016). In case of epidermal burns (grade 1) and superficial dermal burns (grade 2a), the dermo-epidermal junctions are destroyed, and their

regeneration is spontaneous and takes 5 – 21 days without scaring. Deep dermal burns (grade 2b) usually regenerate more than 21 days and create scares, but subdermal burns (grade 3) or pressure sores are not spontaneously healed wounds. Moreover, the size of the damaged area is crucial for cell and tissue surviving. The boundaries between the individual skin layers are extremely thin, therefore it is clinically difficult to estimate the real amount of surviving tissue in the injured skin (Gunter *et al.* 2016).

Wound healing is a process in a human body, which is highly regulated, and in normal conditions it involves various types of cells. The healing process can be divided into four overlapping phases: hemostasis, inflammation, reepithelization (cell proliferation) and remodeling (Olczyk *et al.* 2014; Wu and Chen 2014).

1.2.1 Hemostasis

The process of wound healing begins immediately after a vessel injury occurs. In a very early stage, the vasoconstrictors such as thromboxane A_2, adrenalin and serotonin start with narrowing the vessels, and platelets are activated by their contact with the damaged vessel collagens. The platelets are the main early modulators, which are able to adhere, aggregate and release the key glycoproteins from α-granules. The glycoproteins that play an important role in the healing process are fibrinogen, fibronectin, thrombospondin, vitronectin and von Willebrand factor (Induruwa *et al.* 2018; Olczyk *et al.* 2014). The physiological mechanism of hemocoagulation, i.e. the blood clot formation, is based on the transformation of globular fibrinogen to fibrous fibrin, which is catalyzed by thrombin. The enzyme, thrombin, is formed from prothrombin on the surface of the activated platelets. The blood clot provides a temporary "scaffold" for the formation of an ECM, which can be remodeled in the following healing stages (Fig. 3) (Swieringa *et al.* 2018).

Fibronectin is another key protein of hemostasis, which is concentrated in a wound during the first day of the healing process. Polymerized fibronectin has highly cell-adhesive function; therefore, many different cell types can interact by their integrin receptors with arginylglycylaspartic acid (RGD) domains on fibronectin. Overall, fibronectin supports further adhesion and aggregation of the platelets and stimulates the adhesion and migration of the endothelial cells, fibroblasts and keratinocytes (Prasad and Clark 2018). The aggregated platelets, which are trapped in the temporary ECM, e.g. in a fibrin and fibronectin mesh, release growth factors, such as vascular endothelial growth factor (VEGF), platelet-derived growth factor (PDGF), transforming growth factors α and β (TGF-α, TGF-β), insulin-like growth factor-1 (IGF-1) and basic fibroblast growth factor (bFGF) (Etulain 2018). PDGF and

TGF-β recruit monocytes and neutrophils to the wound, which initiate the inflammation during the healing process (Hosgood 1993). Neutrophils are also chemo-attracted by degradation products of C5a complement and products of bacteria decomposition. VEGF, TGF-α and bFGF initiate angiogenesis by activating the endothelial cells (Ferrari *et al.* 2009; Bao *et al.* 2009). Fibroblasts are activated by PDGF and IGF-1 and are recruited into the wound. The key role of fibroblasts in the wound is to synthesize ECM biomolecules, such as collagens and glycosaminoglycans (Prasad and Clark 2018; Greiling and Clark 1997).

1.2.2 Inflammation

The second phase of the healing process is inflammation, which normally starts during the first 24 hours, and on average lasts up to 48 hours from the moment when an injury happens. Inflammation is accompanied by swelling, body heat, redness and pain around the injured site. The changes of vascular permeability and the constriction of vessels are supported by histamines, prostaglandins, leukotrienes, proteases, nitrogen oxide and reactive oxygen species. These mechanisms are important mainly for leaking plasma to the damaged tissue (Olczyk *et al.* 2014; Wu and Chen 2014).

Neutrophils and monocytes/macrophages are the key cells of inflammation, and their main function is to keep the wound aseptic by debridement and phagocytosis (Fig. 3). They also produce a wide spectrum of growth factors and cytokines. The invasion of neutrophils to the wounded site takes a couple of minutes after the damage occurs, and their function is to create a front barrier against bacteria (Wang 2018). The crucial chemoattractants for neutrophils are thrombin, fibrin decomposition products, bacteria, components of complement C5a, histamine, leukotrienes, TGF-β and PDGF (Olczyk *et al.* 2014; Grotendorst *et al.* 1989). In the later phase of inflammation, the interleukin (IL-1) and tumor necrosis factor (TNF-α) are released from the cells, which further enhances inflammation. The neutrophils undergo apoptosis and they are replaced by monocytes after two or three days of inflammation (Ferrante 1992).

Monocytes are commonly present in blood, but during inflammation, they migrate to the temporary matrix of the wound and transform to macrophages. This process is mediated mainly by the products of fibrin and fibronectin degradation and by TGF-β mediators (Grotendorst *et al.* 1989; Wahl *et al.* 1987). Thrombin has also chemotactic and mitogenic impact on monocytes/macrophages. Macrophages have a double role in the process of wound healing. Firstly, they kill bacteria and participate in phagocytosis. Secondly, they secrete cytokines and growth factors, which stimulate fibroblast proliferation and biosynthesis of

collagen. The removal of debris from a wound by macrophages is done by releasing matrix metalloproteinases, such as collagenase or elastase. Macrophages produce TGF-β, TGF-α, PDGF, bFGF, IL-6, IL-1 and heparin-binding epidermal growth factor (HB-EGF), which modulate epithelialization, collagen production and angiogenesis. Moreover, macrophages cause the removal of the fibrin clot by releasing the activator of plasminogen. The latter stage of inflammation also involves lymphocytes, which influence the growth of fibroblasts and their synthesis of biomolecules (Koh and DiPietro 2011; Rodero and Khosrotehrani 2010).

1.2.3 Proliferation

The end of inflammation is indicated by the reduction of macrophages in the wound, and also by the absence of neutrophils. Proliferation starts after 2 or 3 days when the rebuilding of the destroyed tissue is initiated (Koh and DiPietro 2011). The number of fibroblasts, endothelial cells and keratinocytes is increased in the site of damage, which is correlated with their migration and enhancement of their growth. This stage of the healing process can be divided into three parallel running repairing mechanisms – biosynthesis of extracellular matrix molecules, reepithelization and angiogenesis (Olczyk *et al.* 2014). These mechanisms are modulated by releasing mediators from the cells. Fibroblasts synthesize factors, such as bFGF, PDGF, TGF-β, IGF-1 and epidermal growth factor (EGF), while keratinocytes secrete TGF-α, TGF-β and keratinocyte-derived anti-fibrogenic factor (KDAF). The endothelial cells are the main producers of VEGF, PDGF and bFGF (Behm *et al.* 2012).

1.2.3.1 Biosynthesis of ECM Molecules

The rebuilding of the damaged tissue is caused by replacing the temporary fibrin and fibronectin network with collagen and others glycosaminoglycans, proteoglycans and noncollagenous glycoproteins. The released cytokines and growth factors from different cells support the transformation of undifferentiated mesenchymal cells, that are localized in the surviving dermis, into fibroblasts. Fibroblasts are the key cells for the healing process and they normally migrate to the damaged place in 2 or 3 days after the injury happens (Darby *et al.* 2014). The transformed fibroblasts are attracted by the gradient of chemotactic growth factors in the wounded site, where the proliferation of fibroblasts takes place. The replacement of a temporary matrix starts around the fourth day after the injury by the PDGF and TGF-β mediated activation of fibroblast biosynthesis, which leads to the production of collagens, especially collagen III and V (Zoppi *et al.* 2004). The PDGF is also responsible for

the expression of collagenase, and TGF-β regulates the accumulation of ECM components (Xue and Jackson 2015; Tracy *et al.* 2016). This newly formed tissue is intertwined by capillaries and is called granulation tissue, because of its shape (Fig. 3). Beside collagens, the granulation tissue also contains noncollagenous proteins, such as elastin, glycosaminoglycans and proteoglycans. In the first and the second stages of the healing process, the temporary matrix is enriched by molecules of hyaluronic acid and fibronectin (Tracy *et al.* 2016). In the third stage, the hyaluronic acid mesh structure enables the penetration of migrating cell to the wound area, and collagen fibers are created along the fibronectin scaffolding structure (Tolg *et al.* 2014; Sottile and Hocking 2002). The concentration of hyaluronic acid rapidly decreases after the third day of the healing process, and collagen completely replaces hyaluronic acid in the next three weeks. This mechanism is accompanied by apoptotic decrease of the fibroblast amount until they totally disappear (Webber *et al.* 2009b; Webber *et al.* 2009a). Normally, collagen I and III are present in natural dermis in the ratio 4:1, while in the initial stages of healing, collagen III predominates in order to enhance the mechanical toughness of the newly created granulation tissue (Muller *et al.* 2012; Tracy *et al.* 2016). This tissue substitutes the dermis for a while, but in the last phase of the reparation process, it is remodeled to a scar. The granulation tissue has high metabolic activity, which requires high energy supply, and therefore this tissue has a dense network of capillaries (Fig. 3) (Colwell *et al.* 2005).

1.2.3.2 Reepithelization

Reepithelization is the reconstruction process, in which the epithelial cells from the wound edges and epithelial appendages participate (Fig. 3). This phase of healing comprises the detachment of keratinocytes, their migration to the area of the damage, growth and differentiation (Ter Horst *et al.* 2018). The key mediators of reepithelization, that affect the keratinocyte migration and proliferation, are keratinocyte growth factor (KGF), EGF and TGF-α (Gibbs *et al.* 2000; Yamamoto *et al.* 2005). The proliferation of keratinocytes begins directly on the basement membrane between the epidermis and dermis. The migration of keratinocytes continues until the keratinocytes create a uniform layer of well-connected cells. The detachment of the keratinocytes from the basement membrane is mediated by matrix metalloproteinase MMP-2 (gelatinase-A) and MMP-9 (gelatinase-B), which destroy collagen IV of the basement membrane and collagen VII (Salo *et al.* 1994). It was also found out that MMP-1 (interstitial collagenase) enables the migration of keratinocytes through collagen I and III network, while stromelysin-1 and stromelysin-2 promote the cell migration through

the network of fibronectin, glycosaminoglycans and laminins (Saarialho-Kere *et al.* 1994; Park *et al.* 2011; Pilcher *et al.* 1997).

1.2.3.3 Angiogenesis

The process of the renovation of the blood circulation prevents the wounded area from ischemic necrosis. Simultaneously, the repairing mechanisms are stimulated by mediators from the blood (Fig. 3). Angiogenesis is stimulated by low tension of oxygen, high concentration of lactic acid and by locally decreased pH. However, the proangiogenic activity of macrophages, fibroblasts, keratinocytes and endothelial cells is also significant (Olczyk *et al.* 2014). They produce many soluble stimulation factors, such as angiogenin, angiotropin, VEGF, bFGF, TGF-β and TNF-α, but also many suppression factors of angiogenesis, e.g. hypoxia inducible factor, angiostatin and thrombospondin (Ferrari *et al.* 2009; Colwell *et al.* 2005; Tonnesen *et al.* 2000). Hyaluronic acid plays a special role in angiogenesis, where the low molecular mass hyaluronic acid has a stimulating effect, while the high molecular mass has the opposite effect (Slevin *et al.* 2002). This phase of the healing process is crucial, because the endothelial cells firstly migrate to the temporary matrix, proliferate and then develop new tubular branches of capillary-like network. The endothelial cell migration depends mainly on the activity of metalloproteinases and on the growth factors (Mongiat *et al.* 2016). The dense network of capillaries will be reduced by apoptosis of some endothelial cells in the last phase of healing. The collagen matrix will be replaced by a scar, where the requests for oxygen and nutrients are significantly lower (Olczyk *et al.* 2014; Wang *et al.* 2017).

1.2.4 Remodeling

The last phase of the wound healing is characterized by phenotypic maturation of fibroblasts in the granulation tissue into myofibroblasts (Webber *et al.* 2009a; Webber *et al.* 2009b). These cells contain $\alpha_1\beta_1$ and $\alpha_2\beta_1$ integrin receptors for collagen and α-smooth muscle actin microfilaments, especially in the later phase of remodeling, which enable the contraction of the tissue (Kondo *et al.* 2004; Darby *et al.* 1990). In the second week of the healing process, the myofibroblasts are the dominant cell type in the granulation tissue (Darby *et al.* 2014). During the remodeling stage, the granulation tissue matures to the scar, and the mechanical strength of the tissue is increased. The capillaries in the mature tissue are linked together to the large blood vessels, and the amount of proteoglycans and glycosaminoglycans, as well as the amount of water, is decreased (Dulmovits and Herman 2012; Olczyk *et al.*

2014). The final ratio of collagens is changed; collagen I is more abundant in scar tissue than collagen III. The final density and the covalent cross-links of the collagens are increased, therefore the scarring tissue has a better tensile strength than the tissue during early phases of healing after the injury (Xue and Jackson 2015).

In conclusion, the wound healing process is a highly regulated complex process in which molecules of ECM, cells and mediators play specific roles, and any minor changes in the individual phases can lead to huge skin pathologies.

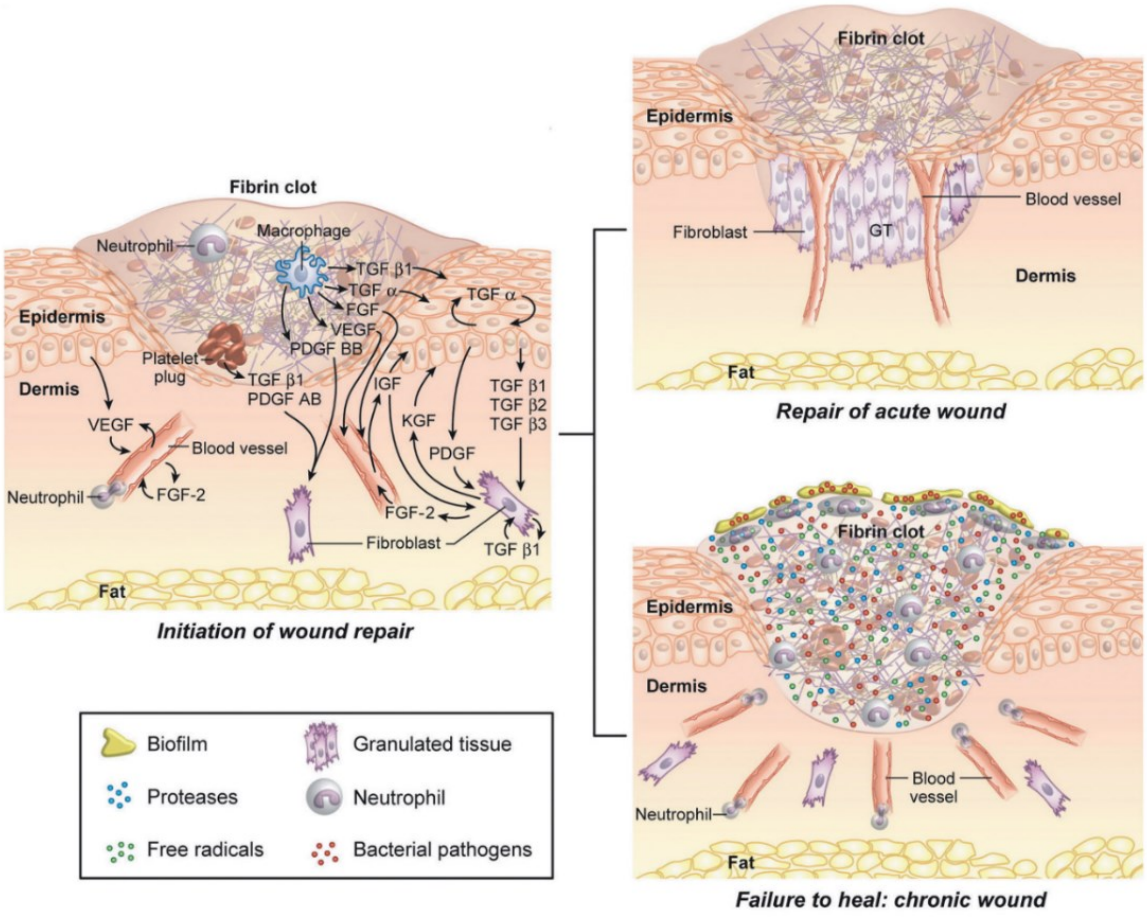

Figure 3. *Wound healing mechanisms – acute and chronic wounds (Clark et al. 2007).*

1.3 Tissue Engineering in the Wound Healing

1.3.1 Conventional Treatments

Deep dermal wounds are usually accompanied with a slow and inadequate healing process due to lack of epidermis. The wound bed is uncovered by keratinocytes, so that pathogens can cause extensive infections. For many centuries, people have tried to solve this problem by covering the injuries. The first frog skin xenograft was reported in the 1500 BC in Papyrus of Ebers (Vig *et al.* 2017). Nowadays, commonly used xenografts are surgically extracted from a porcine skin and are placed to human wounds in order to cover the damaged area and to accelerate the healing process. The main disadvantage of the xenografts is their immunological rejection (Nathoo *et al.* 2014).

Another option of the conventional treatment is a human skin allograft, which was firstly mentioned in 1503 in the work of Branca of Sicily. Human skin allografting has been clinically applied since World War II. Skin allografts can be obtained either from living donors or from cadavers. All over the world, skin burn centers frequently use the allografts, because supplies can be defrosted from skin banks and used immediately (Vig *et al.* 2017). Although the allograft is considered to be an appropriate skin analog, which provides growth factors and cytokines and supports vascularization, it is usually transplanted as a temporary cover due to a possible immunological rejection (Farkas *et al.* 2018). Allogeneic dermal substitutes were cultured and implanted into patients with intractable skin ulcers in order to cover wounds and to improve the wound conditions for subsequent application of autologous skin grafts (Hasegawa *et al.* 2005).

The successful application of an amnion for the treatment of partial thickness burns was firstly described in 1910 (Vig *et al.* 2017). The amnion is collected from the placenta of a donor and is preserved for a future use. Moreover, it was found recently that amnions can be preserved by dehydration (Fetterolf and Snyder 2012). It has been observed that the treatment by the amnion reduces pain, minimizes the loss of electrolytes, fluids and proteins, decreases the infection risk and accelerates the healing process. The amniotic membrane is a suitable source of collagen and growth factors, which supports epithelization and closure of the wounds. In comparison with classical allografts, the amnion lacks immune markers and has a unique ability to reduce pain and bacterial contamination (Snyder *et al.* 2016; Eskandarlou *et al.* 2016).

The most suitable way how to replace the damaged skin is to use an autograft. A thin layer of epidermis and dermis, e.g. split-thickness autograft, can be shaved by dermatome

from the healthy skin of a patient and then placed to the wounded area (Prakash *et al.* 2016). The main benefit of this technique is that there is no risk of an immunological rejection. Moreover, clinicians recently obtained positive results by treating chronic wounds with a meshed split-thickness autograft in the combination with an amniotic membrane as the wound dressing (Lavor *et al.* 2018).

1.3.2 Commercial Tissue-Engineered Products

Nowadays, there are many approaches how to treat wounds, but for the simplification, we can divide commonly used tissue-engineered products into temporary, semi-permanent and permanent. Based on the time of application in a wound, skin dressings are considered as temporary products, while advanced skin substitutes are designed as permanent products. Semi-permanent products are made by the combination of the permanent skin substitutes with the temporary skin dressings. These products can be further classified according to several criteria: presence of cells – cellular or acellular, type of materials – synthetic or biologic, origin of the cells or biomaterials – autologous, allogenic, and xenogeneic. The wound treatment depends on the depth of the damage, therefore the tissue-engineered products are being developed in order to replace certain layers of the damaged skin, e.g. epidermis, dermis or full-thickness skin (Vig *et al.* 2017; Savoji *et al.* 2018).

The easiest way how to enhance the healing process is to cover the wound by suitable acellular material, which can be synthetic, biologic or a combination of both. These materials are mainly used for superficial, mid-dermal partial thickness wound burns or for epidermolysis bullosa and hidradenitis suppurativa diseases (Dagregorio and Guillet 2005; Melkun and Few 2005). The main commercial available products are Integra® and Biobrane®, which combine the bovine collagen with the synthetic materials, such as silicone or nylon mesh (Fig. 4). Alloderm® is one of the most commercially used acellular human lyophilized dermis that was successfully used for example in implant-based breast reconstructions (Fig. 4) (Hinchcliff *et al.* 2017). Other options are xenogeneic substitutes made of decellularized xenogeneic materials, such as porcine dermis (Permacol™), bovine collagen I and elastin (Matriderm®) and the intact matrix from porcine submucosa (Oasis®). Oasis® is considered to be dermo-epidermal composite since it is used for wound closure in extensive acute, chronic and burn wounds (Martinson and Martinson 2016; Min *et al.* 2014; Kalin *et al.* 2015).

More advanced skin substitutes are made from biological or synthetic materials and cells. In case of the cellular allogenic skin substitutes, the most frequently used type of cells are neonatal foreskin fibroblasts growing on synthetic meshes or matrices. Commercial examples

of dermal substitutes are Dermagraft® and Transcyte®, which are successfully used for the treatment of diabetic ulcers and partial-thickness burns (Fig. 4) (Martinson and Martinson 2016; Kumar *et al.* 2004). Apligraf® or OrCel® are full-thickness skin composites containing not only allogenic neonatal foreskin fibroblasts, but also allogenic keratinocytes, which are cultured together on a collagen matrix (Fig. 4) (Martinson and Martinson 2016; Zelen *et al.* 2016; Still *et al.* 2003). Another allogenic full-thickness skin substitute with dermal and fully stratified epidermal layer is StrataGraft™. It is well-tolerated and temporary grafted before autografting in the patients with burns.

Allogenic skin substitutes, which are either cellular or acellular, provide only a temporary dressing of the wounded area. In the case of a large wound, these substitutes have to be replaced by autologous grafts or re-grafted, because the allogenic substitutes are usually rejected. Therefore, the most advanced tissue-engineered substitutes are autologous, that contain the cells or the whole skin tissue from the patient (Boyce *et al.* 2006). Although there are some limitations, keratinocytes are the best accessible skin cells for autotransplantation, therefore the commercial cultured epidermal autografts are commonly available. EpiDex® or Epibase® are cultured keratinocytes in the form of confluent cell sheets (Tausche *et al.* 2003). The production of cell sheets in *in vitro* conditions is simple, however the manipulation after few weeks is challenging, thus some carriers are required for the delivery. Therefore, the more advanced epidermal substitutes use for example a silicone support layer (MySkin®), a fibrin sealant (Bioseed®-S), petrolatum gauze (Epicel®) or a microperformed hyaluronic acid membrane (Laserskin®) (Fig. 4) (Carsin *et al.* 2000; Uccioli *et al.* 2011; Vig *et al.* 2017). Keratinocytes from donor biopsy can also be sprayed into the wound in the form of suspension (CellSpray) (Magnusson *et al.* 2007). Substitutes containing only keratinocytes are inappropriate for healing of the full-thickness skin wounds, because the digestive collagenase enzymes in the wound bed can reduce acceptance of these substitutes. Moreover, these substitutes can cause hyperkeratosis, contracture and scarring. One option how to deal with this problem is to pre-graft the wound bed for four days by an allogenic skin in order to prepare the wounded area for the following application of autologous cell substitutes (Vig *et al.* 2017).

Another strategy to treat a deep dermal wound is based on autologous dermal substitutes, which are typically made from hyaluronic acid scaffolds and autologous fibroblasts. Commercially available products are Hyalograft 3D or similar Hyalomatrix® with an additional outer silicone membrane, which acts as a temporary barrier. The skin substitutes can also be used together; for example, the TissueTech autograft system combines dermal

Hyalurograft 3D and epidermal Laserskin® (Fig. 4) (Uccioli *et al.* 2011). Although TissueTech autograft shows positive results in healing full-thickness ulcers, the clinical applications are limited due to grafting of two different products. Autologous fibroblast seeded on synthetic membranes can be used as a cultured dermal substitute. Commercially available synthetic materials, applicable in the dermal substitution, are based on either biodegradable synthetic polyurethane microfibers or polylactic-*co*-glycolic acid (PLGA) nanofibers combined with chitosan (Rockwood *et al.* 2007; Ajalloueian *et al.* 2014). Further tested synthetic polymers are polylactic acid (PLA), polycaprolactone (PCL) and copolymer of PLGA/PCL and polypyrrole. All of them can be combined with nature-derived polymers, such us hyaluronic acid or chitosan (Franco *et al.* 2011; Pal *et al.* 2017; Akkouch *et al.* 2010).

The most sophisticated substitutes are focused on the treatment of full-thickness skin wounds by a one-step procedure using autologous equivalents of both skin layers, e.g. epidermis and dermis. Permaderm™ is one of the commercially produced composites, which uses collagen and glycosaminoglycan substrate for the cultivation of keratinocytes and fibroblasts. This composite is designed as a permanent replacement, but no clinical trials have been reported yet. Another composite of dermis and epidermis are Tiscover™ and DenovoSkin™ (Oostendorp *et al.* 2017). Both substitutes mimic the natural skin architecture, but the culture time is still long, therefore no clinical trials have been published yet. Tiscover™ is currently undergoing the clinical trials for chronic foot ulcers (Vig *et al.* 2017).

It can be concluded that each of these substitutes has its own advantages, but also many disadvantages, and therefore there is no ideal skin equivalent yet. The vascularization of commercial skin substitutes is limited, which leads to integration failures and subsequently to rejections. Moreover, commonly available substitutes are expensive, the preparation process takes 2 – 3 weeks and large-scale production is problematic, because supplies of tissue from donors are also limited. For the future, it is necessary to improve the vascularization of substitutes in order to better integrate the substitute to the patient tissue (Zimoch *et al.* 2018). Therefore the current research is focused on potential application of adipose-derived stem cells in the revascularization of full-thickness skin substitutes (Klar *et al.* 2017a; Klar *et al.* 2016; Sun *et al.* 2016b). The standardization of the manufacturing process and the preservation are important as well (Sun *et al.* 2016a). Last but not least, the incorporation of additional cell types, such as endothelial cells, cells of skin appendages and stem cells, to the newly developed substitutes is essential for the most physiological imitations of the real skin (Dai *et al.* 2018; Sriram *et al.* 2015). The most advanced method is skin bioprinting (Augustine 2018).

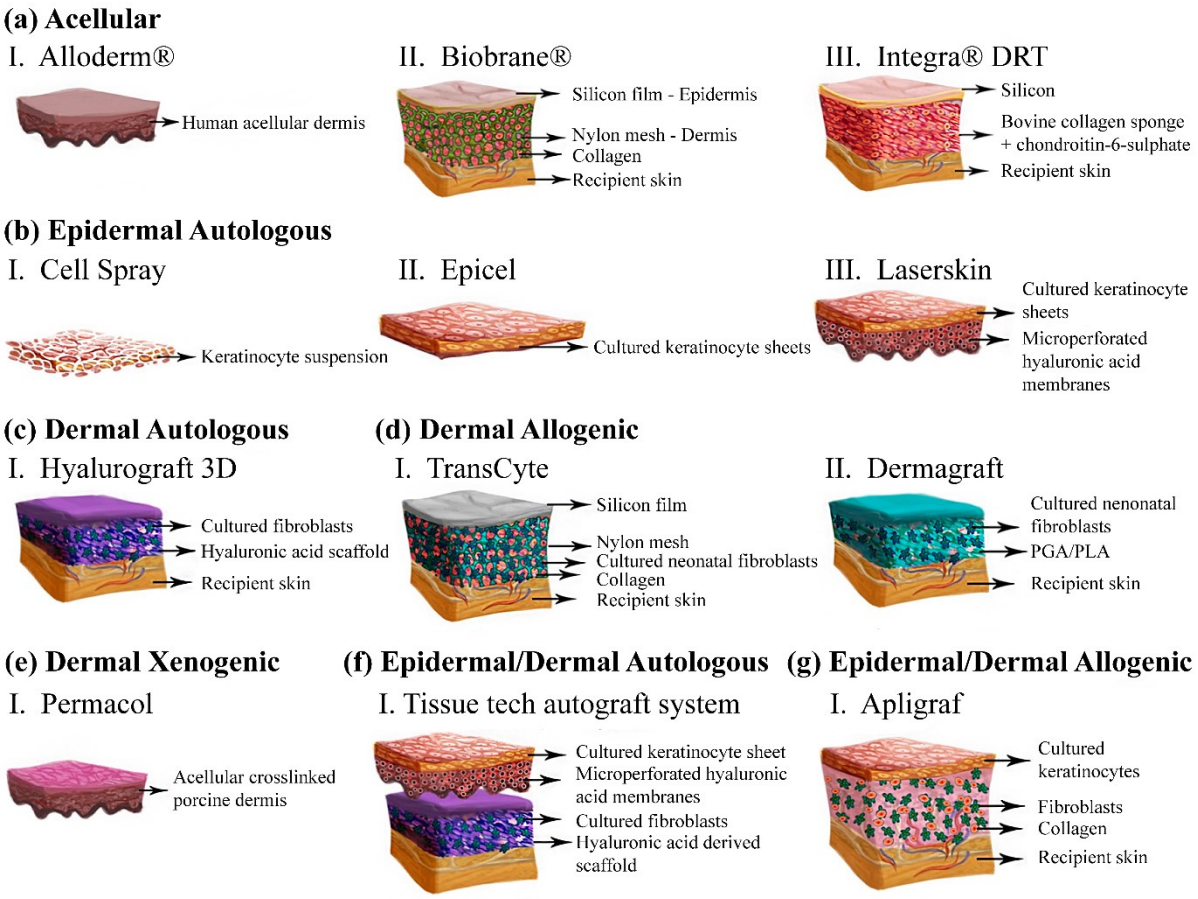

Figure 4. *Commercial tissue-engineered skin substitutes (Vig et al. 2017).*

1.4 Novel Approaches in Skin Tissue Engineering

Two-dimensional (2D) systems have been used for many years for cultivation of cells and as *in vitro* models for studying the cell behavior. The conventionally used 2D Petri dishes, glass slides or coverslips or polystyrene plastics provide mechanical support for the cells and equal amount of nutrients and growth factors from medium, which enable homogeneous proliferation of the cells. Although the basic 2D culture systems do not provide control of cell morphology, the simplicity of these systems make them more attractive for biological and medical applications (Duval *et al.* 2017). However, it is necessary to realize that 2D cultivation systems are not sufficient for the experiments in which the physiological behavior of the cells is evaluated or simulated. Several methods have been described to control the cell behavior by modifying 2D surfaces of the materials. For example, coating by biomolecules (Bacakova *et al.* 2017), cell-adhesive islands (Elineni and Gallant 2011), microwells (Xu *et al.* 2014) or micropillars (Fu *et al.* 2010) are used to customize surfaces of 2D materials (Nguyen *et al.* 2016). Nonetheless, these modified 2D systems still induce an apical-basal polarity and restrict adhesion and migration of the cells in x-y axis, which lead to non-

physiological behavior of the cells, such as fibroblasts or mesenchymal stem cells (Fig. 5) (Ihalainen *et al.* 2015). On the other hand, the apical-basal polarity and adhesion in x-y axis is a typical behavior of epithelial cells, like keratinocytes, for which the 2D surface is required. More complex three-dimensional (3D) microenvironment is desired for a non-prescribed polarity of fibroblasts or mesenchymal stem cells and also for the spreading, and migration in all three dimensions (Duval *et al.* 2017). Novel 3D cultivation systems aim at modeling the physiological environment similar to natural ECM for the cells to study their biomechanical and biochemical interactions. From the tissue-engineering point of view, these 3D cultivation systems provide better results in cell adhesion, spreading, proliferation, migration, matrix proteins production, and differentiation (Fig. 5) (Duval *et al.* 2017; Ahearne 2014).

There are many approaches how to provide the most suitable 3D environment for the cells, but the most advanced ones can be categorized subsequently – cell sheet technology, scaffolds made from synthetic or natural materials, scaffolds from decellularized ECM and cells embedded in hydrogels. The following subsections are focused on each of them in more detail (Chaudhari *et al.* 2016).

1.4.1 Cell Sheet Technology

Cells can be cultivated in the form of sheets in a 2D system, but as it was mentioned above, 2D system affects morphology of the cells and causes the polarization. This effect can be mitigated by cultivating the cells using a layer-by-layer technology with ECM molecules between these layers (Lee *et al.* 2018). The synthesis of ECM molecules by cell sheets provides 3D-like environment for the cells and eliminates apical-basal polarity. According to Rheinward and Green's technique, keratinocytes are cultivated to their confluent state and then placed to a wound; however, a monolayer cell sheet is fragile and its handling is difficult (Rheinwald and Green 1975; O'Connor *et al.* 1981; Auxenfans *et al.* 2015). One of the possible solutions is the cultivation of multi-layered cell sheets on thermally-responsive polymeric substrates, such as a poly(N-isopropylacrylamide) membrane. The confluent layer of the cells can be separated from the substrate without trypsinisation by lowering the temperature under 25°C, which is the lowest critical solution temperature (Nagase *et al.* 2018; Lee *et al.* 2018). This thermo-sensitive membrane can also be modified by fibrin, fibronectin or collagen and can be placed between layers of the cells (Lee *et al.* 2018; Lin *et al.* 2013).

1.4.2 Scaffolds for the Cells

The scaffolds for the cells can be manufactured from many different biodegradable or non-biodegradable food and drug administration (FDA)-approved materials, that can be synthetic, nature-derived or composite. Based on fabrication protocol, the scaffolds can be produced in the different shapes for various applications, e.g. porous, fibrous or microsphere scaffolds (Chaudhari *et al.* 2016).

1.4.2.1 Scaffolds Based on Synthetic Materials

The synthetic materials, such as PLA, PLGA, PCL, polyethylene glycol (PEG), polyglycolic acid (PGA), polyethylene oxide (PEO), polybutylene terephthalate (PBT) and many other synthetic polymers are used due to their flexible properties, high mechanical stiffness, simple processability and non-toxic biodegradability (Chaudhari *et al.* 2016). These materials are commonly processed to fibrous scaffolds by conventional electrospinning, followed by cell seeding (Yari *et al.* 2016; Hejazian *et al.* 2012), and by more advanced techniques, such as electrospinning of polymers with encapsulated cells (Chen *et al.* 2015; Jayasinghe 2013) or *in situ* electrospinning technique, i.e. direct deposition of personalized nanofibrous dressing into a patient wound (Liu *et al.* 2018a; Dong *et al.* 2016; Deng *et al.* 2018). The fibrous scaffolds, especially nanofibrous, are widely used in wound healing either as wound dressings or as substitutes of the damaged skin, according to their degradation capabilities.

Although the synthetic scaffolds are non-toxic and mimic mechanical and morphological properties of native tissue, they usually do not enhance the cell adhesion and proliferation. Therefore, many approaches have been described in order to improve attractiveness of the synthetic materials for cells, and thereby to accelerate the healing process. Commonly used methods are based on coating a surface by substances more physiological for the cells or on encapsulating some agents with therapeutic potency (Chen *et al.* 2017). For example, Bacakova *et al.* modified PLA nanofibers with fibrin or collagen I in order to enhance the adhesion and growth of human dermal fibroblasts and keratinocytes (Bacakova *et al.* 2016; Bacakova *et al.* 2017). Fu *et al.* found out that collagen-coated PCL nanofibers with the presence of exogenous TGF-β1 increased fibroblast proliferation, while fibrinogen-coated nanofibers in the presence of exogenous TGF-β1 decreased the growth of fibroblasts, and supported migration and α-smooth muscle actin expression in these cells, which is typical for fibroblast differentiation to myofibroblasts (Fu *et al.* 2016). Similarly, Cheng *et al.* observed

that PCL/collagen nanofibrous membrane was a suitable matrix to deliver and release controlled amount of TGF-β1, which supports the differentiation of fibroblasts (Cheng *et al.* 2016). It was also found that the PCL/collagen nanofibrous membrane alone did not stimulate migration of keratinocytes, while the coating made by collagen ultrafine fibrous network significantly increases the motility of these cells (Fu *et al.* 2014).

These *in vitro* results can be further applied in the construction of skin dressings or substitutes. The current research is focused on developing 3D nanofiber-based dressings that have high area-to-volume ratio of surface, high porosity and well mimic natural ECM. Therefore, the nanofibrous dressings can absorb wound exudate while the wound stays properly hydrated, and moreover they can release growth factors or other therapeutic agents with anti-bacterial, anti-inflammatory and anti-oxidant effects (Chen *et al.* 2017). For example, Kim and Yoo incorporated human EGF to PCL/PEG nanofibers in order to enhance the healing process of diabetic wounds (Kim and Yoo 2013). Similarly, Liao *et al.* created a nanofibrous composite of carbon nanotubes and polyvinyl alcohol with EGF for wound dressing applications (Liao *et al.* 2017). Polyethylene glycol-poly-DL-lactide scaffold was created for the same purpose, but bFGF was loaded instead of EGF (Yang *et al.* 2011). VEGF and PDGF were encapsulated in PLGA nanoparticles, which were incorporated into nanofibers in order to generate a sustained release of growth factors, and thereby to promote angiogenesis, to increase re-epithelialization and to control granulation tissue formation (Xie *et al.* 2013). Moreover, curcumin and silver particles or antibiotics were used in combination with synthetic nanofibers to reduce microbial infection by covering the wound and by releasing anti-bacterial agents (Shababdoust *et al.* 2018; Chen and Chiang 2010; Heo *et al.* 2013; Chen and Liu 2015). Synthetic nanofibrous scaffolds seeded with both keratinocytes and fibroblasts were also studied under *in vitro* and *in vivo* conditions as skin substitutes for the full-thickness wound repair (Reed *et al.* 2009; Bacakova *et al.* 2017). Mahjour *et al.* used a layer-by-layer method to construct PCL/collagen nanofibers with both types of cells and applied this construct to nude mice onto the full-thickness wound (Mahjour *et al.* 2015).

1.4.2.2 Scaffolds Based on Nature-Derived Materials

Natural polymers are those that are extracted from natural sources like plants, animals or microorganisms. Commonly used natural polymers are either polysaccharides, such as chitosan, hyaluronic acid, heparin and cellulose, or proteins, mainly collagen, fibrin, fibronectin, silk fibroin, laminin and CKs (Raveendran *et al.* 2017). These natural polymers

are frequently combined with synthetic polymers to improve their physical and chemical properties that are crucial for the interactions of cells with biomimetic materials.

Cellulose is a structural polysaccharide which is extracted mainly from cell walls of plants or from bacteria. Therefore, cellulose is plenteous material in nature and its source is relatively inexhaustible. Based on these advantages, cellulose is a promising biomaterial for tissue engineering. The structure of cellulose is formed by linear polysaccharide chains with beta acetal-linked glucose units as monomers (Raveendran *et al.* 2017; Bacakova *et al.* 2014). The most commonly used forms of cellulose for regenerative purposes are nanoparticles, nanocrystals and nanofibers, which are made from native cellulose extracted from plants or bacteria (Foster *et al.* 2018). Cellulose nanoparticles are used for strengthening materials due to their low density, presence of a reactive hydroxyl functional group and high aspect ratio (Zulkifli *et al.* 2017). The most recent publications about wound healing strategies often discuss the positive effect of bacterial or wood-based cellulose nanofibrils (CNFs) in form of hydrogels (Liu *et al.* 2018b). These nanofibrous hydrogels are prepared by cross-linking in sodium hydroxide/urea aqueous solvent media, which increase the water uptake capacity of cellulose (Peng *et al.* 2016). Novel dressing material for wounds are based on 3D-ordered CNF films, which can be made by molding or evaporating CNF hydrogels (Hakkarainen *et al.* 2016; Wu *et al.* 2014; Skogberg *et al.* 2017). Cellulose nanofibers can be also prepared by electrospinning technology (Park *et al.* 2015; Ohkawa 2015). The cellulose nanofibers are often modified in order to improve their mechanical and chemical properties and thereby to enhance cell attachment and growth. For example, CNFs are modified either by a negative charge using 2,2,6,6-tetramethylpiperidinyloxy (TEMPO) oxidation or by a positive charge using 2,3-epoxypropyl trimethylammonium chloride (EPTMAC) (Skogberg *et al.* 2017; Trovatti *et al.* 2018; Shefa *et al.* 2017).

Collagen is the most abundant ECM protein, which constitutes the physiological environment for the cells; therefore it is an extensively used protein in the construction of the wound dressings and substitutes. Commercial dressings and substitutes are made mainly of collagen sponge, fibers, powders or purified skin. Many publications report a positive effect of collagen in any form on the healing process of acute burned wounds. Furthermore, it was found out that elastase level in the wound microenvironment is reduced by presence of collagen, which disrupts the cycle of chronicity in diabetic wounds (Fleck and Simman 2010). Many results show that the nanofibrous scaffolds fabricated from collagen, collagen-containing composites or collagen-coated nanofibers are more suitable for the cells than pure synthetic scaffolds due to higher biocompatibility and biodegradability. For example, Zhou at

al. developed electrospun tilapia collagen nanofibers, which accelerated the healing process by inducing keratinocyte proliferation and differentiation (Zhou *et al.* 2016). Lai *et al.* prepared nanofibers from collagen/hyaluronan and gelatin nanoparticles which were enriched by releasing several growth factors, e.g. bFGF, EGF, VEGF and PDGF-BB, in order to enhance the healing process of diabetic wounds (Lai *et al.* 2014). Bacakova *et al.* used collagen or fibrin coating of synthetic PLA nanofibers to enhance fibroblast and keratinocyte adhesion and proliferation (Bacakova *et al.* 2017). It can be summed up that native collagen in any form increases fibroblast chemotaxis, angiogenesis, keratinocyte migration, but the most recent studies show that the fibroblast behavior is more physiological when the fibroblasts are entrapped in the 3D structure of collagen hydrogels (Miron-Mendoza *et al.* 2012; Klar *et al.* 2014).

1.4.3 Decellularized ECM Scaffolds

Decellularized ECM scaffolds are collagen-rich scaffolds made by the removal of cellular components from the whole tissue in order to reduce the immunological response. These acellular scaffolds can be recellularized by autologous cells, which can further replace the scaffold by their own ECM molecules. The process of decellularization can be performed by various techniques, such as repeating of freeze-thaw cycles, treating with hypotonic and hypertonic solutions, ultra-sonication and enzymatic digestion by trypsin/ ethylenediaminetetraacetic acid (EDTA) (Chaudhari *et al.* 2016; Helliwell *et al.* 2017; Wu *et al.* 2015). Several commonly available commercial products (Alloderm®, DermaMatrix®, Integra®, OASIS Ultra® and Permacol®) are based on acellular scaffolds, but all of them are derived from the exogenous porcine or bovine skin which can cause immune rejection in many patients. In order to solve this complication, Benny *et al.* developed an organotypic skin culture, which is made by decellularization of the ECM molecules deposited by fibroblasts and keratinocytes. The cells, which are seeded on the deposited ECM substrates, produce more ECM molecules and enhance the deposition of dermal-epidermal junction components *in vitro* (Benny *et al.* 2015). On the other hand, Greaves *et al.* used allogenic human decellularised dermis for treatment of acute cutaneous wounds and showed that the acellular dermis can enhance angiogenesis during the healing process (Greaves *et al.* 2015). Spiekstra *et al.* evaluated the secretion of wound-healing factors released by epidermal keratinocytes and dermal fibroblasts, which were reseeded on the acellular donor dermis (Spiekstra *et al.* 2007).

1.4.4 Cells Embedded in Hydrogels

Nature-derived or synthetic polymers are widely used for fabrication of various scaffolds for cells, but their porous or fibrous structure is still more in 2D rather than in 3D form. Therefore, the most recent approach is based on embedding the cells into the hydrogels, which are made up of natural macromolecules (Fig. 5). The hydrogels are able to self-assemble from the liquid monomeric phase to the polymeric mesh network under certain temperature, pH, and enzymatic activity (Chaudhari *et al.* 2016; Shang and Theato 2018). The hydrogels are covalently or non-covalently cross-linked which enable the encapsulation of living cell (Jhon and Andrade 1973). Their biocompatibility is attributed to their similarity with the natural ECM. This system went through many studies, which caused an increase in the number of commercial test systems and hydrogel-based therapies (Chau *et al.* 2013; Tsao *et al.* 2014; Arnette *et al.* 2016). When the cells are entrapped in the hydrogels, the surrounding environment affects their gene expression pattern and stimulates biosynthesis of their own ECM molecules, which results in degradation and remodeling of the hydrogels (Ahearne 2014; Polio and Smith 2014). The degradation time and the time of remodeling should be in balance, and both are highly dependent on the behavior of the encapsulated cells. Various synthesized matrix metalloproteases (MMP-1, MMP-2, MMP-8, MMP-13 and MMP-14), which are involved in the degradation processes and migration of the cells in the hydrogels, have been described. Besides the degradation, the cells can also synthesize their own molecules of ECM, and thereby they can remodel the hydrogels (El Ghalbzouri *et al.* 2009; Raveendran *et al.* 2017).

Various nature-derived hydrogels for wound healing and regeneration applications have been described. These hydrogels are derived mainly from collagen, fibrin, hyaluronan-chitosan or chitosan-gelatin, which are molecules similar to the macromolecular-based components of the body (Miron-Mendoza *et al.* 2012; Franco *et al.* 2011; Braziulis *et al.* 2012; Huang *et al.* 2018). The most advanced hydrogels are based on self-assembled peptides conjugated with substance P (Kim *et al.* 2018). Although the hydrogels have excellent biocompatibility and biodegradability, their mechanical properties are weak with tendency to contract and degrade under traction forces of the embedded cells (Lotz *et al.* 2017; Polio and Smith 2014). In order to develop a large-size clinically applicable transplant, Braziulis *et al.* used plastic compression for collagen type I hydrogel to increase the stability and improve mechanical properties of the material (Braziulis *et al.* 2012). Similarly, Kim *et al.* induced structural and mechanical changes of fibrin-collagen matrix by its compression (Kim *et al.*

2017; Ghezzi *et al.* 2011). Lotz *et al.* cross-linked collagen with succinimidyl glutarate polyethylene glycol, which reduced contraction of collagen hydrogels, and thus increased the applicability of these models (Lotz *et al.* 2017). Another way how to solve the weakness of the hydrogels is to strengthen them using biodegradable synthetic scaffolds, e.g. PCL/PLGA nanofibrous membranes or knitted meshes (Hartmann-Fritsch *et al.* 2016; Franco *et al.* 2011).

It has been reported in many publications that 3D microenvironment of hydrogels provides more physiological conditions for cell spreading, proliferation, migration and differentiation (Arnette *et al.* 2016). The cells embedded in the hydrogels, especially fibroblasts and other mesenchymal cells, tend to be more spread with typical spindle-like morphology and create a network with cell contacts in all three dimensions (Smithmyer *et al.* 2014; Hartmann-Fritsch *et al.* 2016; Miron-Mendoza *et al.* 2012). On the other hand, keratinocytes with their polarity prefer 2D-structured surface of the hydrogels. Fujisaki *et al.* and many others observed that collagen hydrogels, mainly collagen IV and collagen I, support the adhesion, proliferation and stratification of keratinocytes (Fujisaki *et al.* 2008; Stark *et al.* 2004; Klar *et al.* 2018). In addition, the biosynthesis of ECM molecules by fibroblasts and keratinocytes is enhanced by the physiological conditions of the hydrogels, which is important for hydrogel remodeling and for the separation of the cells by the formation of the basement membrane (El Ghalbzouri *et al.* 2009). Although the encapsulated cells are separated from the cells growing on the surface, their communication can be mediated by cytokines and growth factors released from the cells by a paracrine manner or by cell-hydrogel mechanosensation (Witte and Kao 2005; Brohem *et al.* 2011; Ahearne 2014). The paracrine-based relationship of cells can be modulated by changing the permeability and structural properties of cell-encapsulating substances. For examples, Chiu *et al.* modulated the permeability of fibrin constructs by varying the concentration of fibrinogen and thrombin (Chiu *et al.* 2012). Bader *et al.* changed the keratinocyte-fibroblast paracrine communication by gelatin-based semi-interpenetrating networks (Bader and Kao 2009).

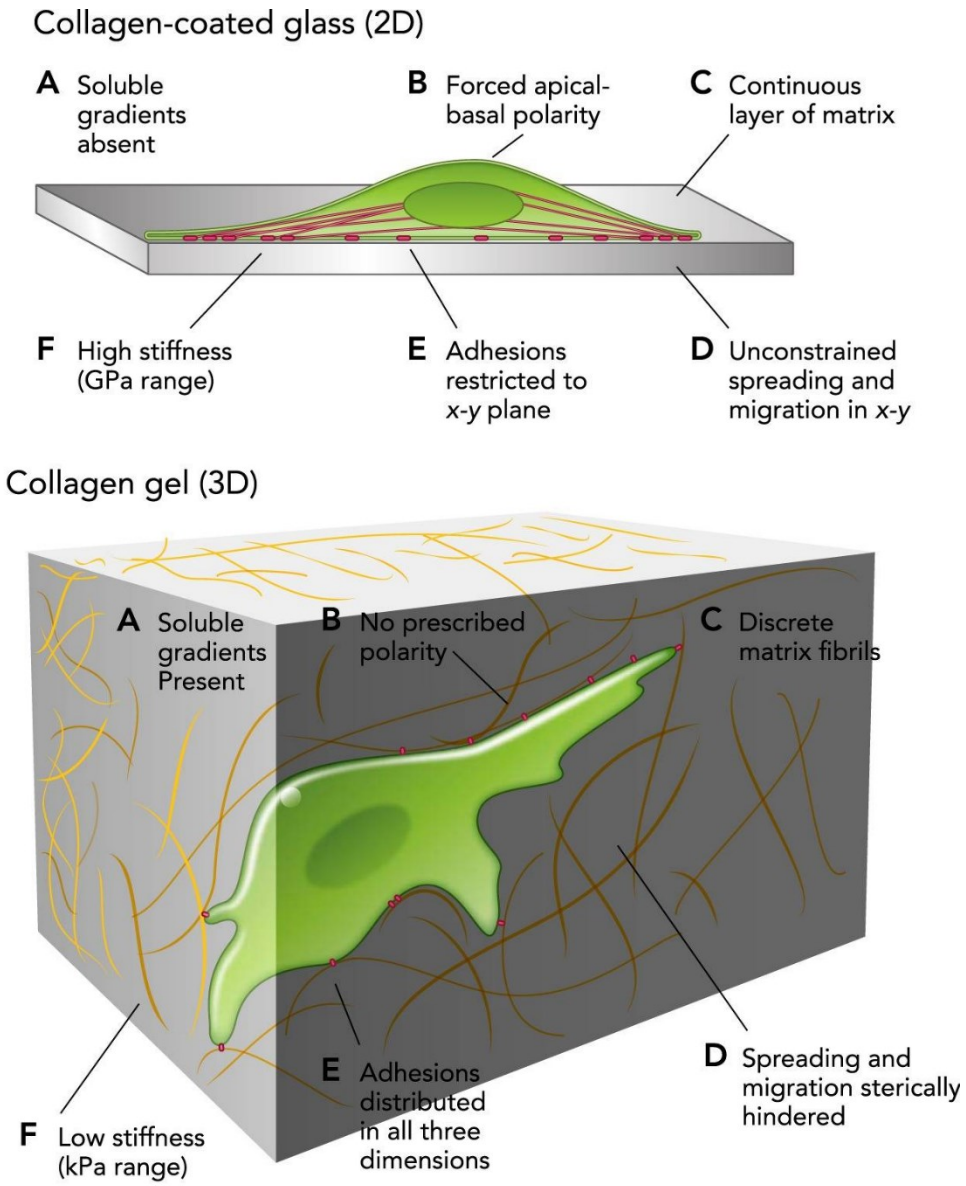

Figure 5. *Behavior of the cells in 2D and 3D microenvironments (Duval et al. 2017).*

2 Objectives and Hypothesis of the Work

The skin tissue engineering is a very quickly developing field, which is focused mainly on the construction of appropriate skin substitutes. The aim of the skin tissue engineers is to understand the molecular mechanisms of the cell interactions during wound healing and to construct a biocompatible and biodegradable skin equivalent. However, this skin equivalent has to fulfill many requirements. It has to substitute functionally the native skin, and at the same time, it has to be easily manufacturable and cost-effective. Therefore, there are still several challenges to overcome.

The objectives and hypothesis of this work can be summarized as follows:

(i) The first main objective of this work was to construct a pre-vascularized skin substitute consisting of a collagen hydrogel reinforced by a biodegradable nanofibrous membrane. This general aim was subdivided into the following specific aims:

- Comparison of the protein-coated nanofibrous membranes poly-lactic acid (PLA), poly-L-lactic acid (PLLA) or polylactic-co-glycolic acid (PLGA) with the non-coated nanofibrous membrane in terms of the skin and stem cell adhesion, morphology and growth. The behavior of normal human dermal fibroblasts (NHDFs), adipose tissue-derived stem cells (ADSCs) and human keratinocytes (hKs) was observed. The hypothesis was that the biodegradable synthetic nanofibrous membranes with fibrin or collagen nanocoatings are suitable substrates for cell growth and for the construction of bioengineered skin substitute.

- Adaptation of the structure of fibrin nanocoatings by altering the parameters in preparation protocols. The fibrin nanocoatings with or without attached fibronectin was optimized in order to enhance adhesion, proliferation and migration of NHDFs and ADSCs. The hypothesis was that the cell behavior directly depends on the structure of fibrin nanocoatings.

- Creating an optimal 3D environment for cell colonization and growth from rat tail and porcine collagen I hydrogels. The migration capability of NHDFs and ADSCs in collagen hydrogels was analyzed. The hypothesis was that the NHDFs and ADSCs are able to migrate from the substrate into the collagen hydrogel representing the dermal part of the substitute.

- Constructing a bi-layered skin substitute using collagen hydrogel reinforced by a protein-coated nanofibrous membrane containing both main skin cell types, i.e. NHDFs colonizing the hydrogel and hKs seeded on the surface of the hydrogel. NHDFs were expected to migrate into the collagen hydrogel from the membrane, while hKs were expected to create stratified layers on the surface of the hydrogel. The hypothesis was that the collagen hydrogel is a suitable substrate for the growth and migration of NHDFs as well as for the adhesion and stratification of hKs, i.e. for the formation of an artificial epidermis.

- Co-culturing the ADSCs with human umbilical vein endothelial cells (HUVECs) in the bi-layered skin construct in order to support the formation of capillary-like network. The hypothesis was that the ADSCs are able to support the spontaneous formation of the tubular structures from the embedded HUVECs and thereby they could accelerate the vascularization of collagen-based skin substitutes.

(ii) The second objective of this work was to develop temporary cellulose-based wound dressings. For this purpose, the cellulose-based materials were coated with fibrin or with charged CNFs to improve the material properties for cell attachment. The hypothesis was that the modified cellulose-based materials enhance the adhesion and proliferation of the cells by specific adsorption of cell adhesion-mediating proteins.

3 Methodology

3.1 Preparation of the Microfibrous and Nanofibrous Membranes

3.1.1 Synthetic Nanofibrous Membranes

Experiments were carried out on nanofibrous membranes made of the PLGA copolymer (ratio 85:15, Purasorb® PLG 8531; Corbion, Netherlands), PLA (Ingeo™ Biopolymer 4032D; NatureWorks, USA) and PLLA (Polyscitech, Akina Inc., USA). The nanofibrous membranes were prepared by needle-free electrospinning technology (Elmarco, Czech Republic). For details; see Bacakova *et al.* (2017), Pajorova *et al.* (2018), Bacakova and Pajorova *et al.* (2019), and Pajorova *et al.* (in preparation). The membranes were fixed in the CellCrown™ inserts (Scaffdex Ltd, Finland) and then put in the wells of 24-, 12- or 6-well plates cultivation plates (TPP Techno Plastic Products AG, Switzerland). The samples were sterilized in 70% ethanol and were rinsed in sterile deionized water.

3.1.2 Nature-Derived Cellulose Meshes

Highly pure spunlace nonwoven cotton fabric PurCotton® (Winner Industrial Park, China) was used as a non-modified cellulose mesh for nanocellulose coatings (Pajorova *et al.* 2020) and also as a prefabricated material for production of the commercially available Hcel® NaT textiles (Holzbecher Bleaching & Dyeing Plant in Zlic, Czech Republic) These Hcel® NaT textiles were prepared by carboxymethylation of the PurCotton® fabric and its conversion to a sodium salt (Bacakova *et al.* 2018b). In Bacakova *et al.* (2018b) study, two textile forms of Hcel® NaT with different structural morphologies and properties were compared, namely homogeneous H form and the porous P form. The textiles were sterilized by 25 kGy of γ-radiation or UV irradiation, were cut into 1.5x1.5 cm^2 samples and were fixed into CellCrowns™ inserts.

3.2 Preparation of the Nanocoatings on the Membranes

3.2.1 Protein Nanocoatings

The fibrin nanocoatings on the nanofibrous membranes and Hcel® NaT meshes were formed by activation of water-soluble human fibrinogen (EMD Millipore, USA) with human thrombin (Sigma-Aldrich Co, USA). The fibrin nanocoatings were utilized in the following works Bacakova *et al.* (2017, 2018b), Pajorova *et al.* (2018), Bacakova and Pajorova *et al.*

(2019), and Pajorova *et al.* (in preparation). In Bacakova *et al.* (2017), only one type of fibrin nanocoating was prepared, however in our further works, two different types of fibrin nanocoatings were prepared on the membranes. The first type of fibrin nanocoating coated the individual fibers in the membrane (referred to as "fibrin coating"). The second type of fibrin nanocoating created a fine homogeneous fibrin mesh on the surface of the membrane in addition to the coating of the individual fibers in the membrane (referred to as "fibrin mesh"). For more details; see Pajorova *et al.* (2018), Bacakova *et al.* (2018b). Briefly, in the first step, fibrinogen at a concentration of 10 μg/mL in trisaminomethane (Tris) buffer (consisting of 50 mM Tris-HCl, 100 nM NaCl, and 2.5 mM $CaCl_2$) was applied on the membrane for 1 hour. The unreacted fibrinogen was rinsed twice with pure Tris buffer. In the second step, the adsorbed fibrinogen was activated with thrombin (2.5 U/mL in Tris buffer) for 15 minutes. In Bacakova *et al.* (2017), the unreacted thrombin was washed twice with the Tris buffer. However, in Pajorova *et al.* (2018) and Bacakova *et al.* (2018b) works, this third step was slightly modified in order to prepare two types of fibrin nanocoatings. For creating the "fibrin coating" type of nanocoating, the unreacted thrombin was washed by incubating the membranes in Tris buffer for 30 minutes, while for creating the "fibrin mesh" type of nanocoating the unreacted thrombin was only aspirated without washing step. Then the fourth step was the same in all our published works. A solution of 200 μg/mL of fibrinogen in Tris buffer and 0.5 U/mL of antithrombin III (Chromogenix, Italy) in deionized water was added to the membranes for 1 hour to form a stable fibrin nanocoatings (Scheme 1).

The collagen nanocoatings were compared with fibrin nanocoatings; see Bacakova *et al.* (2017). The collagen solution (rat tail, 3.37 mg/mL; Corning Incorporated, USA) was diluted in 0.02 M acetic acid to the final concentration of 200 μg/mL. 400 μl of the solution was then applied on the pristine membranes. The samples were exposed to ammonia vapor to neutralize the pH. The unreacted collagen was washed with deionized water (Scheme 1).

To enhance the cell adhesion, we attached fibronectin (Fn) to the surface of all mentioned nanocoatings (Bacakova *et al.* 2017, 2018b; Pajorova *et al.* 2018). Human fibronectin (Roche, Switzerland) was diluted to a final concentration of 50 μg/mL in phosphate-buffered saline (PBS; Sigma-Aldrich Co., USA) and 400 μL of solution was applied on nanocoatings for 12 hours at 4°C. The membranes were rinsed with PBS.

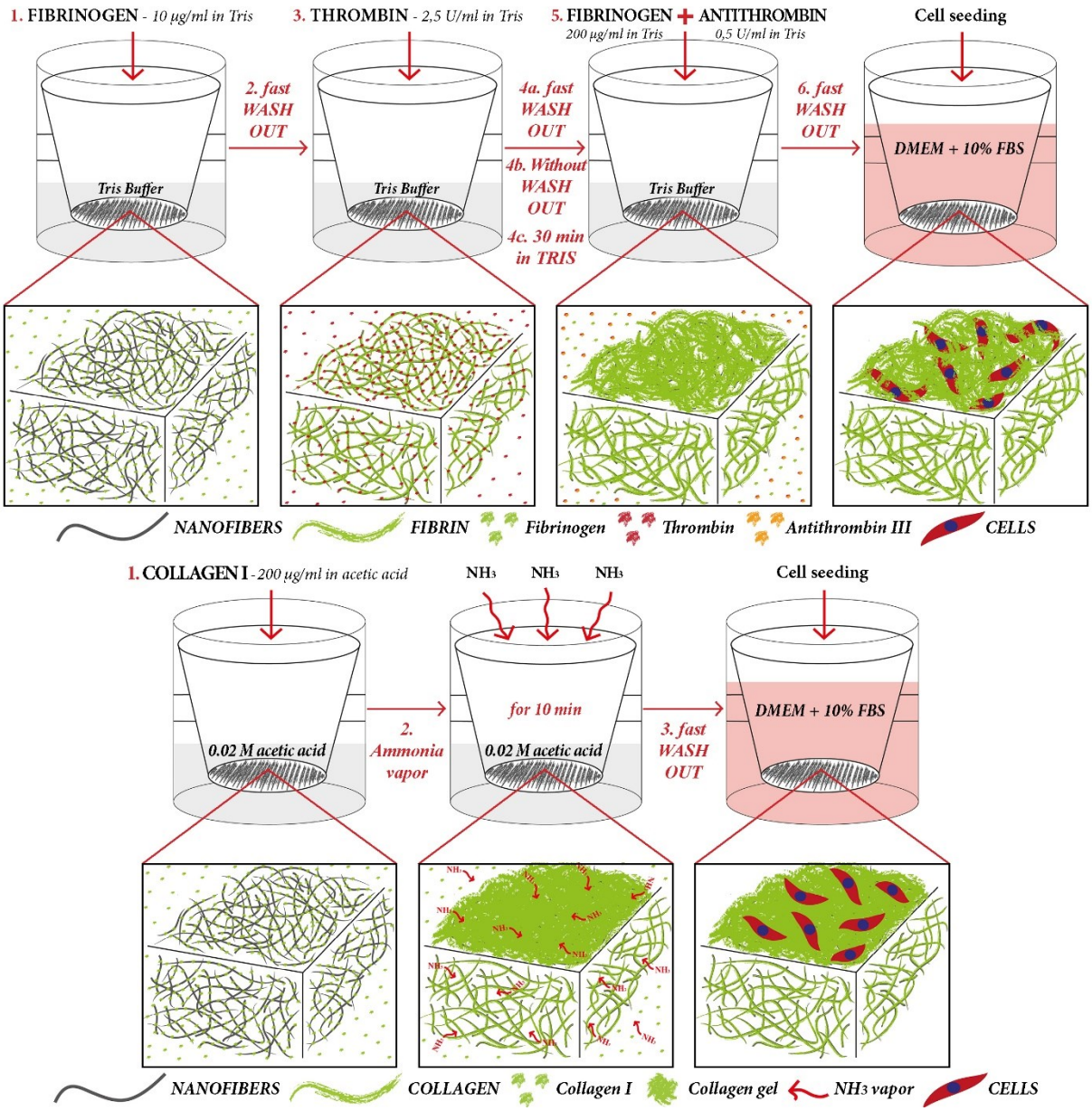

Scheme 1. *Schematic image of the preparation of fibrin and collagen nanocoatings on PLGA and PLA nanofibrous membranes.*

3.2.2 Cellulose Nanofibril Coatings

The CNFs were utilized as coatings to improve the surface properties of the cellulose meshes. The CNF materials were received from VTT Technical Research Centre (Finland). Both anionic (aCNFs) and cationic (cCNFs) grades were produced from once-dried bleached birch kraft pulp. Anionic CNFs were produced using TEMPO oxidation and cationic CNFs were prepared using EPTMAC; for more details; see Pajorova *et al.* (2020). The CNF materials were diluted to 0.15% (w/v) solution in deionized water, sonicated and centrifuged. The CNF-coated meshes were prepared using either 150 µL or 600 µL of cCNF and aCNF

supernatants (further referred to as "c150, c600, a150, a600") and by a combination of these supernatants (c+a). A pristine non-coated mesh was used as the control. The CNF-coated samples were dried (Scheme 2). The samples were sterilized using UV-C irradiation.

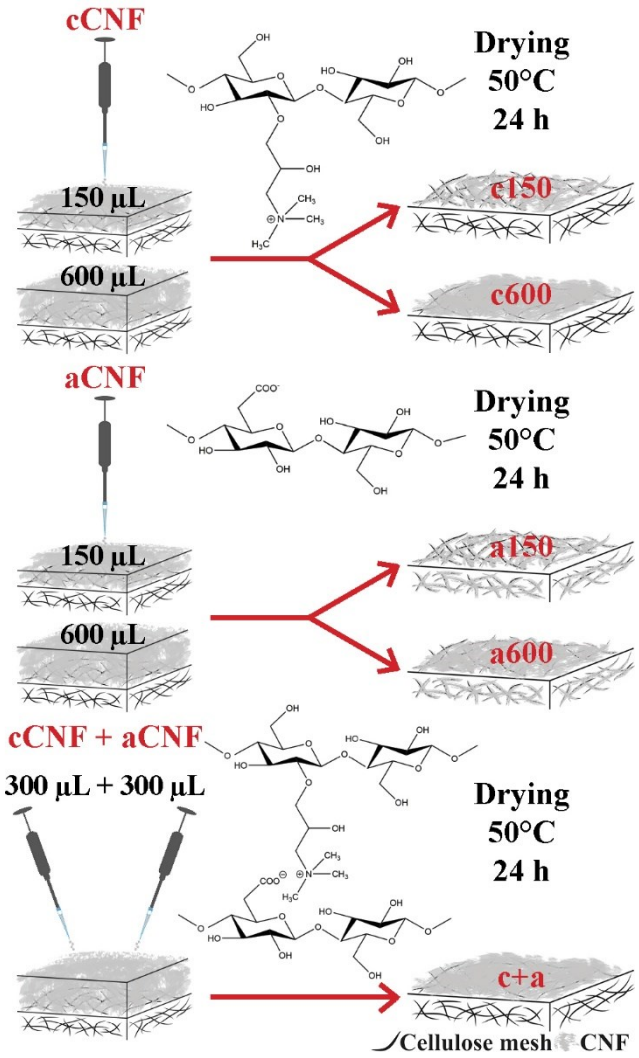

Scheme 2. *Schematic picture of the preparation of the different coating topographies on the cellulose meshes using cCNF and aCNF solutions.*

3.3 Material Characterization

3.3.1 Structure and Topography of Modified Membranes

The surface topography of the nanofibrous membranes, cellulose meshes in their non-coated state, and also with CNF coatings were studied by scanning electron microscopy (SEM). The samples were coated with gold or carbon to avoid charging during the SEM observation. The detailed setup of imaging is described in Bacakova *et al.* (2017, 2018b) and Pajorova *et al.* (2020). The thickness of the membranes was determined from SEM images of a vertical section of the membrane. The diameter of the fibers and the size of the void spaces

among the fibers were measured on the SEM images using Atlas software (Tescan, Czech Republic) or using ImageJ Fiji program. The surface roughness (Ra) of CNF coatings was measured using atomic force microscopy (AFM). The samples in the inserts were mounted into a custom holder and mapped using Olympus IX 81 (Japan) linked with JPK NanoWizard 3 AFM microscope (JPK, Germany). The roughness maps of dry samples were mapped at Hybrid acquisition mode; see Pajorova *et al.* (2020).

3.3.2 Morphology of the Protein Nanocoatings

The morphology of the protein nanocoatings and the collagen hydrogel was studied either by SEM or using immunofluorescence staining and microscopy. For SEM, the nanofibrous membranes with nanocoatings or with collagen hydrogel were fixed with 4% paraformaldehyde in piperazine-N,N′-bis(2-ethanesulfonic acid) (PIPES) buffer (Sigma-Aldrich Co., USA). The samples were dehydrated using the standard gradient of ethanol solutions, aceton and hexamethyldisilazane (HDMS; Sigma-Aldrich Co., USA). Air drying of the sample for a period was followed by coating with gold-palladium; see Bacakova and Pajorova *et al.* (2019).

For immunofluorescence staining of nanocoatings, the fibrin, collagen, and fibronectin nanocoatings were freshly prepared and incubated in Dulbecco's Modified Eagle's Medium (DMEM; Gibco, USA) under the cell culture conditions for one week. The protein-coated membranes were blocked with 1% bovine serum albumin (BSA; Sigma-Aldrich Co., USA) in PBS and then with 1% Tween (Sigma-Aldrich Co., USA) in PBS. The samples were incubated with primary antibodies against human fibrinogen (rabbit, polyclonal; Dako Denmark A/S, Denmark) or collagen I (mouse, monoclonal; Sigma-Aldrich Co., USA), or with a primary antibody against fibronectin (mouse, monoclonal; Sigma-Aldrich Co., USA). The samples with attached Fn were simultaneously stained for two proteins on the same sample, i.e. for fibrinogen+Fn and collagen+Fn. In this case, the second primary antibody against fibronectin (mouse, monoclonal; Sigma-Aldrich Co., USA) was added after rinsing the first primary antibody away. All primary antibodies were diluted in PBS in a ratio 1:200 and were incubated with samples overnight at 4°C (fibrinogen and collagen) or for 3 hours at room temperature (fibronectin). The samples were then incubated with secondary antibodies, namely goat anti-rabbit or goat anti-mouse antibodies conjugated with Alexa Fluor® 488 (both from Molecular Probes, Thermo Fisher Scientific, USA). In case of fibronectin staining, the second secondary antibody goat anti-mouse antibodies conjugated with Alexa Fluor® 633 (Molecular Probes, Thermo Fisher Scientific, USA) was used after first secondary antibody.

All secondary antibodies were diluted in PBS in a ratio 1:400 and were incubated with samples for 1 hour in dark and at room temperature. For detailed protocol; see Bacakova *et al.* (2017, 2018b), Pajorova *et al.* (2018) and Bacakova and Pajorova *et al.* (2019). The samples were scanned on a Leica TCS SPE DM2500 upright confocal microscope and on a Leica TCS SP8 confocal microscope. For image post-processing and analysis, the Fiji (ImageJ) open-source image analysis software was used.

3.3.3 Mechanical and Physico-Chemical Properties

The elasticity of the wet nanofibrous membranes with and without nanocoatings was tested using the puncture testing protocol, described in detail in Bacakova *et al.* (2017) and Pajorova *et al.* (2018). In brief, the samples were punctured with a spherical cup probe at a constant speed while the force was being recorded. The deformation of the nanofibrous membranes was evaluated in MatLab. The stiffness of collagen hydrogel disks reinforced by a nanofibrous membrane without cells was measured by compression test. The mechanical properties of the reinforced hydrogel were characterized by the Young's moduli in the linear parts of the stress-strain curves. The data were analyzed in MatLab; see Bacakova and Pajorova *et al.* (2019). Young's modulus of CNF coatings at the cell perception level was measured by AFM. The dry samples were examined for the mechanical properties at the same setup as the roughness mapping; see above. The mechanical properties of wet samples were probed at the two-time point intervals after watering in DMEM; for details; see Pajorova *et al.* (2020).

The physico-chemical properties were measured on CNF coatings. The wettability of CNF coatings was analyzed by the sessile drop method using an OCA-15 plus optical goniometer (Dataphysics Instruments GmbH, Germany). The swelling ratio of CNF coatings was measured after immersion of the sample into deionized water (dH_2O) or DMEM. The water uptake was calculated after 20 minutes and after 20 hours. The total amount of pre-adsorbed adhesion-modulating proteins on the CNF coatings was evaluated using Pierce™ BCA Protein Assay Kit (Pierce BCA Protein Assay, USA); for details; see Pajorova *et al.* (2020).

3.4 Cell Isolation, Characterization and Culture Conditions

3.4.1 Human Dermal Fibroblasts and Human Keratinocytes

The NHDFs purchased from Lonza (Switzerland) were used in all our publications; see Bacakova *et al.* (2017, 2018b), Bacakova and Pajorova *et al.* (2019) and Pajorova *et al.* (2018, 2020). The human aneuploid immortal keratinocytes of the line HaCaT purchased from Cell Lines Service (Germany) were utilized in Bacakova *et al.* (2017). The HaCaT cell line contains spontaneously transformed and immortal non-tumorigenic human epidermal keratinocytes with full epidermal differentiation capacity. NHDFs and HaCaT cell line were cultured in DMEM supplemented with 10% of fetal bovine serum (FBS; Gibco, USA) and 40 μg/mL of gentamicin (LEK, Slovenia). The primary hKs were isolated from skin of a young adult donor after informed consent at University Hospital Kralovské Vinohrady. They were used in Bacakova and Pajorova *et al.* (2019) for the construction of collagen-based 3D skin construct and for the advanced vascularized 3D ski construct (Pajorova *et al.*, in preparation). The epidermis and dermis were separated by enzymatic digestion using 0.25% trypsin or neutral protease (Dispase®, Worthington, USA). The keratinocytes were further released from the epidermis into the cell culture medium (Bacakova and Pajorova *et al.* 2019) or they were harvested in a higher yields using dynamic trypsinization according to Wang *et al.* (Wang *et al.* 2018). After centrifugation, the isolated keratinocytes were seeded either on adhered or directly with 3T3 mouse embryonic fibroblasts (Sigma-Aldrich Co., USA) that were inactivated using mitomycin C (Sigma-Aldrich Co., USA). The keratinocytes were cultivated in a mixture of the DMEM medium and Ham's Nutrient Mixture F12 medium (DMEM/F12) in a ratio of 3:1. The mixture of the media was supplemented with 10% of FBS, 10 ng/mL of EGF, 10 μg/mL of insulin, 0.4 μg/mL of hydrocortisone, 10^{-10} M of cholera toxin and 1% of antibiotic-antimycotic solution (all from Sigma-Aldrich Co., USA); further referred to as "keratinocyte growth medium" (KGM). The NHDFs were seeded in passages 2 – 6 and primary keratinocytes in passages 1 – 3 and they were cultivated at 37°C in a humidified air atmosphere with 5% CO_2.

3.4.2 Adipose Tissue-Derived Stem Cells

The ADSCs were isolated from subcutaneous adipose tissue from 15 healthy donors (26 – 53 years) after informed consent at Hospital Na Bulovce in Prague (Estes *et al.* 2010; Travnickova *et al.* 2020). The liposuctions were conducted on the thighs (n=10) or on the abdomen (n=9) using low negative pressure (-200mmHg; referred to as "low") and high

negative pressure (-700mmHg; referred to as "high") for each selected harvesting sites, and donor. The fresh lipoaspirates were washed several times with PBS, and then they were digested using type I collagenase 0.1% (w/v) (Worthington, USA) diluted in PBS with 1% (w/v) BSA. After one-hour digestion, the lipoaspirate was centrifuged, and the stromal vascular fraction (SVF) was separated from rest of the digested tissue. The SVF was washed for three times, filtrated using strainer (pore size 100 μm), and seeded into culture flasks (75 cm^2, TPP, Switzerland) in a density of 0.16 mL of the original lipoaspirate/cm^2. The isolated cells were cultured in DMEM (Gibco, USA), supplemented with 10% FBS (Gibco, USA), 40 μg/mL of gentamicin (LEK, Slovenia), and 10 ng/mL of recombinant human basic FGF2 (GenScript, USA). The primary cells in the passage 0 were frozen after they reached confluence, and the rest of them were subcultured and characterized.

The yields of isolated ADSCs were calculated on day 1 after seeding the cells in the passage 0 by counting the adhered cells from randomly taken microscopic fields. The cells were seeded in the 1st passage in 12-well tissue culture plates (TPP, Switzerland) in density of 50 000 cells/well and cultivated for 7 days, then their number, viability, diameter, and doubling time were analyzed. The number, the viability, and the diameter of trypsinized cells in each well were measured using a Vi-CELL XR Cell Viability Analyzer (Beckman Coulter). The cell population doubling time was further calculated. The cell mitochondrial activity of the isolated cells was measured also in the 1st passage by a CellTiter 96® Aqueous One Solution Cell Proliferation Assay (MTS; Promega Corporation, USA) according to the manufacturer's protocol. The MTS assay was performed in three-time point intervals (day 1, 3 and 7) on the cells seeded in 24-well tissue culture plates (TPP, Switzerland) in a density of 25 000 cells/well. The Flow Cytometry analysis was carried out in passage 2 using antibodies against specific surface cluster of differentiation (CD) markers standardized for ADSCs, i.e. CD105, CD90, CD73, CD29, and other CD molecules specific for other cell types, i.e. CD146, CD31, CD34, and CD45. The stained cells were analyzed with the Accuri C6 Flow Cytometer System (BD Biosciences, USA). The cell nuclei and CD markers were also visualized by the immunofluorescence staining and light microscopy. For more details; see Travnickova *et al.* (2020).

The behavior of "low" and "high" abdominal ADSCs isolated from one donor was compared on two different types of fibrin nanocoatings (for review see Bacakova *et al.* 2018a). The "low" abdominal ADSCs form single donor that were more positive for CD146, i.e. a marker of pericytes, than the others, were utilized for the construction of vascularized 3D skin construct (Pajorova *et al.*, in preparation). In order to decrease the variability in the

cell behavior between individual donors for tissue engineering applications, the ADSCs from 10 donors isolated from the same region (thighs or abdomen) under the same pressure ("low" or "high") were mixed in passage 1. The pooled ADSCs were characterized in passage 2 similarly as the cells from individual patients. The pooled ADSCs from thighs and from abdomen were further mixed together in passage 2 to create only "low" and "high" groups of pooled ADSCs. The growth of these two groups of pooled ADSCs were evaluated on the "fibrin mesh" type of nanocoating, and also in collagen hydrogel (unpublished data). The behavior of pooled ADSCs isolated from thighs under the "low" pressure on different CNF coatings was compared with NHDFs; see Pajorova *et al.* (2020). The ADSCs were seeded in passage 1 – 3 and they were cultivated at 37°C in a humidified air atmosphere with 5% CO_2.

3.4.3 Human Umbilical Vein Endothelial Cells

The HUVECs were purchased from Lonza (Switzerland), and they were used for preparation of pre-vascularized 3D skin construct (Pajorova *et al.*, in preparation). The cells were cultured in the endothelial cell growth medium 2 (EGM-2), which was prepared from the endothelial cell basal medium 2 (PromoCell, Germany) supplemented with 0.2 µg/mL of hydrocortisone, 22.5 µg/mL of heparin, 1 µg/mL of ascorbic acid, 5 ng/mL of EGF, 0.5 ng/mL of VEGF, 20 ng/mL of IGF-1, 10 ng/mL of FGF2 and 2% of FBS (EGM-2 supplement pack; PromoCell, Germany), and 1% of antibiotic-antimycotic solution (Sigma-Aldrich, USA).

3.5 Preparation of Collagen-Based Skin Constructs

3.5.1 Bi-Layered Skin Construct

The fibrin homogenous mesh was prepared on the PLLA membrane before the cell seeding based on our protocol published in Pajorova *et al.* (2018); see above. The non-coated and fibrin-coated membranes were seeded with NHDFs at a density 30 000 cells/sample and cultivated for 3 days in DMEM supplemented with 10% FBS and antibiotics. The collagen hydrogels were prepared on the NHDF pre-seeded membranes. The collagen hydrogels were made of the type I collagen isolated from rat tails. The tendons from the rat tails were digested in 0.1 M acetic acid and then they were ultracentrifuged. The supernatant containing the collagen was neutralized with 0.1 M sodium hydroxide and it was centrifuged. The collagen pellet was lyophilized and then it was dissolved in 0.02 M acetic acid to a concentration of 5 mg/mL. For preparing the collagen hydrogels, the final concentration of 3 mg/mL of collagen

was used. In order to neutralize the collagen stock solution (5 mg/mL), the sodium bicarbonate (Sigma-Aldrich Co., USA) in DMEM supplemented with 10% FBS and 40 µg/mL of gentamicin was added and mixed properly. A total volume of 400 µL was applied on the membranes pre-seeded with NHDFs, and it was polymerized in an incubator to reach pH around 7.4. A volume of 1.5 mL of DMEM with 10% FBS was subsequently added to the samples. For more details; see Bacakova and Pajorova *et al.* (2019).

The migration of the NHDFs into the collagen hydrogel from a non-coated membrane and from a fibrin-coated membrane was observed within 2 weeks. The collagen constructs strengthened by the fibrin-coated membrane were chosen for seeding with primary hKs. The keratinocytes were seeded after 4 days of fibroblast gel colonization at a density of 60 000 cells/sample in DMEM/KGM in a ratio of 1:1, and after 24 hours, this medium was replaced by the pure KGM. In order to stimulate the remodeling of the collagen hydrogels by the NHDFs, the 50 µg/mL of 2-phospho-L-ascorbic acid trisodium salt (AA) was added into the medium after 2 days of keratinocyte cultivation, and then the medium with AA was changed every 2 days. The behavior of both cell types in co-culture was observed for 14 days.

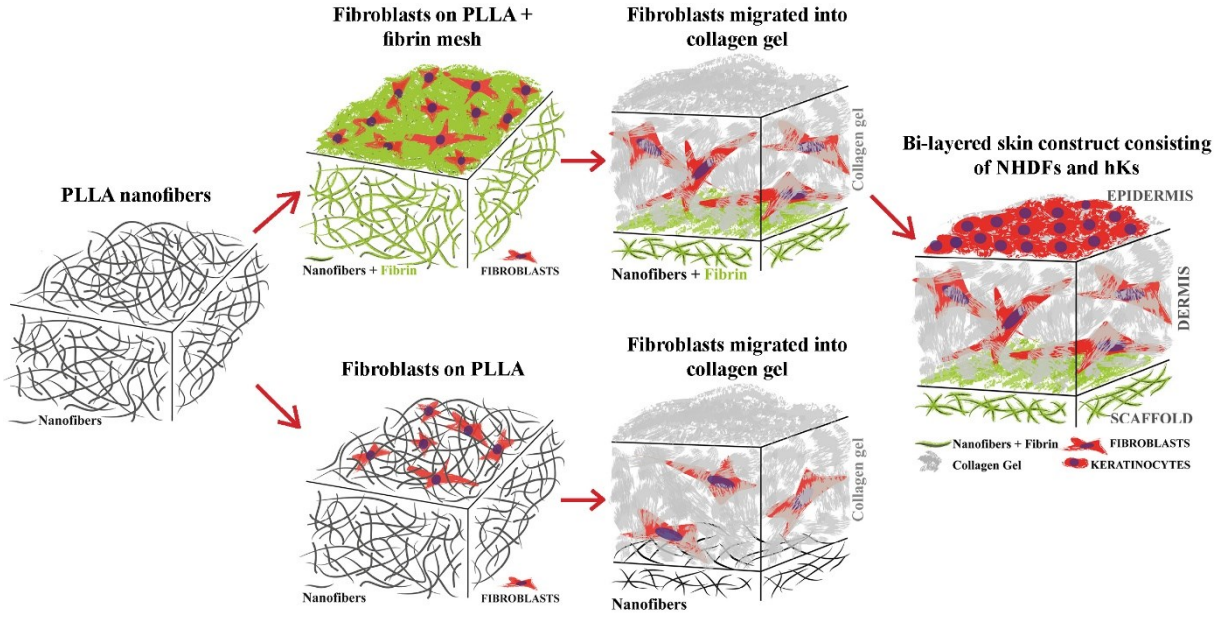

Scheme 3. *Preparation of the constructs for evaluating the migration capability of the NHDFs, consisting of collagen hydrogel reinforced with a non-coated PLLA membrane or a fibrin-coated PLLA membrane seeded with NHDFs. The construct with the fibrin coating was seeded with hKs to create a bi-layered skin construct.*

3.5.2 Bi-Layered Pre-Vascularized Skin Construct

The PLLA membranes coated by fibrin homogenous mesh were seeded with abdominal ADSCs isolated under “low” pressure that were more positive for CD146 marker then the

other ADSCs. These ADSCs were seeded at a density 30 000 cells/sample in DMEM supplemented with 10% FBS, 10 ng/mL of FGF2 and antibiotics. The collagen hydrogels were prepared on the ADSC pre-seeded membranes after 3 days of ADSC cultivation, similarly as in Bacakova and Pajorova *et al.* (2019). However, in this case the collagen I was isolated form the porcine skin and it was polymerized with and without homogeneously dispersed HUVECs. The HUVECs were added at the density of 800 000 cells/sample in the EGM-2 with all supplements described above and sodium bicarbonate into a collagen stock solution (5 mg/mL). A total volume of 500 μL of collagen I with a final concentration of 3 mg/mL was applied on the membranes pre-seeded with ADSCs. A volume of 1.5 mL of EGM-2 with all supplements was added onto the samples after polymerization. The migration of the ADSCs into the collagen hydrogels and their interactions with HUVECs were evaluated after 7 and 14 days of cultivation without keratinocytes. The primary hKs were seeded on pure collagen or on collagen with embedded HUVECs after 7 days of ADSC cultivation, after 4 days of ADSC migration, and at a density of 100 000 cells/sample in EGM-2/KGM in a ratio of 1:1. This medium was replaced after 24 hours either by pure KGM in case of pure collagen or by the fresh EGM-2/KGM in a ratio of 1:1 in case of collagen gel with HUVECs. The AA was added into the medium after 2 days of keratinocyte cultivation and then the medium with AA was changed every 2 days. Some samples were moved above the layer of the medium after 3 days of keratinocyte cultivation to stimulate the stratification of keratinocytes by the air-liquid interface. The interactions between all three cell types in the collagen construct were evaluated after 14 days as described in the next chapter. The data from these experiments will be published in upcoming article (Pajorova *et al.*, in preparation).

3.6 Characterization of the Cell Behavior

3.6.1 Cell Proliferation

The metabolic activity of the cells was measured by MTS assays (Bacakova *et al.* 2017, 2018b; Pajorova *et al.* 2018; Bacakova and Pajorova *et al.* 2019) or by the conversion of resazurin sodium salt (Sigma-Aldrich Co., USA) into water-soluble resorufin by mitochondrial enzymes (Pajorova *et al.* 2020). The principle of an MTS assay is based on conversion of the yellow tetrazolium salt into the water-soluble brown formazan salt by the activity of mitochondrial enzymes in the cells. The products of the metabolic activity of the cells were quantified by measuring the absorbance (formazan) or fluorescence (resorufin) using a spectrophotometer usually at three-time point intervals (days 1, 3, and 7). From the

metabolic activity of cells, the growth dynamics of the cells on different materials were estimated.

3.6.2 Cell Viability

The cell viability was determined using a Live/Dead viability/cytotoxicity kit (Thermo Fisher Scientific, USA) to compare the fibrin-coated and collagen-coated nanofibrous membranes; see Bacakova *et al.* (2017). The principle of this assay is based on the Calcein AM that penetrates the live cells and emits green fluorescence, while ethidium homodimer 1 penetrates the dead cells and stains them with red fluorescence. The number of the live and dead cells was assumed from florescence images.

The viability of NHDFs in extracts from the Hcel® NaT cellulose meshes was tested using the xCELLigence® real-time cell proliferation monitoring system (Roche, Switzerland). The extracts from Hcel® NaT meshes were collected after one week of their incubation in DMEM without FBS. The real-time proliferation of NHDFs in extracts was measured as the electrical impedance in 96-well E-plate View (ACEA Biosciences, USA) for several days; see Bacakova *et al.* (2018).

3.6.3 Cell Morphology

The adhesion, spreading and morphology of the cells were visualized by staining the cells with a combination of fluorescent days; see (Bacakova *et al.* 2017, 2018b; Pajorova *et al.* 2018, 2020; Bacakova and Pajorova *et al.* 2019). Texas red C_2-maleimide cell membrane dye (20 ng/mL, Thermo Fisher Scientific, USA) or phalloidin conjugated with florescent dyes, i.e. tetramethylrhodamine isothiocynate (TRITC; 5 μg/mL) or Atto 488 (0.04 nmol/mL), were used for cytoskeletal protein staining (all from Sigma-Aldrich Co., USA). Hoechst #33258 dye (5 μg/mL) or 4',6-diamidin-2-fenylindol (DAPI; 1 μg/mL; both from Sigma-Aldrich Co., USA) were used for cell nuclei. The vinculin – an important protein of focal adhesion plaques – was stained using primary antibody (mouse, monoclonal; Sigma Sigma-Aldrich Co., USA) and secondary anti-mouse antibody conjugated with Alexa Fluor® 488 (Molecular Probes, Thermo Fisher Scientific, USA) to indicate the level of the specific integrin-mediated adhesion and spreading of the cells (Pajorova *et al.* 2020). Before staining, the cells were fixed with 4% paraformaldehyde. The cells were permeabilized and the non-specific binding sites were blocked using the solution of 1% BSA diluted in 0.1% Triton X-100 and the solution of 1% Tween 20 in PBS (all Sigma-Aldrich Co., USA). Images of the cells were

acquired by epifluorescence microscope (Olympus, Japan), by the Leica TCS SPE DM2500 upright confocal microscope or by Dragonfly 503 (Andor, UK) spinning disk confocal system mounted on inverted microscope Leica DMi8 (Leica, Germany). The morphology of the cells on the CNF coatings was further visualized using SEM (Pajorova *et al.* 2020). The dehydrated samples were coated with gold to avoid the charging of the samples and scanned using ULTRAplus SEM (Carl Zeiss, Germany).

3.6.4 ECM Synthesis by the Cells

The extracellular collagen I and fibronectin production by the cells was evaluated by immunofluorescence staining and the messenger RNA (mRNA) expression of ECM proteins was measured by real-time polymerase chain reaction (PCR) on days 4, 7, and 14 after cell seeding; see Pajorova *et al.* (2018). For the staining, the native cells on the polymer membranes were incubated with primary antibody against collagen I or against fibronectin (both from mouse; Sigma-Aldrich Co., USA) to visualize only the extracellular proteins that were produced by cells. The cells were fixed with 2% paraformaldehyde after incubation with primary antibody. The samples were blocked using 1% FBS and then the secondary anti-mouse antibody conjugated with Alexa Fluor® 488 was incubated with samples. The cell nuclei were stained with Hoechst #33342 (Sigma-Aldrich Co., USA), which penetrates through the non-permeabilized cell membrane. Images were taken using a Leica TCS SPE DM2500 upright confocal microscope.

In order to investigate the relative mRNA expression of ECM proteins, the total RNA was isolated using the Total RNA Purification Micro Kit (Norgen Biotek, Canada). The reverse transcription was performed by the Omniscript Reverse Transcription Kit (Qiagen, Germany) with random hexamers as primers (New England Biolabs, Inc, USA). Both kits were used according to the manufacturer's protocol. The level mRNA expression of target genes was quantified using 5×HOT FIREPol Probe qPCR Mix Plus (ROX; Solis BioDyne, Estonia) with TaqMan Gene Expression Assays (Thermo Fisher Scientific), labeled with FAM reporter dye specific to human collagen I or specific to human fibronectin. The β-actin (ACTB) was used as a reference gene. The relative gene expression level was determined by the Viia™ 7 Real-time PCR System (Applied Biosystems™; Thermo Fisher Scientific), and it was calculated as $2^{-\Delta Ct}$ from cycle threshold (Ct) values of two independent samples for each experimental group and time interval.

3.6.5 Cell Migration into the Hydrogel

The migration of the NHDFs from the membrane into the collagen hydrogel was evaluated in four-time point intervals (day 1, 3, 7 and 14) by the Leica TCS SPE DM2500 confocal microscope and also by MTS assay after separating the hydrogels from the membranes; see Bacakova and Pajorova *et al.* (2019). The cells were stained with phalloidin conjugated with TRITC fluorescent dye (5 μg/mL) and Hoechst #33258 (5 μg/mL). The maximal depth into which the cells were able to migrate from the non-coated or fibrin-coated membranes was observed by Leica TCS SPE software on 3 parallel samples. The MTS assay was carried out on 4 parallel samples, i.e. separated hydrogels and their corresponding non-coated or fibrin-coated membranes.

The shrinkage of the collagen hydrogels caused by the cell traction was also evaluated also in four-time point intervals after the hydrogels were prepared. The contours of the hydrogels sitting on the microscope glass were marked with several points at the edge of the hydrogel and the circle diameters were measured. The shrinkage of the 4 parallel hydrogels with cells was compared with the freshly prepared hydrogels and with the hydrogels cultivated without the cells for 14 days; see Bacakova and Pajorova *et al.* (2019).

3.6.6 Stratification of Human Keratinocytes

In order to visualize the specific CKs in the keratinocyte cytoskeleton, the immunofluorescence staining of CK14, CK5 and CK10 was performed. The primary antibodies to human CK14 (mouse, monoclonal; Abcam, UK) and to human CK5 (rabbit, monoclonal; Abcam, UK, or mouse, monoclonal; Invitrogen, Thermo Fisher Scientific, USA) were utilized for the staining of the basal keratinocytes in the lower layers of forming epidermis. The primary antibody to human CK10 (rabbit or mouse, monoclonal; both from Abcam, UK) was used for the staining of the differentiated keratinocytes in the upper layers of stratified epidermis. All primary antibodies were diluted in PBS or in a blocking solution (1% BSA and 0.1%Tween 20 in PBS) in a ratio 1:200 and incubated with samples for 1 hour in 37°C or overnight in 4°C. The secondary antibodies, namely anti-rabbit or anti-mouse antibodies conjugated either with Alexa Fluor® 488 or with Alexa Fluor® 546 (Molecular Probes, Thermo Fisher Scientific, USA) were used according to the combinations of the primary antibodies. All secondary antibodies were diluted in PBS or in the blocking solution in a ratio 1:400, and were incubated with samples for 1 hour in dark and in room temperature. The images were acquired by the Leica TCS SPE DM2500 upright confocal microscope or by

the Dragonfly 503 (Andor, UK) spinning disk confocal system mounted on inverted microscope Leica DMi8 (Leica, Germany).

The special 3D-printed air-liquid system was developed for the differentiation and stratification of the primary hKs on the collagen surface of pre-vascularized 3D skin models in *in vitro* conditions. The inserts are fitted into the 6-well plate (TPP, Switzerland) and their size is corresponding to the commercial CellCrowns™ (Scaffdex Ltd, Finland) fitted to the 24-well plate (TPP, Switzerland). The position of the inserts, i.e. the distance from the bottom of the 6-well plate, is variable due to the adjustable holder. Approximately three times higher volume (i.e. 5 mL) of the media can be used in comparison with the volume that can be filled into 24-well plates (only 1.5 mL). This enables the cell growing for longer time without changing the media. The most upper position that is the air-liquid position allows adding the volume of 5 mL without complete immersion of the keratinocytes under the media (Scheme 4; Pajorova *et al.*, in preparation).

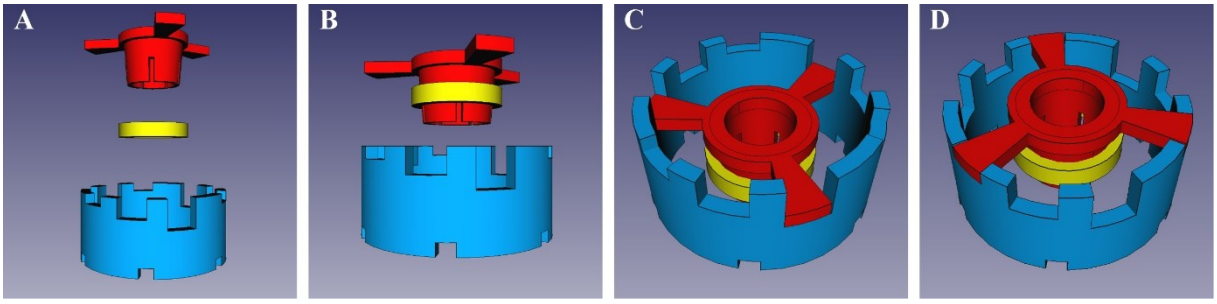

Scheme 4. *A 3D-printed model of the air-liquid insert for all types of the membranes. Separated insert (red), fixing ring (yellow) and holder (blue) (**A**), fixation of the membrane on the insert with ring (**B**), liquid position (**C**) and air-liquid position (**D**).*

3.6.7 Capillary-Like Network Formation

The ADSCs and HUVECs were co-cultured in 3D collagen hydrogels for 14 days to initiate the capillary-like network formation in vascularized 3D skin models. The collagen hydrogels were separated from the underlying membranes before the staining. The specific CD31 marker of endothelial cells was stained using primary and secondary antibodies after the fixation with 4% paraformaldehyde, permeabilization and blocking as is described above. The primary antibody to human CD31 (mouse, monoclonal; Abcam, United Kingdom) was diluted in the blocking solution (1% BSA and 0.1%Tween 20 in PBS) in a ratio 1:200, and was incubated with samples for 1 hour in 37°C. The secondary anti-mouse antibodies conjugated either with Alexa Fluor® 633 (Molecular Probes, Thermo Fisher Scientific, USA) was diluted in the blocking solution in a ratio 1:400, and was incubated with samples for 1

hour in dark and in room temperature. The actin filaments in the cells were stained with phalloidin conjugated with Atto 488 florescent dye (0.04 nmol/mL) and the cell nuclei by DAPI (1 μg/mL). The images were acquired by the Dragonfly 503 (Andor, UK) spinning disk confocal system mounted on inverted microscope Leica DMi8 (Leica, Germany) (Pajorova *et al.*, in preparation).

3.6.8 Protein-Mediated Cell Adhesion on CNF Coatings

The dependence of the cell adhesion on the composition of the pre-adsorbed serum-derived proteins was evaluated in cCNF coatings; see Pajorova *et al.* (2020). The treated group of cCNF coatings was pre-adsorbed with proteins for two hours before cell seeding, while the cCNF coatings in control group was seeded with cells and proteins simultaneously. The adhered NHDFs and ADSCs were stained and visually compared using confocal microscopy. The speed of adhesion of NHDFs and ADSCs was evaluated on cCNF coating by fluorescence live cell imaging (Nikon TiE microscope equipped with a CARVII spinning disk confocal system). Both cell types, stained by different fluorescent dyes (cell trackers), were seeded simultaneously on a single sample. The staining procedure was done according to the manufacturer's protocol before cell seeding. Equal numbers of the stained NHDFs and ADSCs were mixed in DMEM supplemented with 10% FBS and seeded directly on the cCNF-coated glass coverslip. The initial adhesion and spreading of the cells in co-culture was recorded for 18 hours. For more details; see Pajorova *et al.* (2020).

3.7 Statistical Analysis

The statistical significance of the non-Gaussian distributed data was evaluated using the nonparametric analysis of variance (Kruskal-Wallis), with Mann-Whitney U test or Tukey's *post hoc* test for pairwise comparison; see Bacakova and Pajorova *et al.* (2019) and Pajorova *et al.* (2020). The normal distributed data were evaluated using parametric analysis of variance (ANOVA) with Student-Newman-Keuls test or Tukey's *post hoc* test for pairwise comparison; see (Bacakova *et al.* 2017, 2018b; Pajorova *et al.* 2018, 2020; Bacakova and Pajorova *et al.* 2019). Values of $p \leq 0.05$ were considered statistically significant.

4 Results

4.1 Single-Layered Skin Constructs Based on Protein-Coated Nanofibers

(i) Bacakova M., Pajorova J., Stranska D., Hadraba D., Lopot F., Riedel T., Brynda E., Zaloudkova M, Bacakova L. ***Protein nanocoatings on synthetic polymeric nanofibrous membranes designed as carriers for skin cells.*** *Int J Nanomedicine 2017; 12:1143-1160.*

(ii) Pajorova J., Bacakova M., Musilkova J., Broz A., Hadraba D., Lopot F., Bacakova L.* ***Morphology of a fibrin nanocoating influences dermal fibroblast behavior.*** *Int J Nanomedicine 2018; 13:3367-3380.*

Author's contribution: I prepared and improved the nanocoatings and I cultured the cells on them. I participated on planning and realization of all cell related analysis and on writing the manuscripts. *I am the corresponding author of the manuscript.

Both studies follow up on the work of Bacakova *et al.*, in which the fibrin nanocoating on biodegradable synthetic nanofibrous membrane considerably enhanced the adhesion, growth and ECM protein synthesis of dermal fibroblasts (Bacakova *et al.* 2016). In the following work, we compared fibrin nanocoating that was described in Bacakova *et al.* (2016) with collagen nanocoating as a potential substrate for growth of fibroblasts and keratinocytes (Bacakova *et al.* 2017). Furthermore, the preparation of the fibrin nanocoating described in Bacakova *et al.* (2016, 2017) was improved in our next study (Pajorova *et al.* 2018).

In Bacakova *et al.* (2017) work, we focused on the comparison of fibrin and collagen nanocoatings on two different synthetic nanofibrous membranes, i.e. PLA and PLGA polymers. In the first part of this work, the structure and mechanical properties of protein-coated membranes were evaluated using SEM (Fig. 6A), immunofluorescence staining of protein nanocoatings (Fig. 6B) and mechanical puncture testing. Fibers of both PLA and PLGA membranes were randomly oriented and mostly straight. The fiber diameters ranged from tens to thousands nm which corresponded to submicron and micron scale rather than nanoscale (Fig. 6A). Nevertheless, according to the literature, these fibers are usually reffered to as nanofibers. Mechanical puncture testing revealed that the PLGA membranes reached significantly lower ultimate strength than the PLA membranes. Fibrin nanocoatings caused an upward trend in ultimate strength of the membranes, while collagen coatings remained its mechanical properties unchanged or even slightly more brittle.

We further described the structure and stability of the protein nanocoatings on the PLA and PLGA membranes. Fibrin coated individual nanofibers in the membrane and formed a non-homogeneous nanofibrous mesh on the surface of the membrane. Collagen also coated most of the fibers in the membranes and randomly covered the surface with a soft gel. Fibronectin formed an additional nanofibrous mesh that was bound on the fibrin mesh or on the collagen gel (Fig. 6B). Moreover, the structure of protein nanocoatings remained almost unchanged after 7 days in cell culture conditions without the cells.

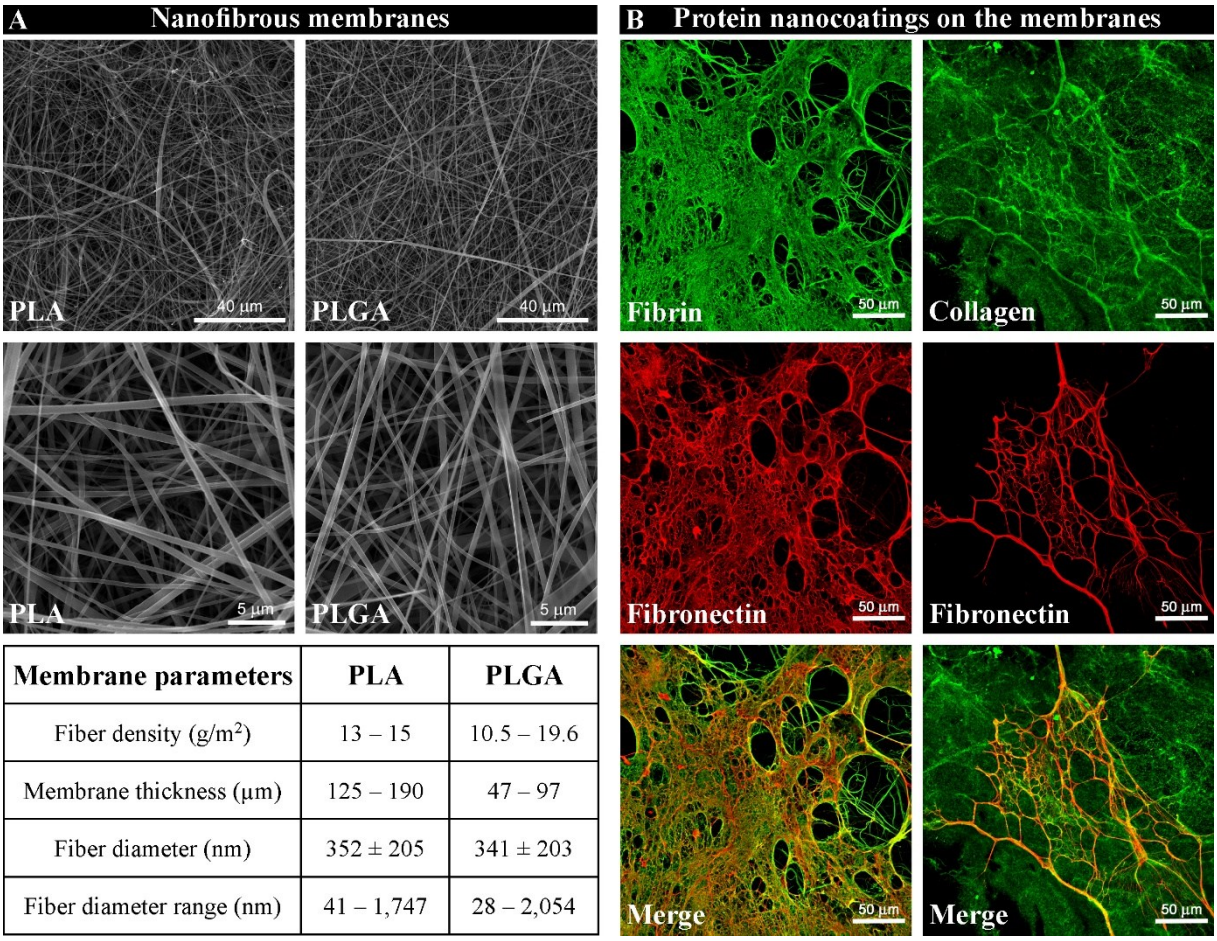

Membrane parameters	PLA	PLGA
Fiber density (g/m^2)	13 – 15	10.5 – 19.6
Membrane thickness (µm)	125 – 190	47 – 97
Fiber diameter (nm)	352 ± 205	341 ± 203
Fiber diameter range (nm)	41 – 1,747	28 – 2,054

Figure 6. *Structure of non-coated PLA and PLGA membranes (**A**) and protein nanocoatings on PLGA membrane (**B**).* Notes: Quanta 450 scanning electron microscope (2,000× and 10,000×). Fiber diameter: mean±SD from 12 SEM images (**A**). Nanocoatings were visualized by immunofluorescence using Alexa 488 (fibrin, collagen; green) or Alexa 633 (fibronectin; red). Leica TCS SPE DM2500 confocal microscope, obj. 40× (**B**).

In the second part of this work, we observed the remodeling of protein nanocoatings by the NHDFs (Fig. 7A, C) and HaCaT keratinocytes (Fig. 7B, D) during their adhesion and growth on these protein nanocoatings. We demonstrated that the structure of nanocoatings can be reorganized by both cell types during their cultivation. NHDFs penetrated and gradually degraded the fibrin nanocoatings, while they were not able to degrade the collagen coatings to

such extent. The structure of fibronectin mesh was altered faster on the fibrin than on the collagen nanocoatings. In addition, the fibrin nanocoatings apparently enhanced the production and deposition of fibronectin by NHDFs (Fig. 7C). HaCaT keratinocytes stacked on the surface of the protein nanocoatings. The fibrin mesh and fibronectin on fibrin were pulled down and degraded by keratinocytes, while the structure of collagen itself and the fibronectin mesh on collagen were resistant against traction forces generated by keratinocytes (Fig. 7D).

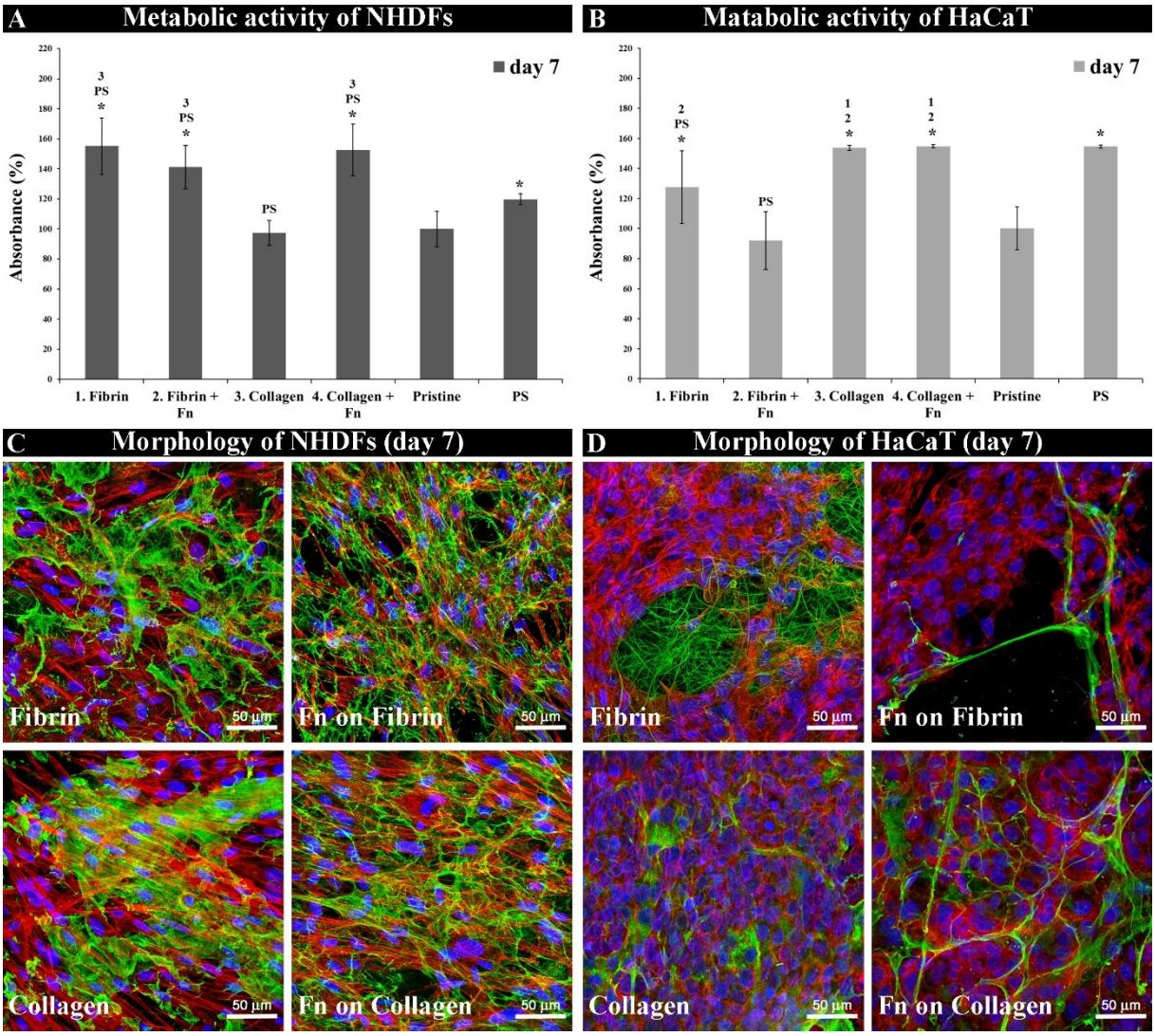

Figure 7. *Metabolic activity and morphology of NHDFs (**A, C**) and HaCaT keratinocytes (**B, D**) on PLGA membranes with protein nanocoatings after 7 days of cultivation.* Notes: The cell metabolic activity (MTS assay) on non-coated and protein-coated PLGA membranes. Polystyrene (PS) was used as control material. Arithmetic mean±SD from 12 measurements. Statistical significance ($p \leq 0.05$; ANOVA, Student-Newman-Keuls) is displayed above each experimental group, indicated by the number of the group or by (*) representing pristine (**A, B**). Fibrin and collagen nanocoatings (+Fn) were visualized by immunofluorescence (Alexa 488; green), F-actin in the cells (phalloidin-TRITC; red), and the cell nuclei (Hoechst #33258; blue). Leica TCS SPE DM2500 confocal microscope, obj. 40× (**C, D**).

We further evaluated the differences in the adhesion, morphology and proliferation of the cells among the various types of samples and cells. The cell proliferation was estimated by measuring cell mitochondrial metabolic activity, the morphology by the immunofluorescence staining and the viability by the Live/Dead assay at three time point intervals. In general, the protein nanocoatings enhanced the cell growth more than the non-coated (pristine) membranes (Fig. 7A, B). The fibrin nanocoating accelerated the attachment, spreading and growth of NHDFs (Fig. 7A, C), while the collagen nanocoating positively influenced the behavior of HaCaT keratinocytes (Fig. 7B, D). The keratinocytes formed larger cell clusters (islands) and they reached confluence after 7 days of cultivation on the collagen nanocoating. NHDFs were in their typical spindle-like morphology on the fibrin nanocoatings, and they were completely confluent after one week. The additionally attached fibronectin to the protein nanocoatings further enhanced the adhesion, spreading and proliferation of both cell types (see images labeled Fn in Fig. 7). The viability of both cell types was almost 100% on both coated and non-coated membranes. The low number of attached cells on non-coated (pristine) membranes did not affect their viability. We detected only negligible differences in cell behavior between PLA and PLGA nanofibers with the protein nanocoatings.

In the article Pajorova *et al.* (2018), we optimized the protocol for fibrin nanocoating preparation that was described earlier in Bacakova *et al.* (2016, 2017) in order to regulate the cell attachment and growth on PLA membranes. In the first part of this study, we clarified the dependence of the fibrin coating structure on the fibrin coating preparation (Fig. 8). We observed that the amount of the unreacted thrombin affected the final formation of fibrin nanocoatings, therefore the structure of fibrin can be regulated by the wash out of the unreacted thrombin. In accordance with the protocol, the fibrin either covered only individual fibers in the PLA membrane (referred to as “F coating”; Fig. 8) or covered individual fibers and in addition formed a fine homogeneous nanofibrous mesh on the whole surface of the membrane (referred to as “F mesh”; Fig. 8). In our previous studies, the fibrin mesh was only on certain parts of the PLA surface (Bacakova *et al.* 2016, 2017). Fibronectin (Fig. 8A; red) was adsorbed predominantly on the top of the fibrin mesh (Fig. 8A; green) and formed an additional nanofibrous mesh (see Fn on “F mesh” in Fig. 8C). We further detected only a minor effect of these two types of fibrin coatings on the mechanical properties of the PLA membrane. However, there was an evident trend towards increasing resistance against mechanical loading for the “F mesh” type of nanocoatings.

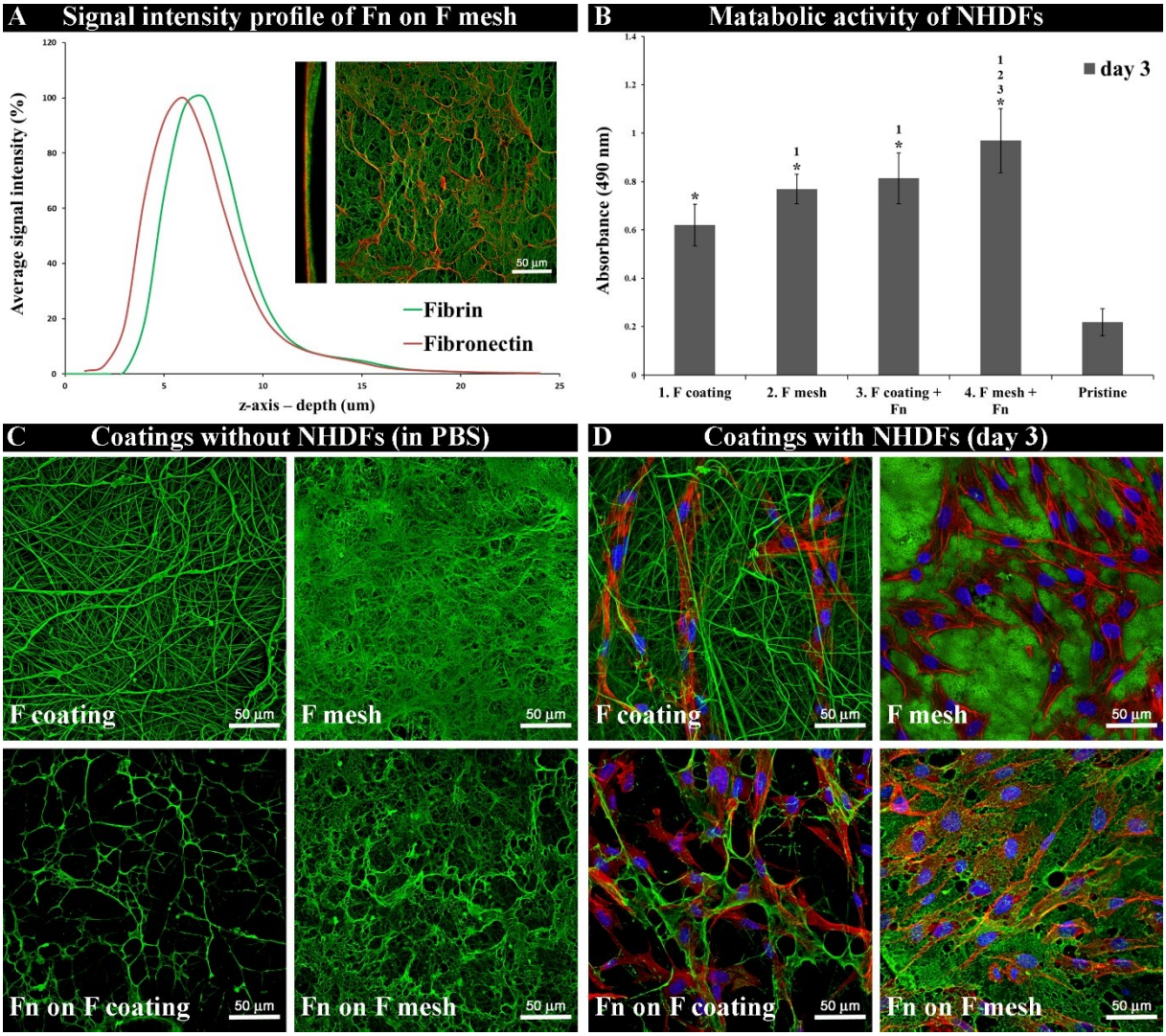

Figure 8. *The signal intensity profile of fibronectin adsorbed on fibrin (**A**), immunofluorescence staining of two different types of fibrin nanocoatings on PLA membrane without cells (**C**), the metabolic activity (**B**) and morphology (**D**) of NHDFs on these fibrin nanocoatings after 3 days of cultivation.* Notes: The membrane with the fibrin nanocoating covering only individual fibers ("F coating"), with fibrin covering individual fibers and forming a mesh on the surface of the membrane ("F mesh"), and fibronectin adsorbed on fibrin (+Fn). A non-coated membrane (pristine) was used as a control material. Maximum intensity projection of Fn on "F mesh" (**A**) – front view and side image. The function plot (**A**) represents the average image plane intensity in a given color channel versus the z-axis (depth) of a confocal z-stack image. Mitochondrial activity (**B**) was measured by MTS assay. Arithmetic mean±SD from 9 measurements. Statistical significance ($p \leq 0.05$; ANOVA, Tukey's test) is displayed above each experimental group, indicated by the number of the group or by (*) representing pristine. Fibrin and fibronectin nanocoatings were visualized by immunofluorescence (Alexa 488; green or Alexa 633; red), F-actin in the cells (phalloidin-TRITC; red), and the cell nuclei (Hoechst #33258; blue). Leica TCS SPE DM2500 confocal microscope, obj. 40× (**A, C, D**).

In the cell-related part of this work, we evaluated the behavior of NHDFs on these two types of fibrin nanocoatings. The morphology of the cells was visualized by staining, and the metabolic activity was measured by MTS assay (Fig. 8 C, D). The expression and synthesis of ECM proteins by NHDFs were detected by real-time PCR and by immunofluorescence

staining of extracellular proteins deposited on the membranes (Fig. 9). Our results showed that the structure of fibrin nanocoating markedly influenced the behavior of NHDFs. The first type of fibrin nanocoating – referred to as "F coating" – supported the elongation of fibroblasts into their typical spindle-like morphology, while the second type of fibrin nanocoating – referred to as "F mesh" – increased the spreading of attached cells into polygonal-like shape (Fig. 8D). The number of adhered cells on "F mesh" nanocoating was significantly higher than the number of cells attached to the "F coating", which consequently accelerated their proliferation on "F mesh" nanocoatings. This was further enhanced by the adsorption of fibronectin on fibrin (see Fn in Fig. 8C, D). After 3 days of cultivation, there were several cells in mitosis present on the membranes with "F mesh" with or without attached Fn, and the cells remained mostly in their polygon-like shape (Fig. 8D). However, after one week of cell cultivation, both fibrin and fibronectin nanocoatings were degraded by NHDFs and replaced by their own ECM proteins (Fig. 9). The cells reached their typical elongated morphology and started to penetrate into the membrane. NHDFs remained round and poorly adhered on the control non-coated membranes for the whole seven days.The dynamics of the replacement of the fibrin nanocoatings by the synthetized ECM proteins were determined by the measurement of relative expression of collagen I and fibronectin in NHDFs. We detected significant increase in the expression of both ECM proteins in case of "F mesh" than of "F coating" type of nanocoatings (Fig. 9A, B). Similarly to the cell adhesion and growth, the rate of the protein replacement was also amplified by the adsorbed fibronectin. Furthermore, these results also correlated with the immunofluorescence microscopy images, in which the deposition of collagen I and fibronectin nanofibers was visualized (Fig. 9C, D). There was clearly visible a difference between the production of extracellular collagen I and fibronectin on PLA membranes with "F mesh" and with "F coating". In accordance with previously described results by Bacakova *et al.* (2016), the positive effect of the nanocoatings on the protein synthesis was evaluated during the continual addition of the AA into the media. This enabled the detection of the extracellular collagen I in its folded triple-helical structure already on day 4 after cell seeding. After one week, the collagen I and fibronectin nanofibers were well-developed, and covered almost the entire surface of the cell monolayer (Fig. 9C, D).

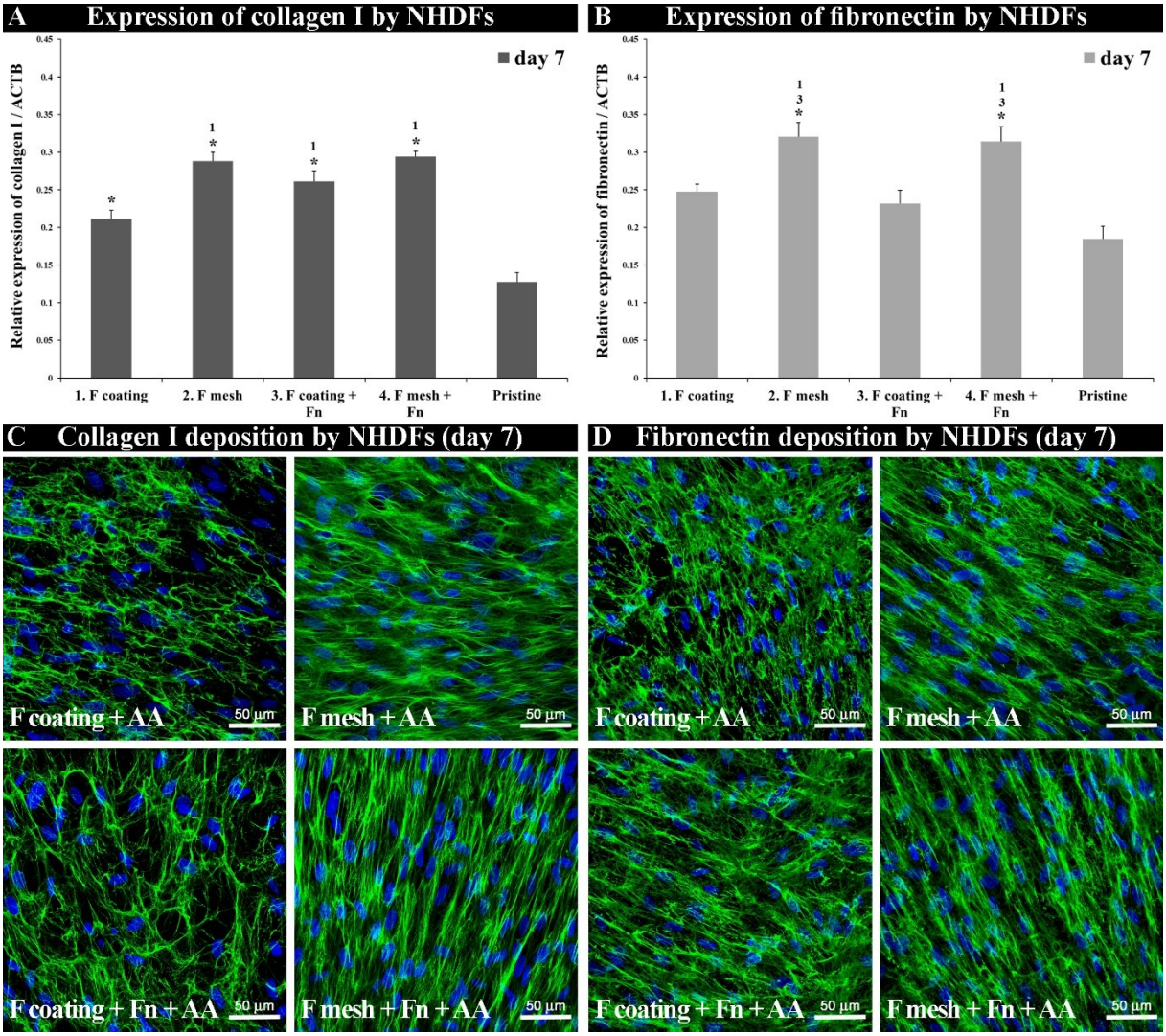

Figure 9. *Relative expression and immunofluorescence staining of extracellular collagen I (**A, C**) and fibronectin (**B, D**) produced by NHDFs on fibrin-coated PLA membranes days 7 after cell seeding.* Notes: The membrane with the fibrin nanocoating covering only individual fibers ("F coating"), with fibrin covering individual fibers and forming a mesh on the surface of the membrane ("F mesh"), and fibronectin adsorbed on fibrin (+Fn). A non-coated membrane (pristine) was used as a control material. The cells were cultivated in the standard cell culture medium with ascorbic acid (AA). The expression was measured by real-time PCR (**A, B**). ACTB was used as a reference gene. The arithmetic mean±SD was calculated from 10 measurements. Statistical significance ($p \leq 0.05$; ANOVA, Tukey's test) is displayed above each experimental group, indicated by the number of the group or by (*) representing pristine. Extracellular proteins were visualized by immunofluorescence (Alexa 488; green) and the cell nuclei (Hoechst #33342; blue). Leica TCS SPE DM2500 confocal microscope, magnification 40× (**C, D**).

4.2 Bi-Layered Skin Constructs Based on Collagen Gel and Nanofibers

(i) Bacakova M.# and Pajorova J.#, Broz A., Hadraba D., Lopot F., Zavadakova A., Vistejnova L, Beno M., Kostic I., Jencova V., Bacakova L. ***A two-layer skin construct consisting of a collagen hydrogel reinforced by a fibrin-coated polylactide nanofibrous membrane.*** *Int J Nanomedicine 2019; 14:5033-5050. # contributed equally*

(ii) Travnickova M., Pajorova J., Zarubova J., Krocilova N, Molitor M., Bacakova L. ***The influence of negative pressure and of the harvesting site on the characteristics of human adipose tissue-derived stromal cells from lipoaspirates.*** *Stem Cells Int 2020; 2020:1016231.*

(iii) Bacakova L., Zarubova J., Travnickova M., Musilkova J., Pajorova J., Slepicka P., Kasalkova N., Svorcik V., Kolska Z., Motarjemi H., Martin Molitor M. ***Stem cells: their source, potency and use in regenerative therapies with focus on adipose-derived stem cells - a review.*** *Biotechnol Adv 2018; 36(4):1111-1126.*

(iv) Pajorova J., Blanquer A., Broz A., Travnickova M., Matejka R., Suca H., Supova M., Bacakova L. ***Pre-vascularized bi-layered skin construct based on collagen hydrogel reinforced by fibrin-coated nanofibrous membrane seeded with adipose-derived stem cells.*** *Manuscript in preparation.*

Author's contribution: I introduced a method of 3D cell cultivation based on collagen hydrogels. I participated on the extraction of collagen from rat tails; isolation of adipose-derived stem cells from lipoaspirate; and isolation of human keratinocytes and fibroblasts from human skin grafts. I participated on their characterization and cultivation. I introduced a method of protein dehydration before the scanning on SEM. I contributed to the planning and realization of all cell related analysis and I participated on writing the manuscripts.

All these studies partially contributed to the construction of a pre-vascularized bi-layered skin construct. We utilized the knowledge from our previous works (Bacakova *et al.* 2017; Pajorova *et al.* 2018) that clarified the behavior of NHDFs and keratinocytes on fibrin and collagen coatings and we prepared the bi-layer construct consisting of both cell types (Bacakova and Pajorova *et al.* 2019). The NHDFs were migrated from the fibrin-coated PLLA membrane into the collagen hydrogel that was subsequently seeded with hKs. This skin construct consisting of the collagen hydrogel reinforced by a fibrin-coated PLLA membrane was further improved by naturally forming capillary-like network (Pajorova *et al.*, in preparation). For this purpose, the NHDFs were replaced by the ADSCs, which were isolated

from the lipoaspirate of human donors (Travnickova *et al.* 2020; Bacakova *et al.* 2018a) and HUVECs were embedded into the collagen hydrogel.

In the first part of Bacakova and Pajorova *et al.* (2019) work, we compared the ability of NHDFs to migrate into the collagen hydrogel from a non-coated membrane and from a fibrin-coated PLLA membrane during two weeks of cultivation (see day 3 and 7 after collagen preparation, i.e. days 6 and 10 after cell seeding, Fig. 10). The hydrogel was prepared after three days of NHDF cultivation and the ability of cells to migrate into the hydrogel was evaluated by indirect measurement of their metabolic activity in four time point intervals. We separately analyzed the metabolic activity of the NHDFs migrating into the collagen hydrogel (referred to as "Gel") and the NHDFs adhered on the membrane beneath the hydrogel (referred to as "PLLA beneath gel"). We measured also the metabolic activity of the NHDFs adhered on the control membranes without the collagen hydrogel (referred to as "PLLA"). There was detected a significant difference between metabolic activity of NHDFs on non-coated and fibrin-coated membranes beneath the gels on day 3 and 7 after the gel preparation (see second pair of columns in Fig. 10A, B), while in case of the control membranes without the gels it was statistically significant only on day 1. Moreover, the fibrin coating also enhanced the NHDF migration from the membrane into the hydrogel and proliferation of these cells, with statistical significance in all time point intervals (see third pair of columns in Fig. 10A, B). Moreover, the results were confirmed by a visualization of the cell morphology using confocal microscopy. We observed that the cells on fibrin-coated PLLA membrane had formed an almost confluent layer before the hydrogel was applied on them. Therefore, the cells were able to migrate into the collagen hydrogel immediately after collagen polymerization. The cells on the non-coated membrane started migrating later. In accordance with our previous studies, the fibrin mesh supported the attachment of cells and their growth, which led to an increase of their migrating capability in all time point intervals (Fig. 10C, D). The depth into which the cells were able to migrate was also influenced by fibrin coating, with statistically significant difference on day 3 after the collagen polymerization. On the fibrin-coated membrane beneath the gel, the cells gradually degraded and reorganized the fibrin mesh; however, some residues of this mesh remained unchanged even on day 14 after the collagen polymerization. In contrast, the fibrin mesh on the control membrane without the gel was completely degraded by cells after 14 days.

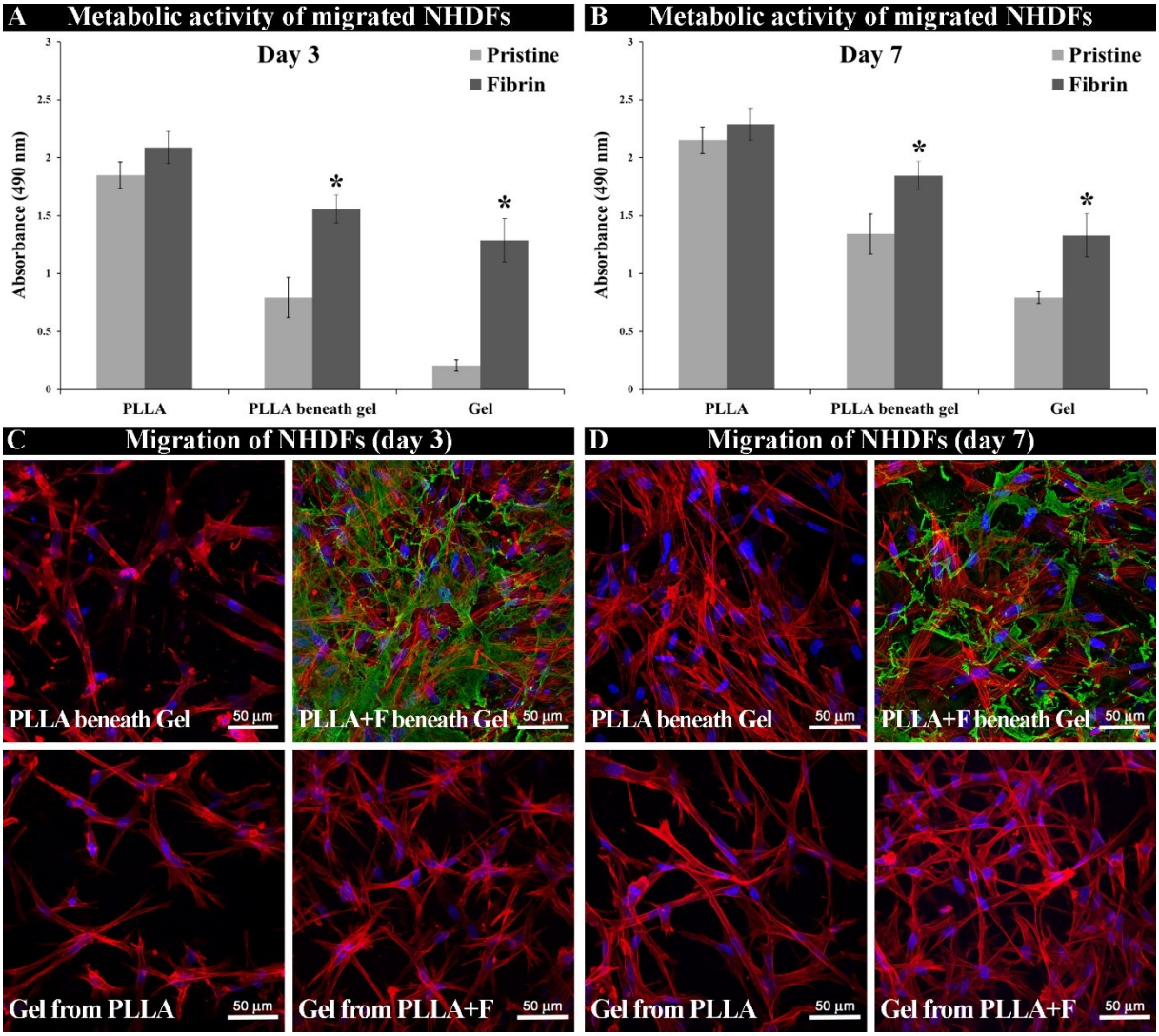

Figure 10. *Metabolic activity (**A, B**) and morphology (**C, D**) of NHDFs migrated into the collagen hydrogel from the non-coated (Pristine) or from the fibrin-coated (Fibrin) PLLA membrane on day 3 (**A, C**), day 7 (**B, D**) after preparation of the collagen.* Notes: Cell metabolic activity on the membrane without the hydrogel (PLLA, first pair of columns), on the membrane separated from the hydrogel (PLLA beneath gel, second pair of columns) and in the hydrogel (Gel, third pair of columns). The arithmetic mean±SD from 8 measurements. Statistical significance ($p \leq 0.05$; ANOVA, Student-Newman-Keuls test): *compared with a non-coated membrane (Pristine) (**A, B**). Fibrin was stained by immunofluorescence (Alexa 488; green), F-actin in the cells (phalloidin-TRITC; red), and the cell nuclei (Hoechst #33258; blue), confocal microscope Leica TCS SPE DM2500, obj. 40× (**C, D**).

In the second part of Bacakova and Pajorova *et al.* (2019) work, a bi-layered skin construct was prepared using the collagen hydrogel with both NHDFs and hKs. The hydrogel was reinforced by the fibrin-coated PLLA nanofibrous membrane from which the NHDFs gradually migrated into the collagen hydrogel (Fig. 11).

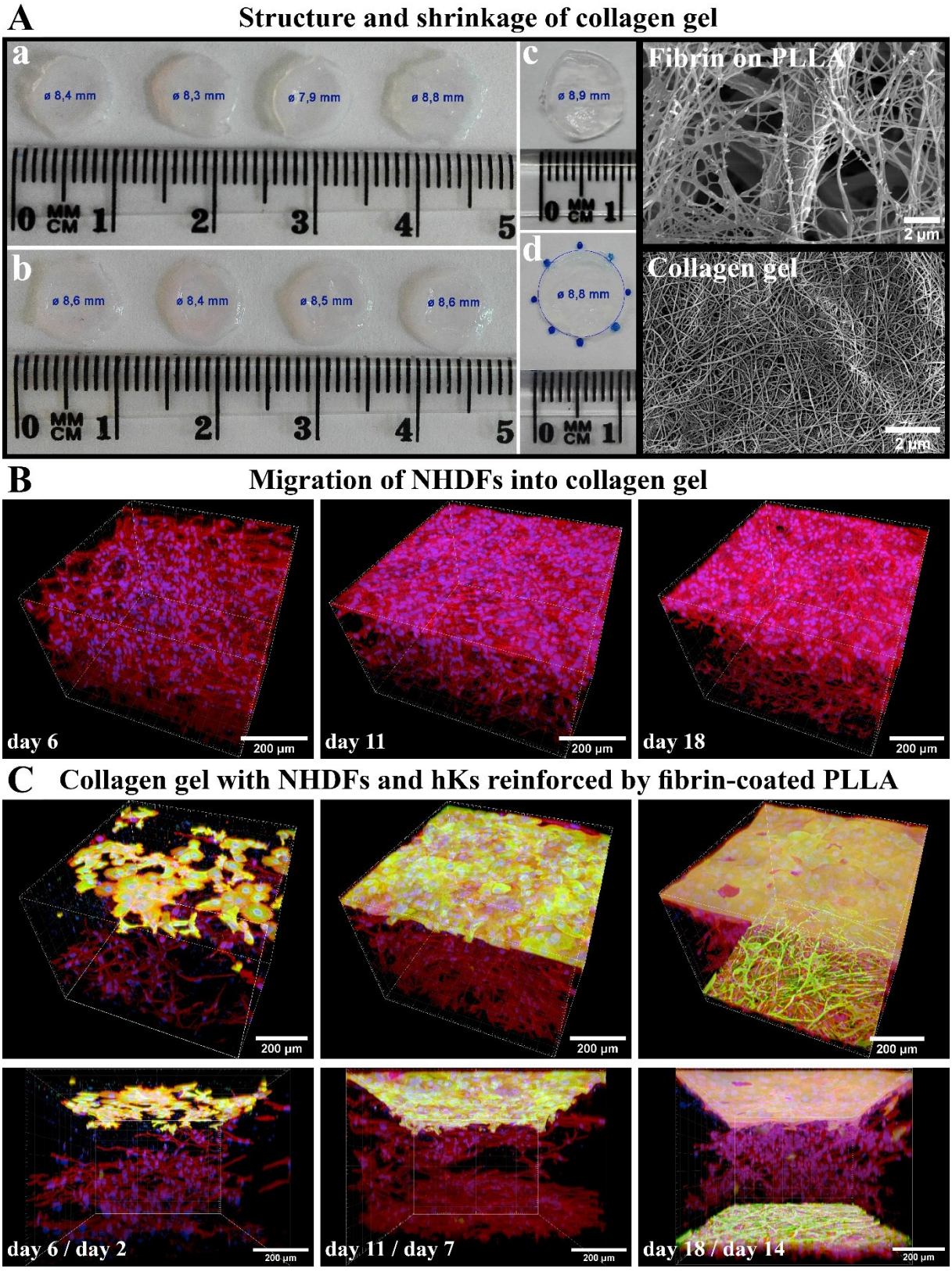

Figure 11. *The structure and shrinkage of the collagen hydrogel (**A**), migration of NHDFs from fibrin-coated PLLA membrane for 6, 11 and 18 days (**B**), and collagen gel with NHDFs and hKs reinforced by fibrin-coated PLLA membrane after 2, 7 and 14 days of hK cultivation (**C**),* Notes: The structure of collagen gel and fibrin coating on PLLA membrane was visualized by SEM. The diameter (Ø) of the gels with NHDFs that migrated from non-coated membrane (a) and from the fibrin-coated membrane (b) for 14 days is presented as mean of the values. The control collagen hydrogel without cells incubated at 37°C, 5% CO_2

for 14 days (c). The measurement principle for hydrogel shrinkage (d) (**A**). Both cell types were stained with phalloidin-TRITC for the cell F-actin cytoskeleton (red), and with Hoechst #33258 for the cell nuclei (blue). The CK14 in the keratinocytes and fibrin coating was stained by immunofluorescence (Alexa 488, green). Dragonfly 503 spinning disk confocal microscope, obj. 20× (**B, C**).

The PLLA membrane consisting of microscale randomly-oriented fibers was firstly coated with fibrin mesh with fiber diameter ranging from ten to approx. 100 nm (see fibrin on PLLA in Fig. 11A). The nanoscale structure of fibrin coating was further enriched with 3D structure of the collagen hydrogel with the diameter in tens of nanometers (see collagen gel in Fig. 11A). The Young's modulus of the collagen hydrogel reinforced by fibrin-coated PLLA membrane was 3.0±1.4 kPa in the first linear region of stress strain response and 89.4±13.2 kPa from approx. 57±10% of compression deformation. Moreover, the collagen hydrogel was not considerably shrunk due to the cell traction forces generated by NHDFs during their two-week migration into the collagen hydrogel (Fig. 11A; a–d). The keratinocytes on the surface of the construct did not promote shrinkage of the collagen hydrogel. The collagen hydrogel prepared after 3 days of NHDF cultivation was seeded by hKs after 4 days of NHDF migration. The cells were visualized by confocal microscopy after 2, 7 and 14 days of the keratinocyte cultivation on top of the collagen hydrogel, which corresponded to the day 6, 11 and 18 of NHDF migration (Fig. 11B, C). Inside the hydrogel, the NHDFs were homogeneously immigrated, spread in all three directions, and showed their typical spindle-like morphology with well-developed F-actin microfilaments. In addition, the NHDFs were able to migrate through the collagen hydrogel from the bottom to the top. They created a cell monolayer on the top of the gel, however only when the surface of the gel was not occupied by hKs (Fig. 11B). The keratinocytes reached a confluent layer on the collagen hydrogel after one week of their cultivation and they created layers. On the hydrogel surface, the keratinocytes formed a basal layer of small still dividing cells with well-developed CK14-containing cytoskeletal filaments, and a suprabasal layer of large cells frequently without cell nuclei (Fig. 11C).

In Travnickova *at al.* (2020) work, we evaluated the influence of the pressure and also harvesting site on the yields, number, viability, diameter, doubling time, mitochondrial activity and the composition of CD surface markers of ADSCs isolated from individual donors. The ADSCs were isolated from lipoaspirate that was harvested under low (-200 mmHg) and high (-700 mmHg) negative pressure from different regions of donors' bodies, i.e. thighs and abdomen.

We found out that the greater cell yields were obtained from the outer thigh region than from the abdomen region. In case of outer thigh region, the yields did not depend on the intensity of the negative pressure, while in case of the abdomen region, the yields were greater under high negative pressure than under low negative pressure (Fig. 12A). These initial differences were equalized in subsequent subculture of the cells, therefore no significant difference was observed in the proliferation capability of ADSCs isolated from thighs and from abdomen under different negative pressures (Fig 12B; left). In general, no significant correlation was detected between the different negative pressures and any other cell characteristic which had been evaluated; for more details; see Travnickova *et al.* (2020). We only noted a slight tendency of ADSCs isolated from inner and other thighs to reach a higher cell number in their second passage compared to the other harvesting regions after one week of cultivation. Moreover, the ADSCs harvested from the abdomen region under low negative pressure from single donors presented more CD146 positive cells than the cells harvested from other regions under low or high negative pressure (Fig. 12B; right). The abdominal ADSCs from single donor were further cultivated on two different types of fibrin coatings on PLLA membrane which were described in Pajorova *et al.* (2018) work. We observed that the abdominal ADSCs obtained under high negative pressure were able to adhere in higher numbers than the abdominal ADSCs harvested under low negative pressure. Therefore, the proliferation of "high" abdominal ADSCs was also faster than the proliferation of "low" abdominal ADSCs on both types of fibrin coatings, i.e. "F coating" and "F mesh". At the same time, both "low" and "high" abdominal ADSCs adhered better and proliferated faster on PLLA membranes modified with "F mesh" type of nanocoating than on "F coating" type of nanocoating (Fig. 12C). The morphology of both types of abdominal ADSCs on non-coated PLLA membrane indicated a very poor cell adhesion on this material. The cells were not spread and took a round shape. The results were in details described in Bacakova *et al.* (2018) review.

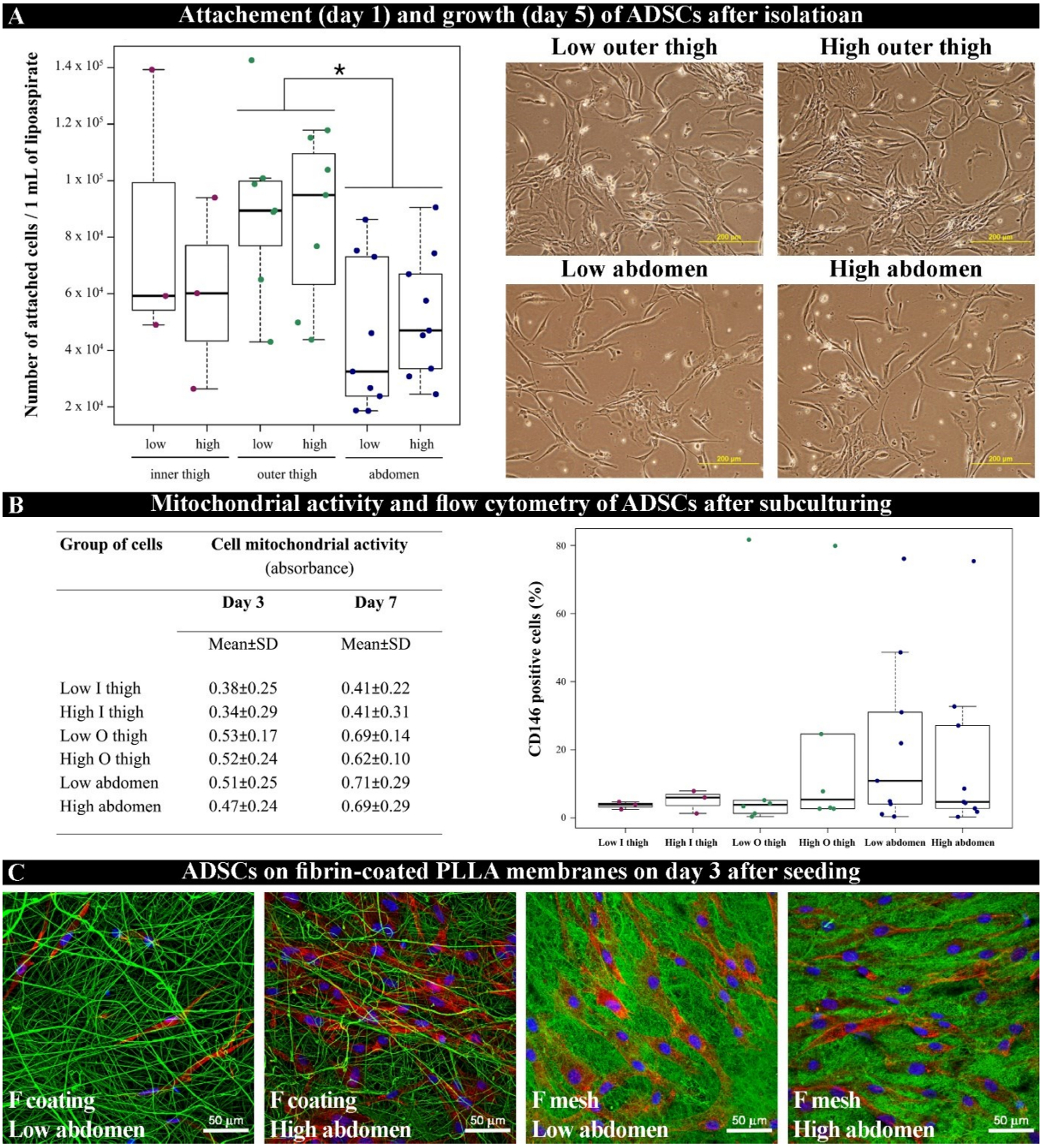

Group of cells	Cell mitochondrial activity (absorbance)	
	Day 3	Day 7
	Mean±SD	Mean±SD
Low I thigh	0.38±0.25	0.41±0.22
High I thigh	0.34±0.29	0.41±0.31
Low O thigh	0.53±0.17	0.69±0.14
High O thigh	0.52±0.24	0.62±0.10
Low abdomen	0.51±0.25	0.71±0.29
High abdomen	0.47±0.24	0.69±0.29

Figure 12. *Characterization of isolated ADSCs form single donors under low negative pressure (-200 mmHg) and under high negative pressure (-700 mmHg) from different areas of their body (thighs and abdomen).* Notes: The cell yields per 1mL of lipoaspirate counted from the number of attached cells after isolation; * statistical significance ($p \leq 0.05$) (**A, left**) and the representative images of isolated cells after 5 days of cultivation; brightfield Olympus IX 51 microscope, obj. 10× (**A, right**). The metabolic activity was measured by MTS assay on days 3 and 7 (**B, left**) and the percentage of CD146-positive cells in each group of cells was measured by flow cytometry (**B, right**). The morphology of ADSCs isolated from abdomen of single donor growing on PLLA with two types of fibrin nanocoatings ("F mesh" vs. "F coating") for 3 days; fibrin was visualized by immunofluorescence (Alexa 488; green), F-actin in the cells (phalloidin-TRITC; red), and the cell nuclei (Hoechst #33258; blue), confocal microscope Leica TCS SPE DM2500, obj. 40× (**C**).

In order to eliminate individual variability in cell behavior between the donors, the ADSCs from ten donors harvested under the same conditions were pooled in the first passage. The proliferation dynamic and morphology of these four groups of pooled ADSCs, i.e. “low” thigh, “high” thigh, “low” abdomen and “high” abdomen, were further analyzed (Fig. 13A). We detected significantly lower growth dynamic of pooled ADSCs compared to the NHDFs. Although there were no significant differences between the groups of pooled ADSCs in their growth and morphology, the pooled ADSCs were able to proliferate during 7 days of cultivation. These cells, namely “low” thigh pooled ADSCs, were utilized in Pajorova *et al.* (2020) work. However, in the next stage we mixed the pooled ADSCs in their second passage into two groups where only the pressure of harvesting was retained (Fig. 13B). These two groups of pooled ADSCs were compared with NHDFs. We observed the decrease of growth capacity of both “low” and “high” pooled ADSCs on polystyrene and also when they were seeded on the fibrin mesh or surrounded by the collagen hydrogel.

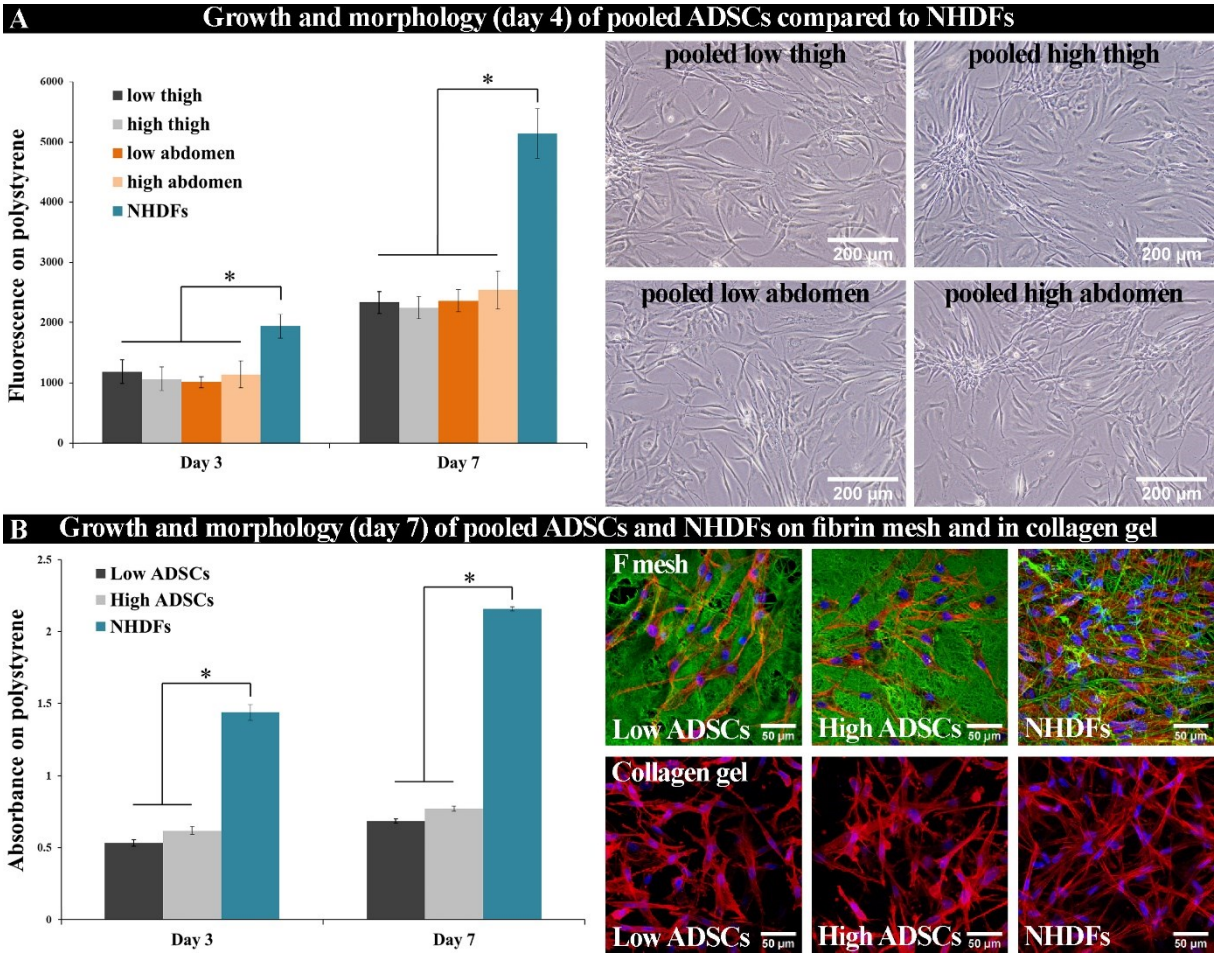

Figure 13. *Metabolic activity and the morphology of pooled ADSCs compared with NHDFs during one week of cultivation.* Notes: The ADSCs were pooled in accordance either with the harvesting area and pressure (**A**) or with harvesting pressure only (**B**). The cell metabolic activity was measured by resazurin

(**A**) or by MTS assay (**B**) on polystyrene after 3 and 7 days of cultivation, * statistical significance ($p \leq 0.05$). The representative images of pooled ADSCs after 4 days of cultivation on polystyrene; brightfield Olympus IX 51 microscope, obj. 10×, scale bar 200 μm (**A**) and on fibrin-coated PLLA membrane or in collagen hydrogel; fibrin was visualized by immunofluorescence (Alexa 488; green), F-actin in the cells (phalloidin-TRITC; red), and the cell nuclei (Hoechst #33258; blue), confocal microscope Leica TCS SPE DM2500, obj. 40×, scale bar 50 μm (**B**).

In the Pajorova *et al.* (in preparation) work, we combined the isolated well-characterized ADSCs with HUVECs in the collagen hydrogel to pre-vascularize the bi-layer skin construct. Due to the slower growth dynamics of pooled ADSCs and their lower migration capability (Fig. 13B), we preferred the ADSCs isolated from a single donor, namely "low" abdominal ADSCs. The selected ADSCs were highly positive for CD146 marker, also called melanoma cell adhesion molecule. Being a receptor for laminin alpha 4, this adhesion molecule is expressed essentially on the vascular system, mainly on the pericytes (Wang *et al.* 2020). Similarly, as it was described in Bacakova and Pajorova *et al.* (2019), we seeded and cultivated the ADSCs on PLLA membrane coated with the fibrin mesh for 3 days before we applied the collagen hydrogel directly on the surface of the membranes with ADSCs. The collagen hydrogel was polymerized both with and without embedded HUVECs. After 4 days of ADSC migration and their interaction with HUVECs, the hKs were seeded on top of the collagen hydrogels and after next 3 days the samples were exposed to the air-liquid interface. The overall cell interactions were evaluated after 14 days of cultivation (Scheme 5).

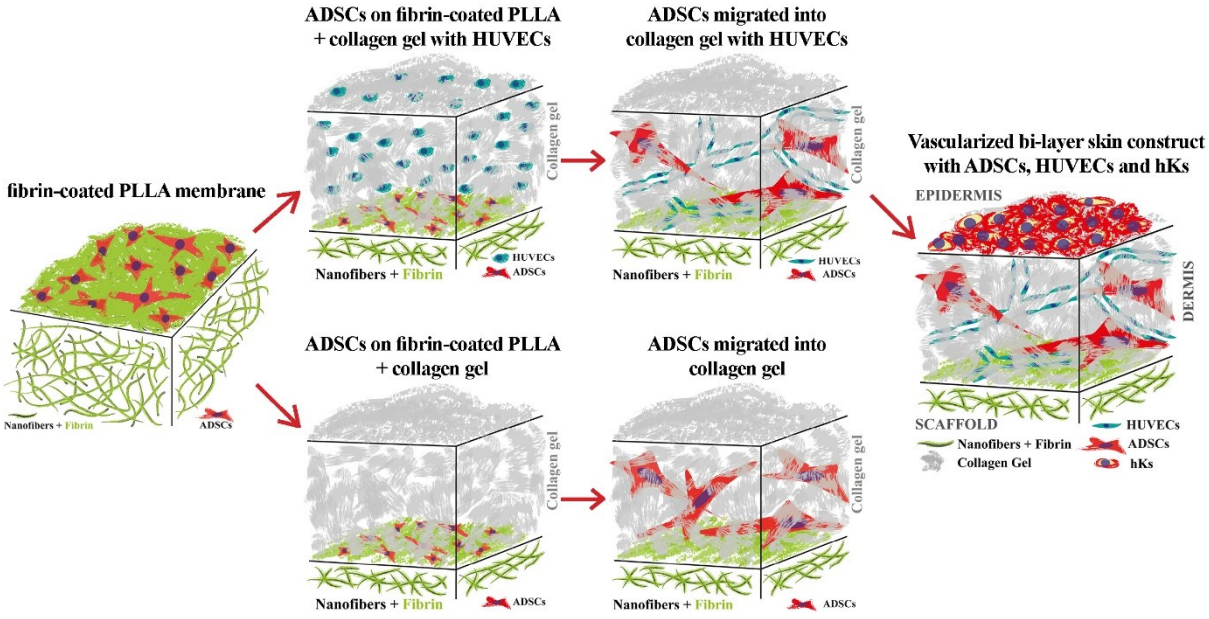

Scheme 5. *Preparation of the pre-vascularized bi-layered skin constructs consisting of a fibrin-coated PLLA membrane seeded with ADSCs, collagen hydrogel with or without embedded HUVECs and hKs on the surface of the hydrogel.*

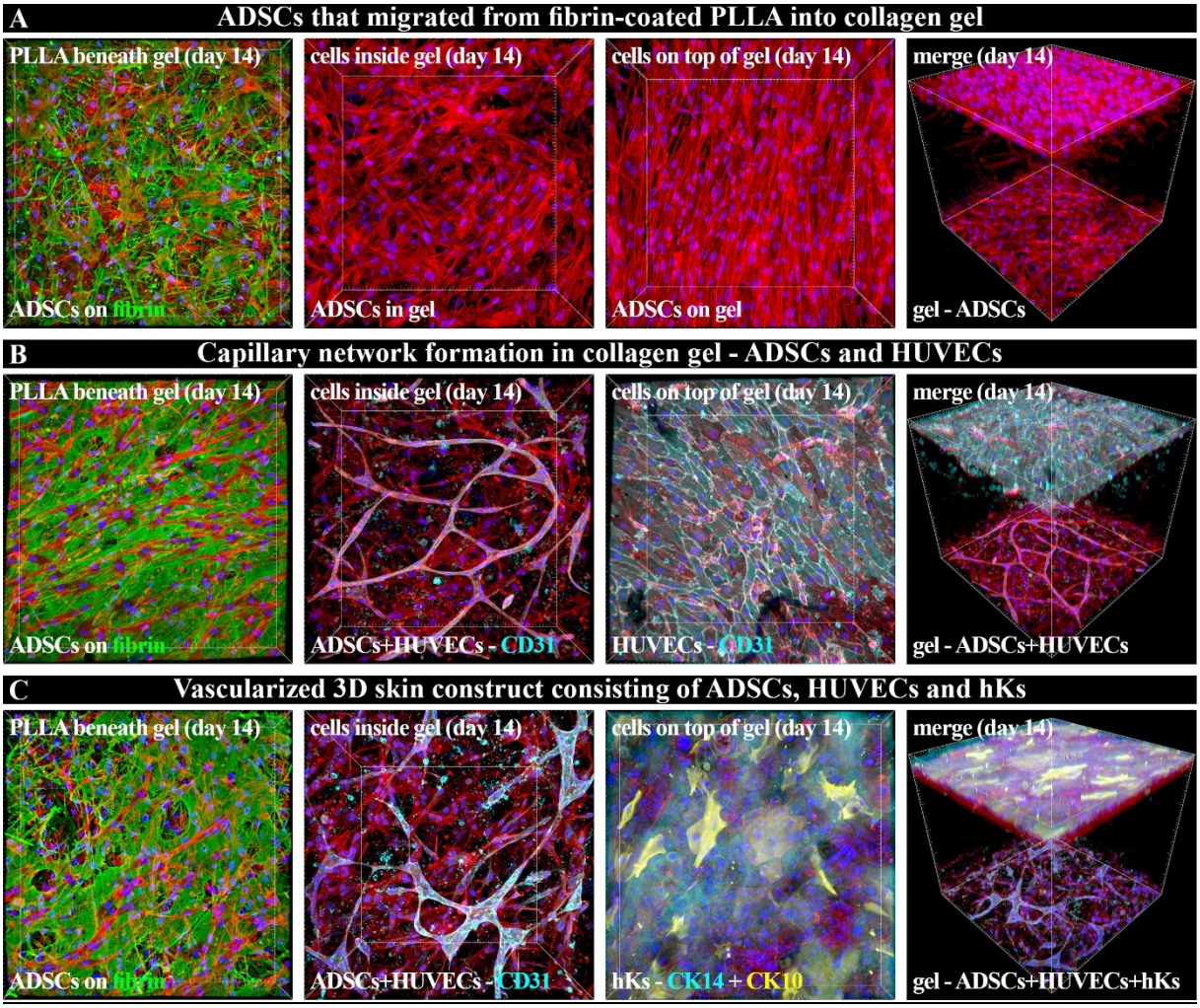

Figure 14. *Preparation of the pre-vascularized bi-layer skin construct consisting of collagen hydrogel reinforced by fibrin-coated PLLA membrane visualized in a three stages.* Notes: ADSCs that migrated from fibrin-coated PLLA membrane into collagen hydrogel during 14 days of cultivation (**A**). Capillary-like network formation in collagen hydrogel with embedded HUVECs and migrated ADSCs after 14 days (**B**). Pre-vascularized bi-layer skin construct containing the migrated ADSCs, embedded HUVECs and stratified layers of hKs (**C**). Front view of fibrin-coated PLLA membrane beneath the collagen gel, of cells inside the gel and of the cells on the top of collagen gel. Side view of merged images. Fibrin was visualized by immunofluorescence (Alexa 488; first column; green). All cell types were stained with phalloidin for the cytoskeletal F-actin (conjugated with TRITC or Atto 488; in all images; red), and with DAPI for the cell nuclei (in all images; blue). CD31 membrane marker of HUVECs (**B** and the 2nd image in **C**) and cytoskeletal CK14 in hKs (the 3rd image in **C**) were visualized by immunofluorescence (Alexa 633; turquoise). CK10 – the late marker of differentiated hKs (the 3rd image in **C**) was visualized by immunofluorescence (Alexa 546; yellow). Dragonfly 503 spinning disk confocal microscope, obj. 20×.

We observed that the ADSCs were able to migrate through the whole hydrogel from the membrane to the surface of the gel when they were cultivated without another cell types. In the collagen hydrogel, the ADSCs prolonged their filopodia in all directions and on the top of the gel they created a confluent layer of the cells (Fig. 14A). In case of the embedded HUVECs in the collagen hydrogel, the ADSCs that were migrated from the membrane into

the hydrogel interacted with the HUVECs, which formed a capillary-like network (Fig. 14B). Although, the network of the capillaries was clearly visible mainly on the fibrin-collagen interface, some short capillary-like branches were also detectable inside the collagen hydrogel. However, this was due to decreased transparency of a milky colored porcine collagen (Fig. 15A). Moreover, the individual slices in the z-axis revealed that the HUVECs tended to form the void space between them, especially at the place where several capillary-like branches were formed (see arrows in Fig. 15A). Interestingly, the HUVECs were also able to colonized the surface of the collagen hydrogel and they formed a monolayer of the cells when they were cultivated without hKs (Figs. 14B and 15B). We noticed that the monolayer of HUVECs was interrupted at some places by the pits with tubular character in *z*-axis that were connected to the deeper located capillary-like branches in the collagen hydrogel (see arrows in Fig. 15B).

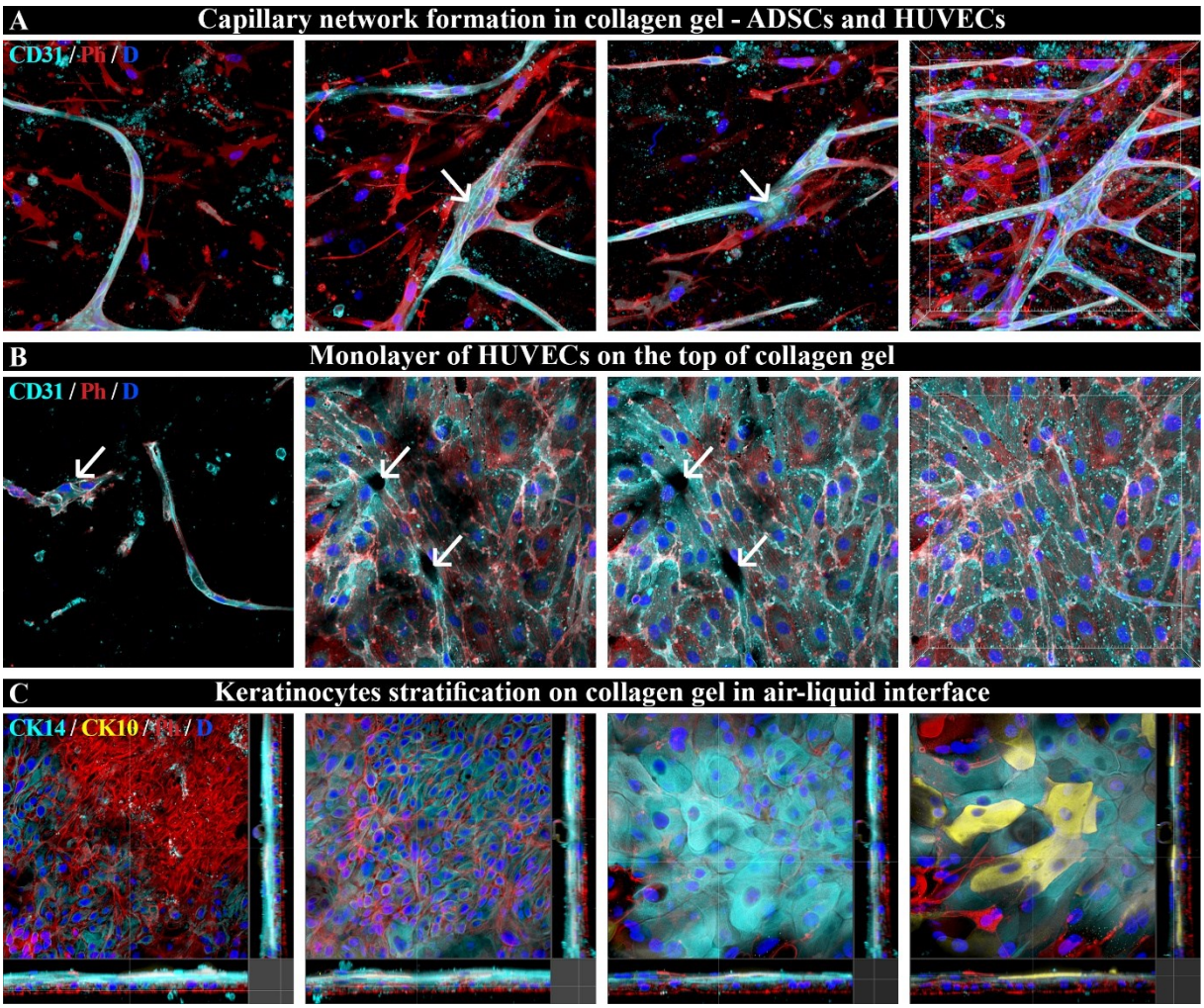

Figure 15. *Visualization of the capillary-like network formation in the collagen hydrogel (**A**), the monolayer of HUVECs (**B**) and the stratified hKs on the hydrogel surface (**C**).* Notes: Series of the representative z-stack images (first three images in **A, B**) and the final 3D front view (last image in **A, B**).

Series of the orthogonal views of the stratified hKs on collagen hydrogel (**C**). The images are ordered from the deepest (left) to the most superficial (right) view of the cells. All cell types were stained with phalloidin for the cytoskeletal F-actin (conjugated with TRITC or Atto 488; all images; red), and with DAPI for the cell nuclei (all images; blue). CD31 membrane marker of HUVECs (**A, B**) and cytoskeletal CK14 in hKs (**C**) were visualized by immunofluorescence (Alexa 633; turquoise). The late marker CK10 of differentiated hKs (**C**) was visualized by immunofluorescence (Alexa 546; yellow). Dragonfly 503 spinning disk confocal microscope, obj. 40×.

The final status of the cell colonization was evaluated after the hKs were seeded and stratified in the air-liquid interface on the surface of the pre-vascularized collagen hydrogel reinforced by the fibrin-coated PLLA membrane (Fig. 14C). We observed that the capillary-like network was slightly reduced when the hKs were cultured on the collagen surface, however they were still capable to form some short branches and connections. The hKs covered the whole surface, and moreover they created several layers of cells with overall thickness approx. 50 μm (Fig. 14C). The individual slices in the z-axis showed that the really small hKs were attached to the collagen hydrogel in their basal layer. In this layer on the cell-collagen interface, the hKs visibly formed a star-like structures from their F-actin filaments in the middle of each individual cell (see red F-actin in Fig. 15C; left). In the basal layer and the next suprabasal layers, the hKs expressed mainly the CK14, which is one of the main CKs of the non-differentiated keratinocytes. However, the cells in the suprabasal layers became to be larger and larger, which corresponds to their more differentiated stage (see turquoise CK14 in Fig. 15C; from left to right). On the air-liquid interface, the most superficial layer of hKs expressed also the CK10 positive cells. In this highly differentiated cell layer, the large hKs expressed more CKs than F-actin microfilaments and their cell nuclei were hardly detected or event they were not present (see yellow CK10 in Fig. 15C; right).

4.3 Temporary Cell-Decorated Wound Dressings Based on Cellulose

(i) Pajorova J.# and Skogberg A.#, Hadraba D., Broz A., Travnickova M., Zikmundova M., Honkanen M., Hannula M., Lahtinen P., Tomkova M., Bacakova L., and Kallio P.* ***Cellulose Mesh with Charged Nanocellulose Coatings as a Promising Carrier of Skin and Stem Cells for Regenerative Applications.*** *Biomacromolecules 2020; 21(12):4857-4870. # contributed equally*

(ii) Bacakova M., Pajorova J., Sopuch T., Bacakova L. ***Fibrin-Modified Cellulose as a Promising Dressing for Accelerated Wound Healing.*** *Materials (Basel) 2018; 11(11):2314.*

Author's contribution: I introduced a method of nanocellulose coatings in collaboration with technical university in Tampere (Finland). I planned and performed the cell related analysis on the nanocellulose coatings and I participated on structural and mechanical characterizations of the nanocellulose coatings, especially I introduced the method of cell dehydration before the scanning on SEM. I prepared the fibrin nanocoatings on cellulose meshes and I cultured the cells on materials. I participated on writing the manuscripts and *I am the corresponding author of the manuscript.

In the third part of my work, I focused on temporary wound dressings. In both studies we utilized a nature-derived cellulose mesh, which is commonly used for covering wound beds. We optimized the physicochemical properties of this mesh for the cell attachment and their carrying into the wound using wood-derived CNFs in Pajorova *et al.* (2020) work and by fibrin nanocoatings in Bacakova *et al.* (2018b) work.

In Pajorova *et al.* (2020) work, we coated a pure cellulose mesh with different types of charged CNFs in order to find the best substrate for NHDFs and ADSCs growth. We observed that the structure of the CNF coatings can be regulated by the volume of applied CNF on the surface of the cellulose mesh (Fig. 16A). The CNF solutions with a volume of 150 μL (a150, c150) covered the individual fibers of the mesh and filled the pores between them, while a volume of 600 μL (c600, a600 and c+a) formed a thin film on the surface of the mesh. The individual differences also depended on the charge of CNFs. The surface roughness (Ra median) determined by AFM reached almost the same values, i.e. 9.04 nm for cCNFs and 10.2 nm for aCNFs, while the Ra median of c+a was 55.76 nm (Fig. 16B). The CNF coatings differed not only in the structure but also in the mechanical and chemical properties. We detected that the swelling ratio of cCNF was higher than the swelling ratio of aCNFs; however, unlike to aCNFs, the swelling ratio of cCNFs stayed unchanged with time. The

significant changes were measured on aCNFs where the swelling ratio was increasing with time. This was also reflected in the mechanical properties measured by AFM in time after the samples were swollen. The cCNF coatings were softer at the beginning compared to the aCNF coatings; however, the aCNF coatings softened with time as the water content of aCNFs increased. The behavior of c+a coatings was comparable with the behavior on aCNF coatings.

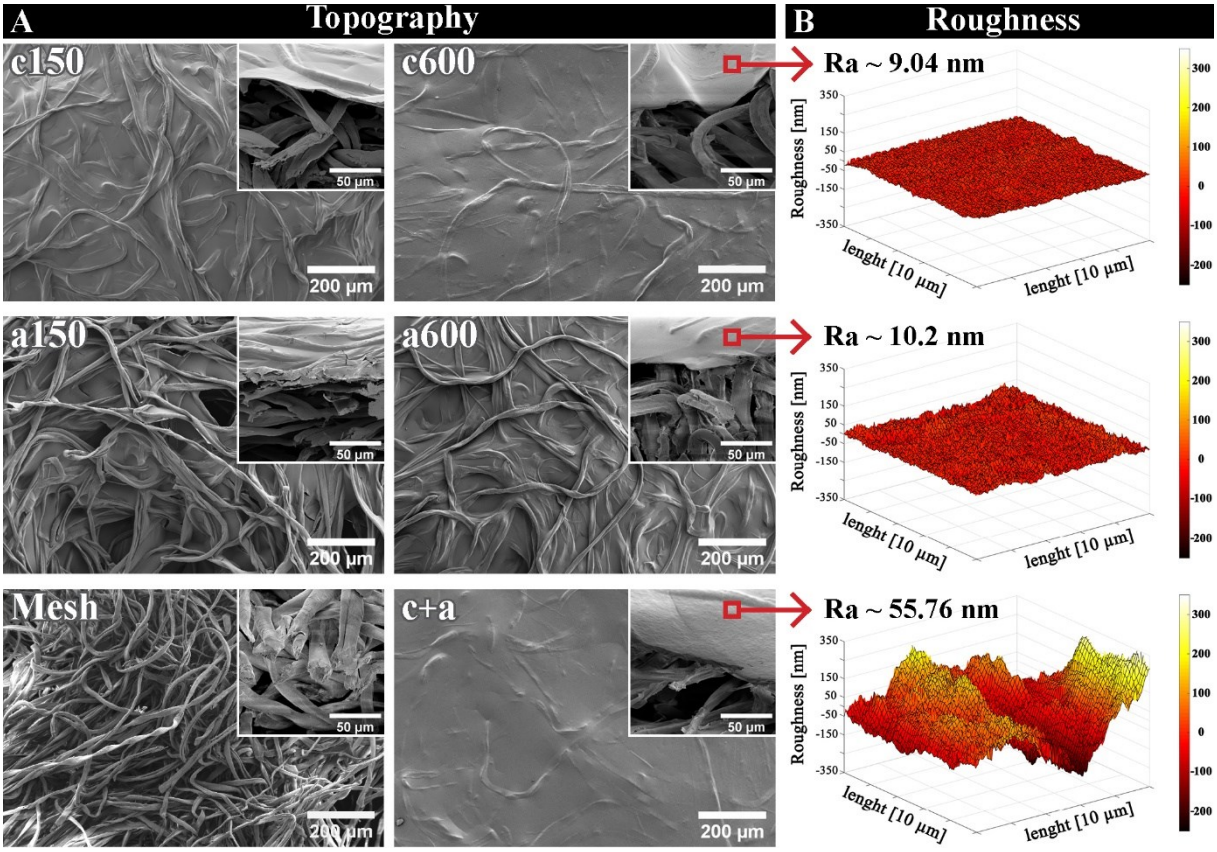

Figure 16. *Topography (**A**) and roughness (**B**) of CNF-coated meshes.* Notes: Front view and side view (inset image) of SEM images of c150, c600, a150, a600, and c+a CNF-coated and non-coated meshes (left and center). The roughness of the c600, a600, and c+a CNF-coated meshes was measured by AFM (right).

In the cell-related part of this work, we evaluated the adhesion, morphology and proliferation of NHDFs and ADSCs on the CNF coatings. The immunofluorescence staining and the values of the cell metabolic activity – an indicator of the cell number – were used to evaluate the overall growth dynamics of the cells within a one-week period (Figs. 17 and 18). The growth of both cell types on aCNF or c+aCNF coatings was comparable or even better than the growth on standard tissue culture polystyrene, while on the cell growth on cCNF coatings was similar to that on the non-coated meshes. Therefore, we further analyzed the mechanisms behind these phenomena.

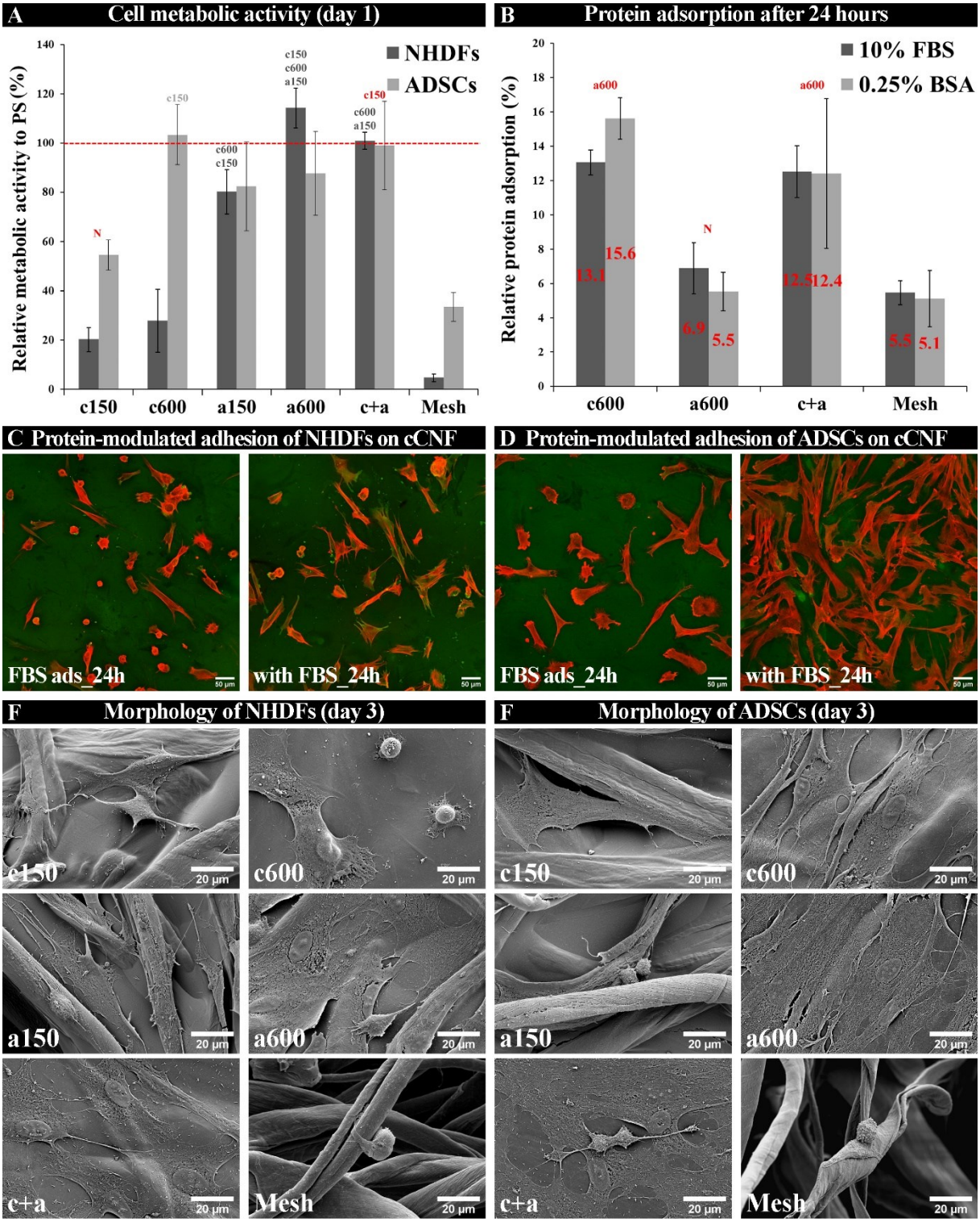

Figure 17. *A response of the NHDFs and ADSCs on CNF coatings after 24 hours (**A, B, C, D**) and 3 days (**E, F**) of cultivation.* Notes: The cell metabolic activity on CNF-coated meshes relative to the activity on polystyrene (PS=100%; red line) after 1 day of cultivation (resazurin assay; **A**), a proportion of adsorbed proteins on CNF coatings after 24 hours of incubation. Relative adsorption of 0.25% BSA (3.75 mg=100%) and 10% FBS (5.46 mg=100%) displayed as a percentage (Pierce BCA Protein Assay Kit; **B**). Arithmetic mean±SD from 8 measurements. Statistical significance ($p \leq 0.05$, ANOVA, Tukey's test) is displayed above each experimental group, indicated by the color (red is for both) of the group or by (N) representing no significant difference compared to the non-coated mesh. Adhesion and spreading of NHDFs (**C**) and ADSCs (**D**) on cCNF-coated meshes with (FBS ads_24h) and without (with FBS_24h) pre-adsorbed

proteins after 24 hours of cell cultivation. Cytoskeletal F-actin (phalloidin-TRITC; red) and vinculin in the cells (Alexa 488; green) were visualized. Dragonfly 503 spinning disk confocal microscope. Obj. 20×. The morphology of NHDFs (**E**) and ADSCs (**F**) on CNF coatings after 3 days of cultivation acquired by SEM.

The initial adhesion of NHDFs and ADSCs on the CNF coatings (Fig. 17A) was characterized after 24 hours of the cultivation. We observed that the number of attached NHDFs was significantly lower on the cCNF coatings than on the aCNF and c+aCNF coatings, while the number of attached ADSCs on the cCNF coatings was similar to that on the aCNF and c+aCNF coatings or even slightly higher. However, all CNF coatings were better than non-coated meshes. In order to explain the different cell behavior on cCNF coatings, the proportion of the adsorbed proteins on these CNF coatings from FBS was measured (Fig. 17B). We detected that the cCNF coatings adsorbed more proteins, especially the most abundant BSA, from the media supplemented with FBS than it was on aCNF coatings. The c+a coatings behaved similarly to the cCNF coatings, but the proportion of adsorbed BSA was slightly lower compared to the cCNF coatings. These results motivated us to compare the adhesion of both cell types seeded either in pure DMEM (without FBS or any proteins) on cCNF coatings with pre-adsorbed FBS or in DMEM supplemented with FBS on pure cCNF coatings (Fig 17C, D). The results confirmed that the ADSCs were able to adhere and spread on cCNF coatings when they were seeded in DMEM with FBS, while the NHDFs remained round and therefore poorly adhered (see with FBS_24h in Fig 17C, D). Interestingly, this difference disappeared on the samples pre-adsorbed with FBS, where suddenly both cell types were not able to attach and spread properly (see FBS ads_24h in Fig 17C, D). This response of the cells indicates that the protein that adsorbed from FBS on the cCNFs was primarily the BSA, which mostly disabled a proper cell adhesion. However, this was probably overcome by the faster adhesion of ADSCs compared to NHDFs when the cells were seeded without protein pre-adsorption. The morphology of the cells was observed after 3 days, when the cells were fully spread and their morphology was well-developed. The flat 2D surface of the c600 coatings markedly enhanced the spreading of ADSCs (Fig. 17F), while the NHDFs remained round and poorly adhered (Fig. 17E). However, the morphology of the NHDFs was improved by the 3D topography of the c150 coatings, where the cells were slightly better adhered and spread. Similarly, both cell types were more elongated on the 3D surface of the a150 coating than on c600 coating even though there were more cells. The cells on non-coated meshes were barely attached.

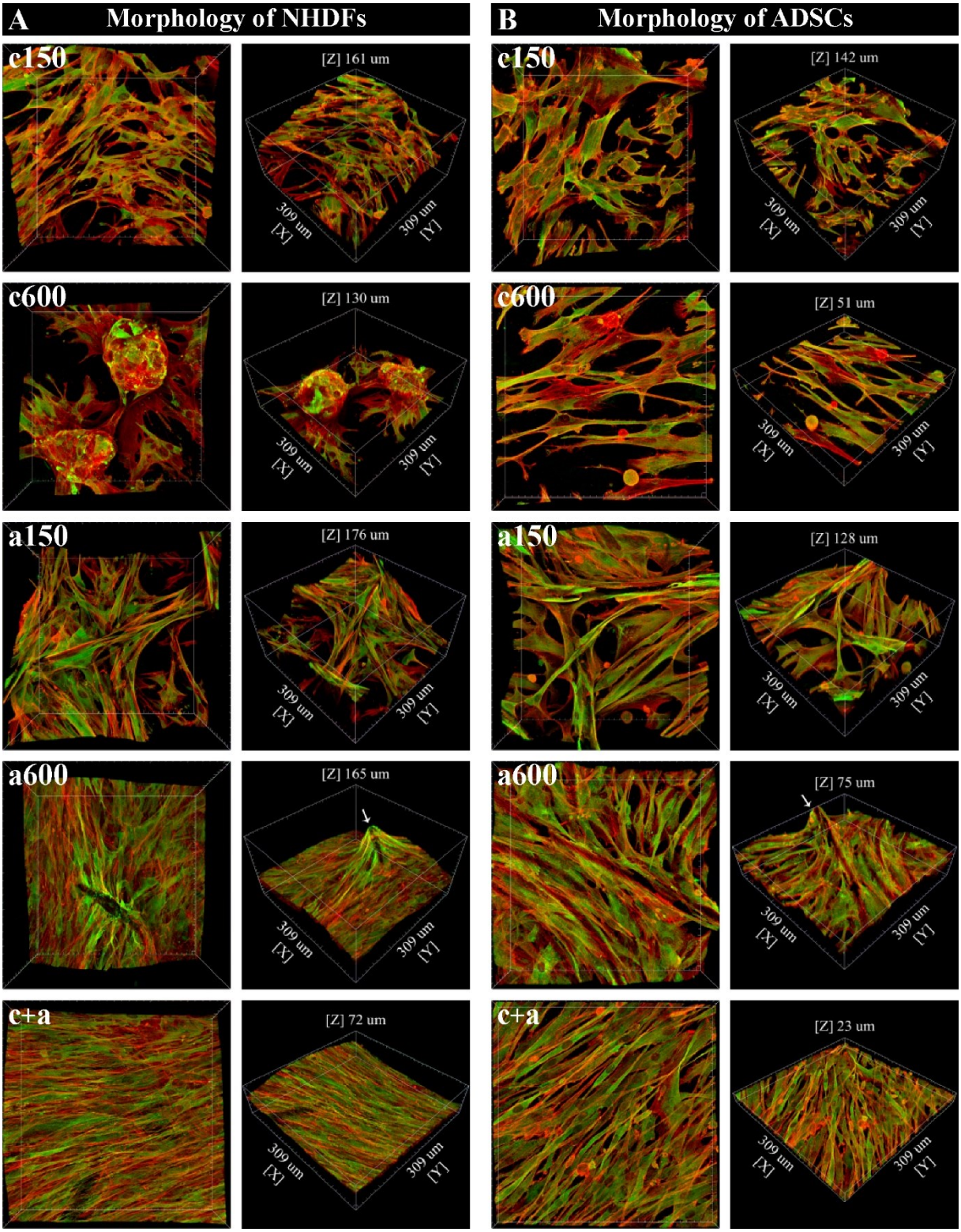

Figure 18. *Morphology of NHDFs (**A**) and ADSCs (**B**), guided by the topography of the CNF-coated meshes after 7 days of cultivation.* Notes: 3D projection of microscopy images (front view and side view) of the cells on CNF coatings. Cytoskeletal F-actin (phalloidin-TRITC; red) and vinculin in the cells (Alexa 488; green) were visualized. Cell focal adhesions (white arrows). Dragonfly 503 spinning disk confocal microscope. Obj. 20×.

The final status of the colonization of the CNF coatings with cells was evaluated on day 7 after the cell seeding (Fig 18A, B). The 3D projections of microscopy images of cells on the CNF coatings revealed that the 2D coatings (c600, a600, c+a) enhanced the proliferation and spreading of both cell types only in the *xy* directions, while the 3D coatings (c150, a150) supported elongation of the cells on the mesh fibers and between them in all *xyz* directions. Both cell types colonized almost the entire space of the aCNF and c+aCNF coatings. The negative effect of cCNFs, mainly of c600 coatings, on cell attachment was manifested by the formation of clusters of ADSCs and spheroids of NHDFs (see c600; Fig. 18A, B). After one week of cultivation, a positive effect of the 3D topography of the a150 coatings and also of the c150 coatings on cell spreading and growth was observed. On the aCNF coatings, the cells were spread along the mesh fibers, and focal adhesions were clearly visible (see a150; Fig. 18A, B). On the a600 coatings, a higher vinculin signal was detected in the cells that migrated upward to the top of the protruding aCNF-coated mesh fibers (arrows in a600; Fig. 18A, B).

In the second work focused on wound dressings (Bacakova *et al.* 2018b), we coated the commercially available Hcel® NaT cellulose mesh with two types of fibrin nanocoatings according to the preparation protocol described in Pajorova *et al.* (2018). The non-toxic nature-derived meshes were in two forms, i.e. porous and homogeneous (referred to as "P form" and "H form"; Fig. 19A; left). In order to increase the attractivness of these meshes for the NHDF attachment, we either covered individual fibers of the mesh by the "F coating" type of nanocoating or we filled the pores and covered the whole surface by the "F mesh" type of nanocoating (Fig. 19A; right). The fibrin functionalization of the Hcel® NaT improved the colonization of the material with NHDFs, which confirmed the results obtained on PLA membranes (Pajorova *et al.* 2018). On the non-coated meshes, the cells were not able to adhere due to the large pores among the micro-scaled fibers of the cellulose mesh. Therefore, the round cells went through the pores of the mesh. The "F mesh" type of nanocoating filled the pores, which significantly improved the cell attachment and the number of cells after 3 days of cultivation. Moreover, the number of NHDFs on "F mesh" was considerably higher than the cell number on "F coating", where the fibrin coated only individual fibers of cellulose mesh. However, after one week, the proliferation of NHDFs on "F mesh" and "F coating" was almost at the same level, especially in case of P form of Hcel® NaT (Fig. 19B).

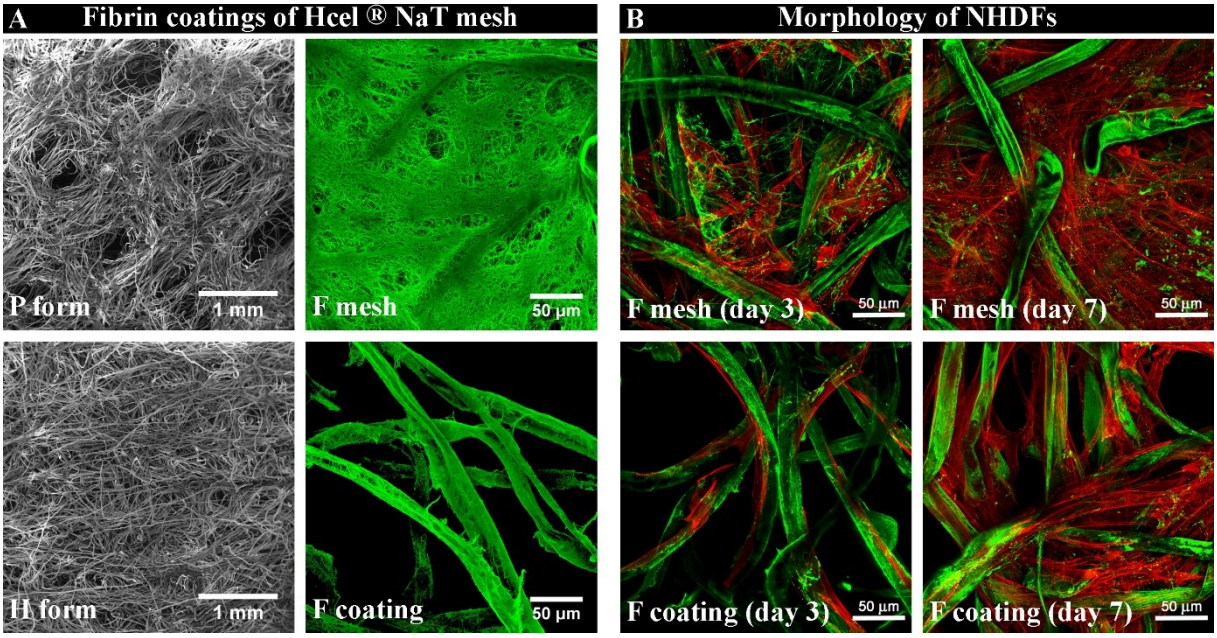

Figure 19. *Structure of the Hcel® NaT meshes with two types of fibrin nanocoatings (**A**) and morphology of NHDFs after 3 and 7 days of cultivation (**B**).* Notes: Structure of Hcel® NaT meshes (P for and H form) was acquired by SEM (1000×) (**A, left**) and the structure of two types of fibrin nanocoatings ("F mesh" and "F coatings") on P form was visualized by immunofluorescence (Alexa 488; green) (**A; right**). Cytoskeletal F-actin was stained with phalloidin-TRITC (red). Leica TCS SPE DM 2500 confocal microscope, obj. 40×.

5 Discussion

5.1 Single-Layered Skin Constructs Based on Protein-Coated Nanofibers

The cell carriers made of various biodegradable synthetic nanofibrous polymers represent one of the current approaches in the treatment of acute or chronic wounds. In our first study (Bacakova *et al.* 2017), we compared electrospun nanofibrous PLA and PLGA membranes with protein nanocoatings. We did not notice apparent differences in the structure of the membranes nor in the formation of protein nanocoatings between these membranes. It has been reported that PLA degrade slower than PLGA; however, it strongly depends on the percentage of PLA in the PLGA copolymer (Kranz *et al.* 2000; Anderson and Shive 1997). Nevertheless, these nanofibrous polymeric membranes in their non-modified state do not provide desired properties for the cell attachment and their growth. Suitable physicochemical properties can be achieved by modifying the surface by biomolecules naturally occurring in the body, i.e. collagen, fibrin and fibronectin (Bacakova *et al.* 2016; Mateos-Timoneda *et al.* 2014). Therefore, we prepared fibrin and collagen nanocoatings with attached fibronectin on PLGA and PLA membranes in order to accelerate the adhesion, proliferation, and ECM synthesis of the skin cells (Bacakova *et al.* 2017).

Our results showed, that the fibrin nanocoating considerably enhanced the adhesion, spreading and growth of fibroblasts, while the growth of keratinocytes was not significantly improved on the fibrin nanocoatings. This behavior might be influenced by the origin of the cells. The fibroblasts naturally migrate into the fibrin clot during wound healing, while the reepithelization occurs normally after the ECM synthesis phase of the healing process, when fibrin particularly is replaced by collagen. The positive effect of fibrin on the fibroblast behavior was described also in many other works (Bacakova *et al.* 2016; Mazlyzam *et al.* 2007; Nair *et al.* 2014); however, consistent conclusions on the role of fibrin in the keratinocyte behavior have not yet been reached. Sese *et al.* found out that the growth of keratinocytes in 3D fibrin constructs was affected by thrombin concentration. They detected that 1 U/mL of thrombin is the optimal concentration for keratinocytes (Sese *et al.* 2011); however, we used a concentration of 2.5 U/mL for our fibrin nanocoatings. Moreover, Kubo *et al.* reported that the important αvβ3 integrin receptors for binding the cells to fibrin molecules was not present on the keratinocyte membrane, which made the fibrin unrecognizable for the keratinocytes (Kubo *et al.* 2001). In our study, the keratinocytes were able to adhere on fibrin nanocoatings, but they were present in significantly lower numbers compared to collagen nanocoatings.

In contrast to the fibrin nanocoatings, the collagen nanocoatings particularly supported keratinocyte adhesion and spreading, while they were not able to resist the traction forces generated by fibroblasts. Eastwood *et al.* showed that most of the contractile forces were generated in the collagen gel during attachment and spreading of the cells, and in addition the contraction forces of the different types of fibroblasts might vary (Eastwood *et al.* 1996). Therefore, we suggested that the fibroblasts and keratinocytes might act on the collagen gel with different traction forces, which resulted into opposite responses of these cells to the collagen coating. In addition, we detected that the collagen nanocoating did not increase the stiffness of the membrane compared to the fibrin nanocoating that provided the fibroblasts with a greater mechanical resistance. On the contrary, the attachment of keratinocytes was probably accelerated by the recognition of the DGEA (Asp-Gly-Glu-Ala) sequence in collagen molecules by α2β1 or α3β1 integrin receptors presented on the keratinocyte membrane (Staatz *et al.* 1991; Scharffetter-Kochanek *et al.* 1992; Engler *et al.* 2004). For this reason, Fu *et al.* also coated the PCL-collagen nanofibrous matrices (331±112 nm in diameter) with an additional ultrafine network of nanofibers (55±26 nm in diameter) in the form of the collagen gel. Similarly to our work, these collagen coatings provided more physiological conditions for the adhesion and migration of keratinocytes (Fu *et al.* 2014).

Fibronectin – the main adhesive protein of ECM containing the RGD sequence – was additionally adsorbed on the nanocoatings to improve the attachment and spreading of the cells (Ruoslahti and Pierschbacher 1987) . The positive effect was more pronounced on the collagen nanocoatings, where the growth of both cell types was increased, compared to the fibrin nanocoatings. However, we observed that the fibrin nanocoatings stimulated the fibroblasts to synthesize their own fibronectin *de novo* as ECM molecules. This was described in many other studies, where the ECM synthesis, mainly collagen I, by the cells was stimulated using a fibrin in various forms (Bacakova *et al.* 2016; Nair *et al.* 2014; Tuan *et al.* 1996).

The dynamic of the degradation and reorganization of the protein nanocoatings by the cells was also different. Similarly, as it was found in our previous study, the fibroblasts continuously degraded and reorganized the protein nanocoatings during the cultivation. In contrast to the fibroblasts, the HaCaT keratinocytes in this study left the collagen coatings almost unchanged, while the fibrin coatings were strongly altered during one week of the cultivation. This can be due to a nonspecific adhesion of keratinocytes on fibrin, which caused the reorganization or even removal of the fibrin as a substrate. Together with the poor adhesion of keratinocytes to fibrin described above, this finding is consistent with the

commonly known ability of keratinocytes to slough the fibrin eschar from the newly formed epidermis.

In Pajorova *et al.* (2018) study, we improved the preparation of fibrin nanocoatings. The first type of nanocoating ("F coating") covered the individual fibers in the membrane, while the second type of nanocoating ("F mesh") formed an additional fine homogeneous nanofibrous mesh on the surface of the membrane (Pajorova *et al.* 2018). Different structures of these fibrin nanocoatings were obtained by controlling the amount of the adsorbed thrombin which reacted with fibrinogen. Previously published studies have found out that the concentration of thrombin above 1 U/mL induced the formation of thin fibrin fibers, while the concentration of thrombin under 0.001 U/mL induced the formation of thick fibrin fibers (Carr and Hermans 1978; Wolberg 2007). In our study, we used the same concentration of thrombin (2.5 U/mL) for both types of coatings, but we regulated the thrombin adsorption by its washing. This resulted either into the formation of the fibrin mesh with thin fibers or into the coverage of the fibers in the membrane. Other research group described that the low concentration of fibrinogen (under 20 μg/mL) allowed for the parallel orientation of the adsorbed fibrinogen molecules with the substrate, while a high concentration (above 100 μg/mL) oriented the fibrinogen molecules perpendicularly (Dyr *et al.* 1998). This might influence the density, the orientation, and the accessibility of the individual fibrinogen domains for the reaction with thrombin. In our study, we firstly adsorbed fibrinogen in a concentration of 10 μg/mL, and then after the activation of the surface by thrombin, the highly concentrated fibrinogen solution (200 μg/mL) was added. This two-step fibrin preparation was previously utilized by Riedel *et al.* and Bacakova *et al.* in order to create stable fibrin nanocoatings on the material surfaces (Riedel *et al.* 2009; Bacakova *et al.* 2016; Bacakova *et al.* 2017). However, in all these studies the fibrin mesh was formed randomly which resulted into nonhomogeneous fibrin nanocoatings.

In this study, we confirmed the results from our previous works (Bacakova *et al.* 2016; Bacakova *et al.* 2017) and in addition we revealed that the behavior of NHDFs can be modulated by the structure of the fibrin nanocoatings. The morphology of adhered NHDFs was guided by the structure of fibrin. The fibrin coating enabled the spreading of the cells in all directions, while fibrin mesh provided the cells with the relatively flat surface. Therefore, the fibrin coating of individual fibers that followed the 3D structure of the membrane caused a typical spindle-like morphology of NHDFs, and the 2D surface of fibrin mesh bridging the gaps between the fibers enhanced the cell attachment and spreading into a polygonal-like shape (Duval *et al.* 2017). Higher initial adhesion of the fibroblasts on fibrin mesh further

accelerated their proliferation rate, which lead to the faster replacement of the fibrin by the synthetized ECM proteins (Mazlyzam *et al.* 2007). In accordance with our previous results, fibrin, mainly in the form of mesh, stimulated the synthesis and deposition of collagen I and fibronectin by the fibroblasts (Bacakova *et al.* 2016; Bacakova *et al.* 2017). Moreover, the additionally adsorbed fibronectin on both types of fibrin nanocoatings increased the expression of ECM proteins by adhering cells. This cell behavior was also observed by other researchers (Sottile and Hocking 2002; Sethi *et al.* 2002). Due to these observations, we assumed that fibrin mesh with adsorbed fibronectin is the most appropriate substrate with the properties approaching the natural environment of the cells.

5.2 Bi-Layered Skin Constructs Based on the Collagen Gel and Nanofibers

An advanced approach in the wound healing is the construction of bi-layered or even three-layered skin constructs to mimic the structure and physiological conditions of natural skin. We focused in the work of Bacakova and Pajorova *et al.* (2019) on 3D collagen hydrogels that are widely used for the various applications in tissue engineering (Bacakova *et al.* 2019b; Arnette *et al.* 2016; Duval *et al.* 2017). We cultured the HNDFs in 3D microenvironment of a collagen hydrogel and hKs on the 2D flat surface of collagen to create a bi-layered skin construct. The embedding of fibroblasts and other mesenchymal cells into collagen hydrogels has been previously reported by many other researchers. They found that the cells in hydrogels were well-spread in all three dimensions and they created a cell network through the whole 3D scaffold (Miron-Mendoza *et al.* 2012; Sriram *et al.* 2015). Moreover, the flat surface of a hydrogel, mainly collagen IV and collagen I, supported the adhesion, proliferation and stratification of keratinocytes (Sriram *et al.* 2015; Fujisaki *et al.* 2008; Klar *et al.* 2018). It has been also detected that the separated cell layers in the hydrogels were able to communicate by paracrine release of certain cytokines and growth factors or by cell-hydrogel mechanotransduction (Tuan *et al.* 1994; Wojtowicz *et al.* 2014; Doyle and Yamada 2016; Stunova and Vistejnova 2018). The paracrine communication between the cells can be regulated by the structural properties of the cell-encapsulating hydrogels, i.e. by void ratio, thickness and density (Chiu *et al.* 2012; Moreno-Arotzena *et al.* 2015). In addition, the collagen hydrogel stimulated the synthesis of the ECM molecules by the cells, which enhanced the remodeling of the hydrogel and the formation of the basement membrane between the cells (El Ghalbzouri *et al.* 2009; Marionnet *et al.* 2006; Breitkreutz *et al.* 2013). Although the collagen hydrogels have been utilized as 3D culture systems for different purposes in many *in vitro* studies, there are still many limitations that need to be overcome.

First of all, the mechanical stability of the hydrogels has to be improved for wound healing applications. The standard stiffness of the collagen hydrogels that is desirable for the growth of embedded cells varies around units of kPa, depending on collagen concentration, temperature, pH, and duration of neutralization (Achilli and Mantovani 2010; Lopez-Garcia *et al.* 2010). However, the physiological conditions that are required for the cell survival during polymerization caused the softening of the hydrogels (Achilli and Mantovani 2010; Antoine *et al.* 2015) which lead to the contraction of the gel under traction forces of the spreading cells. In order to balance the mechanical stability and the relatively low stiffness of the collagen hydrogels that are both necessary for the proper spreading, growth and migration of the cells, the different strategies were developed. Braziulis *et al.* and Kim *et al.* used plastic compression to improve mechanical stability of the hydrogels (Braziulis *et al.* 2012; Kim *et al.* 2017). Lotz *et al.* decreased the fibroblast-mediated shrinkage of the collagen hydrogel by its cross-linking (Lotz *et al.* 2017). Another approach is to reinforce or to strengthen the hydrogel with other mechanically stable scaffolds. For example, Franco *et al.* combined PCL/PLGA membranes with chitosan-gelatin hydrogels and Hartmann-Fritsch *et al.* strengthened a bi-layered skin construct based on bovine collagen I hydrogel with nanofibrous PLGA membrane or with knitted mesh (Franco *et al.* 2011; Hartmann-Fritsch *et al.* 2016). In our study, we reinforced the collagen hydrogel with the fibrin-coated nanofibrous PLLA membrane, which was tested in our previous studies (Bacakova *et al.* 2016; Bacakova *et al.* 2017; Pajorova *et al.* 2018). However, in contrast to the works where the cells were embedded directly into the collagen hydrogel, we pre-seeded the fibrin-coated membrane with NHDFs and we let them migrate form the membrane into the collagen. Moreover, as we constructed a composite scaffold, the collagen hydrogel and PLLA membrane formed a serial mechanical connection. The collagen hydrogel (up to 21% of compression) had approx. 3 kPa which was in accordance with other studies that measured the collagen stiffness formed in physiological conditions (Achilli and Mantovani 2010; Antoine *et al.* 2015; Xie *et al.* 2017), while the PLLA membrane started to dominate over 56% of compression. The presence of the membrane increased the mechanical stiffness of collagen from approx. 3 kPa to 90 kPa at the membrane-collagen interface.

Another strategy that has been newly described in our work was the migration of fibroblasts from the substrate into the collagen hydrogel. This novel approach reduced the contraction of the collagen hydrogel due to the optimal dynamics of collagen degradation and synthesis by NHDFs during their migration (Miron-Mendoza *et al.* 2012; Sriram *et al.* 2015). Moreover, the cells under the collagen hydrogel were already spread and they gradually

colonized the collagen hydrogel, which generated considerably weaker traction forces on the collagen fibers compared to the traction forces generated by embedded cells. The round embedded cells transmitted intensive traction forces on collagen fibers during their spreading phase, which resulted into massive collagen shrinkage. In addition, based on our previous experiences with nanocoatings, we utilized the fibrin mesh type of nanocoating to increase mechanical properties and the attractiveness of the PLLA membrane for the cells (Pajorova *et al.* 2018). In this study, we found out that the fibrin nanocoating accelerated not only the adhesion and growth but also the migration of NHDFs. Fu *et al.* reported similar results with fibrinogen-coated PCL nanofibers that enhanced fibroblast migration capability and their differentiation to myofibroblasts in the presence of TGF-β1 (Fu *et al.* 2016).

The bi-layered skin construct consisting of the collagen hydrogel colonized by spontaneously immigrated NHDFs was further seeded with hKs. A monolayer of dividing cells was formed after 7 days and the cells stratified into layers. The positive effect of the collagen was reported also in our previous work with HaCaT keratinocytes (Bacakova *et al.* 2017). However, it seems that the structure of the collagen determined the behavior of the keratinocytes (Fu *et al.* 2014). Based on our observations and the results of other researchers, the collagen in the form of hydrogel is a suitable substrate for the growth and stratification of the keratinocytes (Braziulis *et al.* 2012; El Ghalbzouri *et al.* 2009; Hartmann-Fritsch *et al.* 2016). In order to stimulate the differentiation of keratinocyte and their stratifications, the hydrogel properties and the cultivation conditions were optimized. In Bacakova and Pajorova *et al.* (2019) work, the keratinocytes were seeded on a hydrogel made of the rat tail collagen and they were cultured under a liquid surface (Bacakova *et al.* 2019b). However, when we created a pre-vascularized skin construct (Figs. 14 and 15) the hKs were seeded on a perceptibly tougher hydrogel made of porcine collagen, which additionally supported the formation of the layers. Moreover, the stratification of hKs into several layers was further enhanced by the air-liquid interface. We confirmed that collagen in the form of the hydrogel is able to host more than one cell type and provide them with a physiological 3D (micro)environment with sufficient permeability of nutrients (Pajorova *et al.*, manuscript in preparation).

The absence of a functional capillary-like network is still one of the major unresolved tasks of tissue-engineered fully functional skin substitutes. The non-vascularized bi-layered skin constructs after implantation suffer by insufficient supplies of oxygen, nutrients and growth factors (Huang *et al.* 2012; Du *et al.* 2017). Therefore, we pre-vascularized our previously described collagen-based bi-layered skin construct using ADSCs and HUVECs

(Pajorova *et al.*, manuscript in preparation). Similarly, as it was described with the NHDFs in the work of Bacakova and Pajorova *et al.* (2019), we let the ADSCs migrate from the fibrin-coated membrane into the collagen hydrogel. However, in order to create a capillary-like network, we embedded the HUVECs into the collagen hydrogel during the polymerization. The formation of capillaries was supported by supplements such as VEGF that is the most potent proangiogenic factor and by bFGF that stimulates the growth and migration of endothelial cells (Xue and Greisler 2002). It has been reported that biological activity of bFGF bounded to fibrin or to fibrinogen remained unchanged compared to unbounded bFGF, which additionally stimulated the proliferation of endothelial cells (Otrock *et al.* 2007). Therefore, we utilized the "fibrin mesh" type of nanocoating to accelerate the growth and migration of both cell types (Pajorova *et al.* 2018).

It has been detected that the mural cells, i.e. smooth muscle cells (Heydarkhan-Hagvall *et al.* 2003) or pericytes (Jain 2003) are able to surround and stabilize endothelial cells, which positively stimulate the angiogenesis. Since pericytes produce proangiogenic growth factors that lead the endothelial cells into a capillary formation (Bergers and Song 2005), we selected the most CD146 positive group of ADSCs that might have the most similar behavior to the pericytes, i.e. the proangiogenic effect. The similar strategy was described by Chan *et al.* who used the ADSCs isolated from burned military patients to create a three-layered skin construct consisting of a collagen–polyethyleneglycol–fibrin hydrogel. They found out that the adipose-derived stem cells isolated from discarded burned skin (dsADSCs) are capable to grow and differentiate even though the percentage of burned total body surface area was great. Moreover, they detected that dsADSCs in the collagen layer exhibited spindle-like morphology, while dsADSCs in the polyethyleneglycol–fibrin layer formed tubular structures and eventually created a dense network (Chan *et al.* 2012). Based on their results and our observations, we suppose that the constructs consisting of fibrin and ADSCs enhanced the vascularization of the dermal equivalents.

However, unlike to the Chan *et al.*, we additionally embedded the HUVECs into the collagen to accelerate the formation of the tubular structure. Although the endothelial cells (ECs) and endothelial progenitor cells (EPCs) has been previously utilized in many works related to the construction of pre-vascularized skin substitutes (Tremblay *et al.* 2005; Marino *et al.* 2014), they usually required the presence of another mesenchymal stem cells (MSCs) to achieve a mature vascular character. Therefore, we combined the HUVECs embedded in collagen gel with ADSCs that migrated from fibrin-coated membrane. Using the ADSCs that were not embedded in collagen gel, we supported the gradual capillary-like network

formation especially on the fibrin-collagen interface, where the ADSCs can interact with embedded HUVECs. A similar cell setup was used by Duttenhoefer *et al.* who pre-vascularized a synthetic polyurethane-based 3D scaffold by seeding the EPCs together with MSCs (Duttenhoefer *et al.* 2013). In another work, Baltazar *et al.* used the method of 3D printing to create a pre-vascularized skin substitute. In order to form the pre-vascularized dermis, they embedded human ECs with the human foreskin dermal fibroblasts and the human placental pericytes instead of ADSCs into the printed rat tail collagen type I. The human foreskin keratinocytes were further printed on this dermal construct to form an epidermis (Baltazar *et al.* 2020). Due to the similar results that we achieved, we could assume that the ADSCs can fully substitute the functions of fibroblasts and also of pericytes in a newly formed pre-vascularized dermis. Interestingly, we also noticed in our experiments (Figs. 14 and 15) that the embedded HUVECs were able to create not only a capillary-like network in the collagen hydrogel, but they also formed a cell monolayer on the surface of the hydrogel when the hKs were absent (Pajorova *et al.*, manuscript in preparation). The same behavior of endothelial cells was described by Abe *et al.* with ECs cultivated on the collagen gel that were affected by EPCs embedded between the layers of the collagen hydrogel (Abe *et al.* 2013).

Karl *et al.* described another strategy, in which they used fresh stromal vascular fraction (SVF) isolated from human fat instead of ADSCs and HUVECs (Klar *et al.* 2014). This enabled them to avoid the complicated isolation process, while the SVF – a mixture of multipotent stem cells, endothelial cells, stromal cells, pericytes, preadipocytes, and hematopoietic cells – was able to spontaneously develop the capillaries (Koh *et al.* 2011; Klar *et al.* 2017b). This strategy seems to be promising for clinical applications due to short time of cultivation and less immunogenicity compared to the use of ADSCs and HUVECs. However, the composition of the cells in SVF might differ, which makes the behavior of the cells in the final construct less predictable. Therefore, in their next study (Klar *et al.* 2016), they isolated and separated the ADSCs and ECs from SVF and they observed the behavior only of these two cell types in the collagen and in fibrin hydrogels. In contrast to our study, Klar *et al*. in both works embedded the cells directly into the hydrogels, which probably increased the shrinkage of the hydrogels as it was discussed in Bacakova and Pajorova *et al.* (2019).

The pre-vascularization of 3D scaffolds seems to be promising strategy that can accelerate blood supply into a wound bed. The capillaries formed before the engraftment of the skin substitute are capable to anastomose with the host vessel, which can increase the cell survival and decreases the rejection of a skin substitute (Laschke and Menger 2012; Baranski

et al. 2013; Moon and West 2008). Moreover, it has been demonstrated that the pre-vascularized skin constructs with rapid perfusion reduced the contraction of a wound bed by increasing the collagen type I deposition and by supporting the proliferation of both dermal and epidermal cells (Klar *et al.* 2014).

5.3 Temporary Cell-Decorated Wound Dressings Based on Cellulose

Last but not least strategy is the coverage of the wounds by intelligent wound dressings that can be enriched with gradually releasing drugs or other substances promoting the healing process (Zikmundova *et al.* 2020; Tavakoli and Klar 2020). These dressings can also be temporary cell carriers, which can simultaneously regulate the amount of exudates and maintain the optimum moisture level, oxygen permeability, and sterility in the wound (Bacakova *et al.* 2019a; Tavakoli and Klar 2020). In order to increase the attachment of NHDFs or ADSCs on the wound dressings, we covered the cellulose-based meshes with nature-derived nanocoatings. In Pajorova *et al.* (2020), we combined cellulose mesh with CNFs with different surface charges and in Bacakova *et al.* (2018) we coated Hcel® NaT cellulose mesh with fibrin nanocoatings (Pajorova *et al.* 2020; Bacakova *et al.* 2018b). Since the beneficial effect of fibrin on the fibroblast attachment and growth has been already discussed (Pajorova *et al.* 2018; Bacakova *et al.* 2017), this part will be focused mainly on nanocoatings made of CNFs (Pajorova *et al.* 2020).

In the first part of Pajorova *et al.* (2020) study, we focused on the preparation and characterization of the CNF-based coatings, especially their structure, roughness, wettability and stiffness. Based on the amount of the CNF solutions and the charge of CNF solutions, we were able to modulate the surface properties, which further affected the cell behavior. The responses of NHDFs and ADSCs were then evaluated in the second part of this study. We proposed 2D film-like coatings and 3D coatings made of negatively-charged (aCNFs), positively-charged (cCNFs) and combined (c+aCNFs) nanocellulose. Although the CNF coatings were much softer than the conventional cell culture substrates (GPa) (Skardal *et al.* 2013), they were still relatively stiff for the cells. For example, Achterberg et al. found out that the Young's modulus of native human dermis at the cell perception level range between 0.1 and 10 kPa, which is at least 10 times softer than our CNF coatings (Achterberg *et al.* 2014). However, not only the stiffness but also the alterations in the surface roughness can influence the initial adhesion of the cells. We observed that the roughness of c+aCNFs (Ra ~ 55.76 nm) was significantly higher compared to aCNFs and cCNFs. The roughness of c+aCNFs corresponds to the surfaces with lower studied roughness measured by Hou with co-

authors. They showed that the substrates with the lowest studied roughness (Ra ~ 31.49 nm) supported cell adhesion and spreading, while the intermediate roughness (Ra ~ 183.16 nm) positively affected also the cell−substrate tension forces and differentiation of mesenchymal stem cells (Hou *et al.* 2020).

Although the studied CNF coatings differ in many parameters, we assume that the main cell adhesion-modulating factor is the surface chemistry of CNFs. The surface chemistry can determine the composition of proteins adsorbed on CNF coatings (Syverud 2017). These adhesion-mediating proteins can further influence the cell behavior via specific amino acid sequences that can be recognized by integrin receptors on the cells. We observed that the dynamics with which the proteins were adsorbed and interchanged in time on CNF surfaces – i.e., the Vroman effect – probably strongly affected the attachment of NHDFs and ADSCs (Vroman *et al.* 1980; Bacakova *et al.* 2011). We detected that positively charged trimethylammonium ($-N(CH_3)_3^+$) tails of cCNFs adsorbed more proteins, mainly BSA, than negatively charged carboxyl ($-COO^-$) functional groups of aCNFs. The cCNF surface with a positive charge probably attracted the negatively-charged proteins such as fibronectin, vitronectin, and BSA. However, due to the 100 – 1000 times higher concentration of BSA than the other proteins in FBS, we can expect that the most abundant protein present on cCNFs was cell-non-adhesive BSA (Hoshiba *et al.* 2018; Arima and Iwata 2007). The cell-non-adhesive BSA might cause the poor adhesion of the cells after 7 days of cultivation in our study. Similar results were also observed by Courtenay *et al.*, who quantified the proteins adsorbed from FBS, specifically BSA, on cCNF scaffolds (Courtenay *et al.* 2019; Attwood *et al.* 2019). However, Hoshiba *et al.* showed the protein composition of the most superficial layer is more important for cell adhesion and growth than the absolute amount of adsorbed proteins (Hoshiba *et al.* 2018). Therefore, the negatively charged CNFs promoted the cell attachment better than cCNFs. Although aCNFs adsorbed less proteins, they probably contained more cell adhesion-mediating proteins in a superficial layer that can be perceived by the cells. The comparable results were reported also by many other researchers with negatively charged $-COO^-$-terminated surfaces (Courtenay *et al.* 2017; Hoshiba *et al.* 2018; Faucheux *et al.* 2004).

In addition, we also found that the adsorbed BSA on cCNF coatings decreased the amount of initially adhered NHDFs, but it did not affect the number of attached ADSCs. Based on results described by Courtenay *et al.*, we can assume that both cells were electrostatically attracted by the positive charge of the cCNFs in a serum-free medium (Courtenay *et al.* 2018; Courtenay *et al.* 2017). However, in contrast to their results, the

ADSCs were able to adhere also in a serum-containing medium, which could be due to the faster adhesion of ADSCs compared to NHDFs. We suppose that the adsorption of BSA in a large quantity was slower than the adhesion of ADSCs. This hypothesis was confirmed by pre-adsorption of BSA or FBS proteins on cCNFs and subsequent inability of both cells to adhere. In contrast to cCNFs, the negatively charged aCNFs enabled the adhesion of both cells only in the serum-containing medium. In case of combined c+aCNFs the adhesion and proliferation of both cells was comparable with aCNFs, while the yields of proteins from FBS, mainly BSA, were similar to cCNFs. This opposite response of the cells on abundantly adsorbed BSA on c+aCNFs can be explained by the comparable wettability of c+aCNFs with aCNFs. While c+aCNFs with aCNFs had hydrophilic character, the cCNFs were rather hydrophobic. In the work of Arima and Iwata, it has been detected that moderately hydrophilic surfaces increased the cell adhesion even though they were pre-adsorbed with BSA, while hydrophobic surfaces pre-adsorbed with BSA inhibited cell adhesion. They assume that the strongly adsorbed BSA on hydrophobic surfaces cannot be replaced with cell adhesion-mediating proteins as effectively as on hydrophilic surfaces. This behavior corresponds to that on hydrophilic c+aCNF coatings, where the cell adhesion rate was high although there was adsorbed a lot of cell-non-adhesive BSA from FBS (Arima and Iwata 2007).

Based on our results, we suggest that the 2D film-like coatings ("fibrin mesh" type of nanocoating or c+aCNFs), where the cells created a confluent layer, can be applicable in the cell sheet technology. The cell sheet can be manually separated from a dressing or as it has been previously described, the cell monolayers can be easily released from the CNFs using cellulase enzymes. These enzymes are noncytotoxic for the cells and preserve the cell-to-cell contacts (Sakai *et al.* 2009). In contrast to the 2D film-like CNF coatings, the 3D substrates made of aCNFs or "fibrin coating" type of nanocoatings mesh might provide a physiological microenvironment for long-term cell cultivation with better diffusion of nutrients than the widely used hydrogels (Duval *et al.* 2017).

6 Conclusion

This work is focused mainly on the construction of a pre-vascularized skin substitute and partially on the development of cellulose-based wound dressing. The first main objective of this work was divided into separate tasks and the results were published in five impacted papers.

The first task on a way to create the pre-vascularized skin substitute was to find an appropriate substrate on which would be this bi-layered skin construct built up, i.e. the biodegradable membrane with suitable properties for cell adhesion and growth. The hypothesis was that the protein-coated nanofibrous membranes (PLA, PLLA, PLGA) are suitable for the construction of a bioengineered skin substitute. We confirmed that the cell colonization of the membranes was accelerated by the protein nanocoatings; specifically, the proliferation of NHDFs and ADSCs was enhanced by the fibrin nanocoatings, while HaCaT keratinocytes grew better on the collagen nanocoatings. Moreover, we showed that the behavior of the cells depended not only on the presence of the fibrin nanocoatings on the membranes but also on the structure of the fibrin nanocoatings. The fibrin nanocoatings in the form of the fibrin mesh was selected as the most appropriate protein modification of nanofibrous membranes for adhesion and growth of NHDFs and ADSCs.

The second task was to create an optimal 3D environment which would mimic the physiological properties of dermis and epidermis. We used the rat tail and porcine collagen to prepare the collagen hydrogel on the surface of the fibrin-coated PLLA membranes that were pre-seeded with NHDFs or ADSCs. The hypothesis was that the NHDFs and ADSCs are able to migrate from the substrate into the collagen hydrogel and the keratinocytes are able to grow and stratify on the surface of the collagen hydrogel. We proved that the collagen in the form of a hydrogel with optimal mechanical properties attracted the NHDFs and ADSCs growth on the fibrin-coated membrane, and it also provided the keratinocytes with an appropriate surface for their growth and stratification.

The third task was to develop the pre-vascularized skin substitute. In order to support the formation of capillary-like network, we co-cultured ADSCs with HUVECs in the collagen hydrogel. The hypothesis was that the ADSCs are able to support the spontaneous formation of the tubular structures from the embedded HUVECs and thereby they could accelerate the vascularization of the collagen-based skin substitutes. We demonstrated that the ADSCs migrated from the membrane into the collagen and that they interacted with embedded HUVECs that formed tubular structures in several layers of the collagen hydrogel. This layer,

which can be referred to as dermal equivalent, was simultaneously seeded by keratinocytes that were able to create several layers of differentiated cells, which can be referred to epidermal equivalent.

The second objective of this work was to develop temporary cellulose-based wound dressings. The results were described in two impacted papers. In order to improve the material properties for cell adhesion, the cellulose-based materials were coated with fibrin or with charged CNFs. The hypothesis was that the modified cellulose-based materials enhanced the adhesion and growth of the cells by specific adsorption of cell adhesion-mediating proteins. We confirmed that both fibrin and charged CNFs improved the cell adhesion on the cellulose mesh, however the fibrin was degraded within one week by the cells. Therefore, we used more stable CNF coatings, on which the cells were able to create sheet of the cells that could be carried into the wound and detached by the cellulase enzymes. We additionally observed that the negatively-charged aCNFs accelerated the cell adhesion and growth, while positively-charged cCNFs rather decreased the cell adhesion and spreading. However, it depended on the cell type and on the spectrum of cell adhesion-modulating proteins, adsorbed on the surface of different CNF coatings.

We can sum up that the skin cells and adipose-derived stem cells can be cultured in 3D environment of the collagen hydrogel reinforced by the fibrin-coated mesh as well as on the modified cellulose-based materials to develop a pre-vascularized skin substitute or a temporary wound dressing.

7 Summary

The creation of a bi-layered pre-vascularized skin construct as well as the development of nature-derived wound dressings were the main areas of our focus. Partial results were presented in seven impacted publications and in one prepared manuscript.

Firstly, we developed single-layered skin substitutes based on protein-coated biodegradable nanofibrous membranes that preceded the bi-layered skin constructs. We demonstrated that the adhesion and growth of human fibroblasts and adipose-tissue derived stem cells (ADSCs) were accelerated using fibrin nanocoatings, while the collagen nanocoating had a positive effect on keratinocyte behavior. These observations were further utilized for the construction of the bi-layered skin constructs where the fibroblasts or ADSCs migrated from a fibrin-coated nanofibrous membrane into the collagen hydrogel and keratinocytes were seeded on the surface of the collagen. Moreover, we optimized the structure of the fibrin to increase the efficiency of the cell initial attachment and their further growth. The development of the pre-vascularized bi-layered skin construct was highly motivated by the lack of the nutrition supplies in the destroyed tissue. In order to vascularize our bi-layered skin construct, we combined ADSCs isolated from donors and endothelial cells. The embedded endothelial cells in the collagen hydrogel were able to form a capillary-like network in the presence of the ADSCs that migrated from the nanofibrous membrane. This part of the construct was created to mimic the dermis, while the differentiating and stratifying keratinocytes were cultured on the surface of the collagen hydrogel to create the epidermis. We assume that the pre-vascularization can improve the acceptability of a tissue-engineered skin substitute by the host, however there are still many tasks to be solved on the way to develop a fully functional skin construct.

Secondly, we contributed to the research on cellulose-based wound dressings. The commercially available cellulose mesh was coated with two types of fibrin nanocoatings or with cellulose nanofibers (CNFs). Using the fibrin coatings, we increased the cell adhesion and proliferation on the cellulose mesh. However, both types of fibrin coatings were degraded by the cells after one week of cultivation and the cells penetrated into the mesh, which might cause undesirable attachment of the dressing to a wound. Therefore, we further coated the cellulose mesh by CNFs that are stable due to absence of cellulase enzyme expression in human cells. In this work, we observed that anionic CNFs accelerated the colonization of the cellulose mesh by the cells, while cationic CNFs rather decreased it. However, this was strongly dependent on the cell types and the cell culture conditions.

8 Souhrn

Naším hlavním záměrem bylo zhotovení dvouvrstvé prevaskularizované kožní náhrady a vývoj kožního krytu z přírodního materiálu. Jednotlivé výsledky byly publikovány v sedmi impaktovaných publikacích a jsou zahrnuty i v jedné připravované publikaci.

Jako první jsme vytvořili jednovrstvou kožní náhradu z biodegradabilní nanovlákenné membrány potažené proteiny, která předcházela dvouvrstvé kožní náhradě. Ukázali jsme, že fibrinová nanovrstva zlepšuje adhezi a růst lidských fibroblastů a kmenových buněk z tukové tkáně, zatímco kolagenní nanovrstva má pozitivní vliv spíše na keratinocyty. Tyto poznatky jsme využili pro konstrukci dvouvrstvé kožní náhrady. Fibroblasty a kmenové buňky z tukové tkáně migrovaly z nanovláken potažených fibrinem do kolagenového gelu, který byl následně osazen keratinocyty. Navíc jsme také vylepšili strukturu fibrinové nanovrstvy za účelem zrychlení adheze buněk a jejich následného růstu. Vývoj prevaskularizovaného dvouvrstvého kožního konstruktu byl motivován nedostatečným zásobením poraněné tkáně nutrienty. Za účelem prevaskularizace našeho dvouvrstvého konstruktu jsme zkombinovali izolované kmenové buňky z tukové tkáně s endotelovými buňkami. Endotelové buňky zalité v kolagenovém hydrogelu v přítomnosti kmenových buněk z tukové tkáně formovaly útvary podobné kapilární síti. Tato část konstruktu byla vytvořena za účelem napodobení dermis, zatímco diferencující a stratifikující keratinocyty byly kultivovány na povrchu kolagenového hydrogelu za účelem vytvoření epidermis. Domníváme se, že prevaskularizace může zlepšit přijetí uměle vytvořené kožní náhrady, avšak pro vytvoření plně funkční kožní náhrady je nutno vyřešit ještě mnoho problémů.

Ve druhé části jsme přispěli k výzkumu kožních krytů vytvořených z celulózy. Komerčně dostupnou celulózovou textilii jsme potáhli dvěma typy fibrinových nanovrstev nebo celulózovými nanovlákny (CNFs). Použitím fibrinových nanovrstev jsme zlepšili adhezi a proliferaci buněk na celulózových textiliích. Nicméně oba typy fibrinových nano-vrstev degradovaly týden po kultivaci a tím buňky prorůstaly do textilie. To by mohlo způsobit nežádoucí přihojení kožního krytu k ráně, a proto jsme celulózovou textilii zkusili potáhnout také celulózovými nanovlákny, které jsou stabilní díky absenci exprese enzymů celuláz v lidských buňkách. V této prací jsme pozorovali, že vrstva anionických CNFs zrychluje kolonizaci celulózové textilie buňkami, zatímco vrstva kationických CNFs snižuje adhezi a rozprostření buněk. Výsledky však závisely na typu buněk a podmínkách buněčné kultivace.

9 References

1. Abe Y, Ozaki Y, Kasuya J, Yamamoto K, Ando J, Sudo R, Ikeda M, Tanishita K (**2013**). Endothelial Progenitor Cells Promote Directional Three-Dimensional Endothelial Network Formation by Secreting Vascular Endothelial Growth Factor. *PLoS One,* 8 (12).
2. Ahearne M (**2014**). Introduction to Cell-Hydrogel Mechanosensing. *Interface Focus,* 4 (2):20130038.
3. Achilli M, Mantovani D (**2010**). Tailoring Mechanical Properties of Collagen-Based Scaffolds for Vascular Tissue Engineering: The Effects of Ph, Temperature and Ionic Strength on Gelation. *Polymers,* 2 (4):664-680.
4. Achterberg VF, Buscemi L, Diekmann H, Smith-Clerc J, Schwengler H, Meister JJ, Wenck H, Gallinat S, Hinz B (**2014**). The Nano-Scale Mechanical Properties of the Extracellular Matrix Regulate Dermal Fibroblast Function. *J Invest Dermatol,* 134 (7):1862-1872.
5. Ajalloueian F, Tavanai H, Hilborn J, Donzel-Gargand O, Leifer K, Wickham A, Arpanaei A (**2014**). Emulsion Electrospinning as an Approach to Fabricate Plga/Chitosan Nanofibers for Biomedical Applications. *Biomed Res Int,* 2014:475280.
6. Akkouch A, Shi G, Zhang Z, Rouabhia M (**2010**). Bioactivating Electrically Conducting Polypyrrole with Fibronectin and Bovine Serum Albumin. *J Biomed Mater Res A,* 92 (1):221-231.
7. Anderson JM, Shive MS (**1997**). Biodegradation and Biocompatibility of Pla and Plga Microspheres. *Adv Drug Deliv Rev,* 28 (1):5-24.
8. Antoine EE, Vlachos PP, Rylander MN (**2015**). Tunable Collagen I Hydrogels for Engineered Physiological Tissue Micro-Environments. *PLoS One,* 10 (3).
9. Arima Y, Iwata H (**2007**). Effect of Wettability and Surface Functional Groups on Protein Adsorption and Cell Adhesion Using Well-Defined Mixed Self-Assembled Monolayers. *Biomaterials,* 28 (20):3074-3082.
10. Arnette C, Koetsier JL, Hoover P, Getsios S, Green KJ (**2016**). In Vitro Model of the Epidermis: Connecting Protein Function to 3d Structure. *Methods Enzymol,* 569:287-308.
11. Attwood SJ, Kershaw R, Uddin S, Bishop SM, Welland ME (**2019**). Understanding How Charge and Hydrophobicity Influence Globular Protein Adsorption to Alkanethiol and Material Surfaces. *J. Mater. Chem. B,* 7 (14):2349-2361.
12. Augustine R (**2018**). Skin Bioprinting: A Novel Approach for Creating Artificial Skin from Synthetic and Natural Building Blocks. *Prog Biomater*.
13. Auxenfans C, Menet V, Catherine Z, Shipkov H, Lacroix P, Bertin-Maghit M, Damour O, Braye F (**2015**). Cultured Autologous Keratinocytes in the Treatment of Large and Deep Burns: A Retrospective Study over 15 Years. *Burns,* 41 (1):71-79.

14. Bacakova L, Filova E, Parizek M, Ruml T, Svorcik V (**2011**). Modulation of Cell Adhesion, Proliferation and Differentiation on Materials Designed for Body Implants. *Biotechnol Adv,* 29 (6):739-767.

15. Bacakova L, Novotna K, Parizek M (**2014**). Polysaccharides as Cell Carriers for Tissue Engineering: The Use of Cellulose in Vascular Wall Reconstruction. *Physiol Res,* 63 Suppl 1:S29-47.

16. Bacakova L, Pajorova J, Bacakova M, Skogberg A, Kallio P, Kolarova K, Svorcik V (**2019a**). Versatile Application of Nanocellulose: From Industry to Skin Tissue Engineering and Wound Healing. *Nanomaterials (Basel),* 9 (2).

17. Bacakova L, Zarubova J, Travnickova M, Musilkova J, Pajorova J, Slepicka P, Kasalkova NS, Svorcik V, Kolska Z, Motarjemi H, Molitor M (**2018a**). Stem Cells: Their Source, Potency and Use in Regenerative Therapies with Focus on Adipose-Derived Stem Cells - a Review. *Biotechnol Adv,* 36 (4):1111-1126.

18. Bacakova M, Musilkova J, Riedel T, Stranska D, Brynda E, Zaloudkova M, Bacakova L (**2016**). The Potential Applications of Fibrin-Coated Electrospun Polylactide Nanofibers in Skin Tissue Engineering. *Int J Nanomedicine,* 11:771-789.

19. Bacakova M, Pajorova J, Broz A, Hadraba D, Lopot F, Zavadakova A, Vistejnova L, Beno M, Kostic I, Jencova V, Bacakova L (**2019b**). A Two-Layer Skin Construct Consisting of a Collagen Hydrogel Reinforced by a Fibrin-Coated Polylactide Nanofibrous Membrane. *Int J Nanomedicine,* 14:5033-5050.

20. Bacakova M, Pajorova J, Sopuch T, Bacakova L (**2018b**). Fibrin-Modified Cellulose as a Promising Dressing for Accelerated Wound Healing. *Materials (Basel),* 11 (11).

21. Bacakova M, Pajorova J, Stranska D, Hadraba D, Lopot F, Riedel T, Brynda E, Zaloudkova M, Bacakova L (**2017**). Protein Nanocoatings on Synthetic Polymeric Nanofibrous Membranes Designed as Carriers for Skin Cells. *Int J Nanomedicine,* 12:1143-1160.

22. Bader RA, Kao WJ (**2009**). Modulation of the Keratinocyte-Fibroblast Paracrine Relationship with Gelatin-Based Semi-Interpenetrating Networks Containing Bioactive Factors for Wound Repair. *J Biomater Sci Polym Ed,* 20 (7-8):1005-1030.

23. Baltazar T, Merola J, Catarino C, Xie CB, Kirkiles-Smith NC, Lee V, Hotta S, Dai GH, Xu XW, Ferreira FC, Saltzman WM, Pober JS, Karande P (**2020**). Three Dimensional Bioprinting of a Vascularized and Perfusable Skin Graft Using Human Keratinocytes, Fibroblasts, Pericytes, and Endothelial Cells. *Tissue Engineering Part A,* 26 (5-6):227-238.

24. Bao P, Kodra A, Tomic-Canic M, Golinko MS, Ehrlich HP, Brem H (**2009**). The Role of Vascular Endothelial Growth Factor in Wound Healing. *J Surg Res,* 153 (2):347-358.

25. Baranski JD, Chaturvedi RR, Stevens KR, Eyckmans J, Carvalho B, Solorzano RD, Yang MT, Miller JS, Bhatia SN, Chen CS (**2013**). Geometric Control of Vascular

Networks to Enhance Engineered Tissue Integration and Function. *Proc Natl Acad Sci U S A,* 110 (19):7586-7591.

26. Behm B, Babilas P, Landthaler M, Schreml S (**2012**). Cytokines, Chemokines and Growth Factors in Wound Healing. *J Eur Acad Dermatol Venereol,* 26 (7):812-820.

27. Bell E, Ivarsson B, Merrill C (**1979**). Production of a Tissue-Like Structure by Contraction of Collagen Lattices by Human Fibroblasts of Different Proliferative Potential in Vitro. *Proc Natl Acad Sci U S A,* 76 (3):1274-1278.

28. Benny P, Badowski C, Lane EB, Raghunath M (**2015**). Making More Matrix: Enhancing the Deposition of Dermal-Epidermal Junction Components in Vitro and Accelerating Organotypic Skin Culture Development, Using Macromolecular Crowding. *Tissue Eng Part A,* 21 (1-2):183-192.

29. Bergers G, Song S (**2005**). The Role of Pericytes in Blood-Vessel Formation and Maintenance. *Neuro-Oncology,* 7 (4):452-464.

30. Boyce ST, Kagan RJ, Greenhalgh DG, Warner P, Yakuboff KP, Palmieri T, Warden GD (**2006**). Cultured Skin Substitutes Reduce Requirements for Harvesting of Skin Autograft for Closure of Excised, Full-Thickness Burns. *J Trauma,* 60 (4):821-829.

31. Braziulis E, Diezi M, Biedermann T, Pontiggia L, Schmucki M, Hartmann-Fritsch F, Luginbuhl J, Schiestl C, Meuli M, Reichmann E (**2012**). Modified Plastic Compression of Collagen Hydrogels Provides an Ideal Matrix for Clinically Applicable Skin Substitutes. *Tissue Eng Part C Methods,* 18 (6):464-474.

32. Breitkreutz D, Koxholt I, Thiemann K, Nischt R (**2013**). Skin Basement Membrane: The Foundation of Epidermal Integrity--Bm Functions and Diverse Roles of Bridging Molecules Nidogen and Perlecan. *Biomed Res Int,* 2013:179784.

33. Brohem CA, Cardeal LB, Tiago M, Soengas MS, Barros SB, Maria-Engler SS (**2011**). Artificial Skin in Perspective: Concepts and Applications. *Pigment Cell Melanoma Res,* 24 (1):35-50.

34. Candi E, Schmidt R, Melino G (**2005**). The Cornified Envelope: A Model of Cell Death in the Skin. *Nat Rev Mol Cell Biol,* 6 (4):328-340.

35. Carr ME, Hermans J (**1978**). Size and Density of Fibrin Fibers from Turbidity. *Macromolecules,* 11 (1):46-50.

36. Carsin H, Ainaud P, Le Bever H, Rives J, Lakhel A, Stephanazzi J, Lambert F, Perrot J (**2000**). Cultured Epithelial Autografts in Extensive Burn Coverage of Severely Traumatized Patients: A Five Year Single-Center Experience with 30 Patients. *Burns,* 26 (4):379-387.

37. Clark RA, Ghosh K, Tonnesen MG (**2007**). Tissue Engineering for Cutaneous Wounds. *J Invest Dermatol,* 127 (5):1018-1029.

38. Colwell AS, Beanes SR, Soo C, Dang C, Ting K, Longaker MT, Atkinson JB, Lorenz HP (**2005**). Increased Angiogenesis and Expression of Vascular Endothelial Growth Factor During Scarless Repair. *Plast Reconstr Surg,* 115 (1):204-212.

39. Converse JM, Smahel J, Ballantyne DL, Jr., Harper AD (**1975**). Inosculation of Vessels of Skin Graft and Host Bed: A Fortuitous Encounter. *Br J Plast Surg,* 28 (4):274-282.

40. Costanzo A, Fausti F, Spallone G, Moretti F, Narcisi A, Botti E (**2015**). Programmed Cell Death in the Skin. *Int J Dev Biol,* 59 (1-3):73-78.

41. Courtenay JC, Deneke C, Lanzoni EM, Costa CA, Bae Y, Scott JL, Sharma RI (**2018**). Modulating Cell Response on Cellulose Surfaces; Tunable Attachment and Scaffold Mechanics. *Cellulose,* 25 (2):925-940.

42. Courtenay JC, Filgueiras JG, deAzevedo ER, Jin Y, Edler KJ, Sharma RI, Scott JL (**2019**). Mechanically Robust Cationic Cellulose Nanofibril 3d Scaffolds with Tuneable Biomimetic Porosity for Cell Culture. *Journal of Materials Chemistry B,* 7 (1):53-64.

43. Courtenay JC, Johns MA, Galembeck F, Deneke C, Lanzoni EM, Costa CA, Scott JL, Sharma RI (**2017**). Surface Modified Cellulose Scaffolds for Tissue Engineering. *Cellulose,* 24 (1):253-267.

44. Dagregorio G, Guillet G (**2005**). Artificial Skin as a Valuable Adjunct to Surgical Treatment of a Large Squamous Cell Carcinoma in a Patient with Epidermolysis Bullosa. *Dermatol Surg,* 31 (4):474-476.

45. Dai NT, Huang WS, Chang FW, Wei LG, Huang TC, Li JK, Fu KY, Dai LG, Hsieh PS, Huang NC, Wang YW, Chang HI, Parungao R, Wang Y (**2018**). Development of a Novel Pre-Vascularized Three-Dimensional Skin Substitute Using Blood Plasma Gel. *Cell Transplant,* 27 (10):1535-1547.

46. Darby I, Skalli O, Gabbiani G (**1990**). Alpha-Smooth Muscle Actin Is Transiently Expressed by Myofibroblasts During Experimental Wound Healing. *Lab Invest,* 63 (1):21-29.

47. Darby IA, Laverdet B, Bonte F, Desmouliere A (**2014**). Fibroblasts and Myofibroblasts in Wound Healing. *Clin Cosmet Investig Dermatol,* 7:301-311.

48. Deng A, Yang Y, Du S, Yang S (**2018**). Electrospinning of in Situ Crosslinked Recombinant Human Collagen Peptide/Chitosan Nanofibers for Wound Healing. *Biomater Sci,* 6 (8):2197-2208.

49. Dong RH, Jia YX, Qin CC, Zhan L, Yan X, Cui L, Zhou Y, Jiang X, Long YZ (**2016**). In Situ Deposition of a Personalized Nanofibrous Dressing Via a Handy Electrospinning Device for Skin Wound Care. *Nanoscale,* 8 (6):3482-3488.

50. Doyle AD, Yamada KM (**2016**). Mechanosensing Via Cell-Matrix Adhesions in 3d Microenvironments. *Exp Cell Res,* 343 (1):60-66.

51. Du P, Suhaeri M, Ha SS, Oh SJ, Kim SH, Park K (**2017**). Human Lung Fibroblast-Derived Matrix Facilitates Vascular Morphogenesis in 3d Environment and Enhances Skin Wound Healing. *Acta Biomater,* 54:333-344.

52. Dulmovits BM, Herman IM (**2012**). Microvascular Remodeling and Wound Healing: A Role for Pericytes. *Int J Biochem Cell Biol,* 44 (11):1800-1812.

53. Duttenhoefer F, de Freitas RL, Meury T, Loibl M, Benneker LM, Richards RG, Alini M, Verrier S (**2013**). 3d Scaffolds Co-Seeded with Human Endothelial Progenitor and Mesenchymal Stem Cells: Evidence of Prevascularisation within 7 Days. *Eur Cell Mater,* 26:49-65.

54. Duval K, Grover H, Han LH, Mou Y, Pegoraro AF, Fredberg J, Chen Z (**2017**). Modeling Physiological Events in 2d Vs. 3d Cell Culture. *Physiology (Bethesda),* 32 (4):266-277.

55. Dyr JE, Tichy I, Jirouskova M, Tobiska P, Slavik R, Homola J, Brynda E, Houska M, Suttnar J (**1998**). Molecular Arrangement of Adsorbed Fibrinogen Molecules Characterized by Specific Monoclonal Antibodies and a Surface Plasmon Resonance Sensor. *Sensors and Actuators B-Chemical,* 51 (1-3):268-272.

56. Eastwood M, Porter R, Khan U, McGrouther G, Brown R (**1996**). Quantitative Analysis of Collagen Gel Contractile Forces Generated by Dermal Fibroblasts and the Relationship to Cell Morphology. *J Cell Physiol,* 166 (1):33-42.

57. El Ghalbzouri A, Commandeur S, Rietveld MH, Mulder AA, Willemze R (**2009**). Replacement of Animal-Derived Collagen Matrix by Human Fibroblast-Derived Dermal Matrix for Human Skin Equivalent Products. *Biomaterials,* 30 (1):71-78.

58. Elineni KK, Gallant ND (**2011**). Regulation of Cell Adhesion Strength by Peripheral Focal Adhesion Distribution. *Biophys J,* 101 (12):2903-2911.

59. Engler A, Bacakova L, Newman C, Hategan A, Griffin M, Discher D (**2004**). Substrate Compliance Versus Ligand Density in Cell on Gel Responses. *Biophys J,* 86 (1 Pt 1):617-628.

60. Eskandarlou M, Azimi M, Rabiee S, Seif Rabiee MA (**2016**). The Healing Effect of Amniotic Membrane in Burn Patients. *World J Plast Surg,* 5 (1):39-44.

61. Estes BT, Diekman BO, Gimble JM, Guilak F (**2010**). Isolation of Adipose-Derived Stem Cells and Their Induction to a Chondrogenic Phenotype. *Nature Protocols,* 5 (7):1294-1311.

62. Etulain J (**2018**). Platelets in Wound Healing and Regenerative Medicine. *Platelets,* 29 (6):556-568.

63. Farkas AM, Baranyi U, Bohmig GA, Unger L, Hopf S, Wahrmann M, Regele H, Mahr B, Schwarz C, Hock K, Pilat N, Kristo I, Mraz J, Lupinek C, Thalhamer J, Bond G, Kuessel L, Wlodek E, Martin J, Clatworthy M, Pettigrew G, Valenta R, Wekerle T (**2018**). Allograft Rejection Is Associated with Development of Functional Ige Specific for Donor Mhc Antigens. *J Allergy Clin Immunol*.

64. Faucheux N, Schweiss R, Lutzow K, Werner C, Groth T (**2004**). Self-Assembled Monolayers with Different Terminating Groups as Model Substrates for Cell Adhesion Studies. *Biomaterials,* 25 (14):2721-2730.

65. Ferrante A (**1992**). Activation of Neutrophils by Interleukins-1 and -2 and Tumor Necrosis Factors. *Immunol Ser,* 57:417-436.

66. Ferrari G, Cook BD, Terushkin V, Pintucci G, Mignatti P (**2009**). Transforming Growth Factor-Beta 1 (Tgf-Beta1) Induces Angiogenesis through Vascular Endothelial Growth Factor (Vegf)-Mediated Apoptosis. *J Cell Physiol,* 219 (2):449-458.

67. Fetterolf DE, Snyder RJ (**2012**). Scientific and Clinical Support for the Use of Dehydrated Amniotic Membrane in Wound Management. *Wounds,* 24 (10):299-307.

68. Flaten GE, Palac Z, Engesland A, Filipovic-Grcic J, Vanic Z, Skalko-Basnet N (**2015**). In Vitro Skin Models as a Tool in Optimization of Drug Formulation. *Eur J Pharm Sci,* 75:10-24.

69. Fleck CA, Simman R (**2010**). Modern Collagen Wound Dressings: Function and Purpose. *J Am Col Certif Wound Spec,* 2 (3):50-54.

70. Foster EJ, Moon RJ, Agarwal UP, Bortner MJ, Bras J, Camarero-Espinosa S, Chan KJ, Clift MJD, Cranston ED, Eichhorn SJ, Fox DM, Hamad WY, Heux L, Jean B, Korey M, Nieh W, Ong KJ, Reid MS, Renneckar S, Roberts R, Shatkin JA, Simonsen J, Stinson-Bagby K, Wanasekara N, Youngblood J (**2018**). Current Characterization Methods for Cellulose Nanomaterials. *Chem Soc Rev,* 47 (8):2609-2679.

71. Franco RA, Nguyen TH, Lee BT (**2011**). Preparation and Characterization of Electrospun Pcl/Plga Membranes and Chitosan/Gelatin Hydrogels for Skin Bioengineering Applications. *J Mater Sci Mater Med,* 22 (10):2207-2218.

72. Fu J, Wang YK, Yang MT, Desai RA, Yu X, Liu Z, Chen CS (**2010**). Mechanical Regulation of Cell Function with Geometrically Modulated Elastomeric Substrates. *Nat Methods,* 7 (9):733-736.

73. Fu X, Xu M, Jia C, Xie W, Wang L, Kong D, Wang H (**2016**). Differential Regulation of Skin Fibroblasts for Their Tgf-B1-Dependent Wound Healing Activities by Biomimetic Nanofibers. *Journal of Materials Chemistry B,* 4 (31):5246-5255.

74. Fu X, Xu M, Liu J, Qi Y, Li S, Wang H (**2014**). Regulation of Migratory Activity of Human Keratinocytes by Topography of Multiscale Collagen-Containing Nanofibrous Matrices. *Biomaterials,* 35 (5):1496-1506.

75. Fujisaki H, Adachi E, Hattori S (**2008**). Keratinocyte Differentiation and Proliferation Are Regulated by Adhesion to the Three-Dimensional Meshwork Structure of Type Iv Collagen. *Connect Tissue Res,* 49 (6):426-436.

76. Ghezzi CE, Muja N, Marelli B, Nazhat SN (**2011**). Real Time Responses of Fibroblasts to Plastically Compressed Fibrillar Collagen Hydrogels. *Biomaterials,* 32 (21):4761-4772.

77. Gibbs S, Silva Pinto AN, Murli S, Huber M, Hohl D, Ponec M (**2000**). Epidermal Growth Factor and Keratinocyte Growth Factor Differentially Regulate Epidermal Migration, Growth, and Differentiation. *Wound Repair Regen,* 8 (3):192-203.

78. Greaves NS, Lqbal SA, Morris J, Benatar B, Alonso-Rasgado T, Baguneid M, Bayat A (**2015**). Acute Cutaneous Wounds Treated with Human Decellularised Dermis Show Enhanced Angiogenesis During Healing. *PLoS One,* 10 (1):e0113209.

79. Greiling D, Clark RA (**1997**). Fibronectin Provides a Conduit for Fibroblast Transmigration from Collagenous Stroma into Fibrin Clot Provisional Matrix. *J Cell Sci,* 110 (Pt 7):861-870.

80. Groen D, Poole DS, Gooris GS, Bouwstra JA (**2011**). Investigating the Barrier Function of Skin Lipid Models with Varying Compositions. *Eur J Pharm Biopharm,* 79 (2):334-342.

81. Grotendorst GR, Smale G, Pencev D (**1989**). Production of Transforming Growth Factor Beta by Human Peripheral Blood Monocytes and Neutrophils. *J Cell Physiol,* 140 (2):396-402.

82. Gunter CI, Bader A, Machens H (**2016**). Regenerative Therapies. In *Regenerative Medicine - from Protocol to Patient*, edited by G Steinhoff. *Springer International Publishing*, 367-386.

83. Haftek M (**2015**). Epidermal Barrier Disorders and Corneodesmosome Defects. *Cell Tissue Res,* 360 (3):483-490.

84. Hakkarainen T, Koivuniemi R, Kosonen M, Escobedo-Lucea C, Sanz-Garcia A, Vuola J, Valtonen J, Tammela P, Makitie A, Luukko K, Yliperttula M, Kavola H (**2016**). Nanofibrillar Cellulose Wound Dressing in Skin Graft Donor Site Treatment. *J Control Release,* 244 (Pt B):292-301.

85. Hartmann-Fritsch F, Biedermann T, Braziulis E, Luginbuhl J, Pontiggia L, Bottcher-Haberzeth S, van Kuppevelt TH, Faraj KA, Schiestl C, Meuli M, Reichmann E (**2016**). Collagen Hydrogels Strengthened by Biodegradable Meshes Are a Basis for Dermo-Epidermal Skin Grafts Intended to Reconstitute Human Skin in a One-Step Surgical Intervention. *J Tissue Eng Regen Med,* 10 (1):81-91.

86. Hasegawa T, Suga Y, Mizoguchi M, Muramatsu S, Mizuno Y, Ogawa H, Kubo K, Kuroyanagi Y (**2005**). An Allogeneic Cultured Dermal Substitute Suitable for Treating Intractable Skin Ulcers and Large Skin Defects Prior to Autologous Skin Grafting: Three Case Reports. *J Dermatol,* 32 (9):715-720.

87. Hejazian LB, Esmaeilzade B, Moghanni Ghoroghi F, Moradi F, Hejazian MB, Aslani A, Bakhtiari M, Soleimani M, Nobakht M (**2012**). The Role of Biodegradable Engineered Nanofiber Scaffolds Seeded with Hair Follicle Stem Cells for Tissue Engineering. *Iran Biomed J,* 16 (4):193-201.

88. Helliwell JA, Thomas DS, Papathanasiou V, Homer-Vanniasinkam S, Desai A, Jennings LM, Rooney P, Kearney JN, Ingham E (**2017**). Development and Characterisation of a Low-Concentration Sodium Dodecyl Sulphate Decellularised Porcine Dermis. *J Tissue Eng,* 8:2041731417724011.

89. Henry J, Toulza E, Hsu CY, Pellerin L, Balica S, Mazereeuw-Hautier J, Paul C, Serre G, Jonca N, Simon M (**2012**). Update on the Epidermal Differentiation Complex. *Front Biosci (Landmark Ed),* 17:1517-1532.

90. Heo DN, Yang DH, Lee JB, Bae MS, Kim JH, Moon SH, Chun HJ, Kim CH, Lim HN, Kwon IK (**2013**). Burn-Wound Healing Effect of Gelatin/Polyurethane Nanofiber Scaffold Containing Silver-Sulfadiazine. *J Biomed Nanotechnol,* 9 (3):511-515.

91. Heydarkhan-Hagvall S, Helenius G, Johansson BR, Li JY, Mattsson E, Risberg B (**2003**). Co-Culture of Endothelial Cells and Smooth Muscle Cells Affects Gene Expression of Angiogenic Factors. *J Cell Biochem,* 89 (6):1250-1259.

92. Hinchcliff KM, Orbay H, Busse BK, Charvet H, Kaur M, Sahar DE (**2017**). Comparison of Two Cadaveric Acellular Dermal Matrices for Immediate Breast Reconstruction: A Prospective Randomized Trial. *J Plast Reconstr Aesthet Surg,* 70 (5):568-576.

93. Hosgood G (**1993**). Wound Healing. The Role of Platelet-Derived Growth Factor and Transforming Growth Factor Beta. *Vet Surg,* 22 (6):490-495.

94. Hoshiba T, Yoshikawa C, Sakakibara K (**2018**). Characterization of Initial Cell Adhesion on Charged Polymer Substrates in Serum-Containing and Serum-Free Media. *Langmuir,* 34 (13):4043-4051.

95. Hou Y, Xie WY, Yu LX, Camacho LC, Nie CX, Zhang M, Haag R, Wei Q (**2020**). Surface Roughness Gradients Reveal Topography-Specific Mechanosensitive Responses in Human Mesenchymal Stem Cells. *Small,* 16 (10).

96. Hsu YC, Li L, Fuchs E (**2014**). Emerging Interactions between Skin Stem Cells and Their Niches. *Nat Med,* 20 (8):847-856.

97. Huang J, Ren J, Chen G, Li Z, Liu Y, Wang G, Wu X (**2018**). Tunable Sequential Drug Delivery System Based on Chitosan/Hyaluronic Acid Hydrogels and Plga Microspheres for Management of Non-Healing Infected Wounds. *Mater Sci Eng C Mater Biol Appl,* 89:213-222.

98. Huang SP, Hsu CC, Chang SC, Wang CH, Deng SC, Dai NT, Chen TM, Chan JYH, Chen SG, Huang SM (**2012**). Adipose-Derived Stem Cells Seeded on Acellular Dermal Matrix Grafts Enhance Wound Healing in a Murine Model of a Full-Thickness Defect. *Ann Plast Surg,* 69 (6):656-662.

99. Chan RK, Zamora DO, Wrice NL, Baer DG, Renz EM, Christy RJ, Natesan S (**2012**). Development of a Vascularized Skin Construct Using Adipose-Derived Stem Cells from Debrided Burned Skin. *Stem Cells International,* 2012.

100. Chau DY, Johnson C, MacNeil S, Haycock JW, Ghaemmaghami AM (**2013**). The Development of a 3d Immunocompetent Model of Human Skin. *Biofabrication,* 5 (3):035011.

101. Chaudhari AA, Vig K, Baganizi DR, Sahu R, Dixit S, Dennis V, Singh SR, Pillai SR (**2016**). Future Prospects for Scaffolding Methods and Biomaterials in Skin Tissue Engineering: A Review. *Int J Mol Sci,* 17 (12):1974.

102. Chen DW, Liu SJ (**2015**). Nanofibers Used for Delivery of Antimicrobial Agents. *Nanomedicine (Lond).* 10 (12):1959-1971.

103. Chen H, Liu Y, Hu Q (**2015**). A Novel Bioactive Membrane by Cell Electrospinning. *Exp Cell Res,* 338 (2):261-266.

104. Chen JP, Chiang Y (**2010**). Bioactive Electrospun Silver Nanoparticles-Containing Polyurethane Nanofibers as Wound Dressings. *J Nanosci Nanotechnol,* 10 (11):7560-7564.

105. Chen S, Liu B, Carlson MA, Gombart AF, Reilly DA, Xie J (**2017**). Recent Advances in Electrospun Nanofibers for Wound Healing. *Nanomedicine (Lond),* 12 (11):1335-1352.

106. Cheng W, Xu R, Li D, Bortolini C, He J, Dong M, Besenbacher F, Huang Y, Chen M (**2016**). Artificial Extracellular Matrix Delivers Tgfb1 Regulating Myofibroblast Differentiation. *RSC Advances,* 6 (26):21922-21928.

107. Chiu CL, Hecht V, Duong H, Wu B, Tawil B (**2012**). Permeability of Three-Dimensional Fibrin Constructs Corresponds to Fibrinogen and Thrombin Concentrations. *Biores Open Access,* 1 (1):34-40.

108. Chu PG, Weiss LM (**2002**). Keratin Expression in Human Tissues and Neoplasms. *Histopathology,* 40 (5):403-439.

109. Ihalainen TO, Aires L, Herzog FA, Schwartlander R, Moeller J, Vogel V (**2015**). Differential Basal-to-Apical Accessibility of Lamin a/C Epitopes in the Nuclear Lamina Regulated by Changes in Cytoskeletal Tension. *Nat Mater,* 14 (12):1252-1261.

110. Induruwa I, Moroi M, Bonna A, Malcor JD, Howes JM, Warburton EA, Farndale RW, Jung SM (**2018**). Platelet Collagen Receptor Glycoprotein Vi-Dimer Recognizes Fibrinogen and Fibrin through Their D-Domains, Contributing to Platelet Adhesion and Activation During Thrombus Formation. *J Thromb Haemost,* 16 (2):389-404.

111. Jain RK (**2003**). Molecular Regulation of Vessel Maturation. *Nat Med,* 9 (6):685-693.

112. Jayadev R, Sherwood DR (**2017**). Basement Membranes. *Curr Biol,* 27 (6):R207-R211.

113. Jayasinghe SN (**2013**). Cell Electrospinning: A Novel Tool for Functionalising Fibres, Scaffolds and Membranes with Living Cells and Other Advanced Materials for Regenerative Biology and Medicine. *Analyst,* 138 (8):2215-2223.

114. Jhon MS, Andrade JD (**1973**). Water and Hydrogels. *J Biomed Mater Res,* 7 (6):509-522.

115. Kalin M, Kuru S, Kismet K, Barlas AM, Akgun YA, Astarci HM, Ustun H, Ertas E (**2015**). The Effectiveness of Porcine Dermal Collagen (Permacol((R))) on Wound Healing in the Rat Model. *Indian J Surg,* 77 (Suppl 2):407-411.

116. Kim HS, Yoo HS (**2013**). In Vitro and in Vivo Epidermal Growth Factor Gene Therapy for Diabetic Ulcers with Electrospun Fibrous Meshes. *Acta Biomater,* 9 (7):7371-7380.

117. Kim JE, Lee JH, Kim SH, Jung Y (**2018**). Skin Regeneration with Self-Assembled Peptide Hydrogels Conjugated with Substance P in a Diabetic Rat Model. *Tissue Eng Part A,* 24 (1-2):21-33.

118. Kim OV, Litvinov RI, Chen J, Chen DZ, Weisel JW, Alber MS (**2017**). Compression-Induced Structural and Mechanical Changes of Fibrin-Collagen Composites. *Matrix Biol,* 60-61:141-156.

119. Klar AS, Biedermann T, Simmen-Meuli C, Reichmann E, Meuli M (**2017a**). Comparison of in Vivo Immune Responses Following Transplantation of Vascularized and Non-Vascularized Human Dermo-Epidermal Skin Substitutes. *Pediatr Surg Int,* 33 (3):377-382.

120. Klar AS, Guven S, Biedermann T, Luginbuhl J, Bottcher-Haberzeth S, Meuli-Simmen C, Meuli M, Martin I, Scherberich A, Reichmann E (**2014**). Tissue-Engineered Dermo-Epidermal Skin Grafts Prevascularized with Adipose-Derived Cells. *Biomaterials,* 35 (19):5065-5078.

121. Klar AS, Guven S, Zimoch J, Zapiorkowska NA, Biedermann T, Bottcher-Haberzeth S, Meuli-Simmen C, Martin I, Scherberich A, Reichmann E, Meuli M (**2016**). Characterization of Vasculogenic Potential of Human Adipose-Derived Endothelial Cells in a Three-Dimensional Vascularized Skin Substitute. *Pediatr Surg Int,* 32 (1):17-27.

122. Klar AS, Michalak K, Bottcher-Haberzeth S, Reichmann E, Meuli M, Biedermann T (**2018**). The Expression Pattern of Keratin 24 in Tissue-Engineered Dermo-Epidermal Human Skin Substitutes in an in Vivo Model. *Pediatr Surg Int,* 34 (2):237-244.

123. Klar AS, Zimoch J, Biedermann T (**2017b**). Skin Tissue Engineering: Application of Adipose-Derived Stem Cells. *Biomed Res Int,* 2017.

124. Koh TJ, DiPietro LA (**2011**). Inflammation and Wound Healing: The Role of the Macrophage. *Expert Rev Mol Med,* 13:e23.

125. Koh YJ, Koh BI, Kim H, Joo HJ, Jin HK, Jeon J, Choi C, Lee DH, Chung JH, Cho CH, Park WS, Ryu JK, Suh JK, Koh GY (**2011**). Stromal Vascular Fraction from Adipose Tissue Forms Profound Vascular Network through the Dynamic Reassembly of Blood Endothelial Cells. *Arteriosclerosis Thrombosis and Vascular Biology,* 31 (5):1141-U1539.

126. Kondo S, Kagami S, Urushihara M, Kitamura A, Shimizu M, Strutz F, Muller GA, Kuroda Y (**2004**). Transforming Growth Factor-Beta1 Stimulates Collagen Matrix

Remodeling through Increased Adhesive and Contractive Potential by Human Renal Fibroblasts. *Biochim Biophys Acta,* 1693 (2):91-100.

127. Kranz H, Ubrich N, Maincent P, Bodmeier R (**2000**). Physicomechanical Properties of Biodegradable Poly(D,L-Lactide) and Poly(D,L-Lactide-Co-Glycolide) Films in the Dry and Wet States. *J Pharm Sci,* 89 (12):1558-1566.

128. Kubo M, Van De Water L, Plantefaber LC, Mosesson MW, Simon M, Tonnesen MG, Taichman L, Clark RAF (**2001**). Fibrinogen and Fibrin Are Anti-Adhesive for Keratinocytes: A Mechanism for Fibrin Eschar Slough During Wound Repair. *Journal of Investigative Dermatology,* 117 (6):1369-1381.

129. Kumar A, Jagannathan N (**2018**). Cytokeratin: A Review on Current Concepts. *International Journal of Orofacial Biology,* 2 (1):6-11.

130. Kumar RJ, Kimble RM, Boots R, Pegg SP (**2004**). Treatment of Partial-Thickness Burns: A Prospective, Randomized Trial Using Transcyte. *ANZ J Surg,* 74 (8):622-626.

131. Lai HJ, Kuan CH, Wu HC, Tsai JC, Chen TM, Hsieh DJ, Wang TW (**2014**). Tailored Design of Electrospun Composite Nanofibers with Staged Release of Multiple Angiogenic Growth Factors for Chronic Wound Healing. *Acta Biomater,* 10 (10):4156-4166.

132. Laschke MW, Menger MD (**2012**). Vascularization in Tissue Engineering: Angiogenesis Versus Inosculation. *European Surgical Research,* 48 (2):85-92.

133. Lavor MA, Michael GM, Tamire YG, Dorofee ND (**2018**). Meshed Split-Thickness Autograft with a Viable Cryopreserved Placental Membrane Overlay for Lower-Extremity Recipient Sites with Increased Risk of Graft Failure. *Eplasty,* 18:e22.

134. Lee YB, Lee JY, Byun H, Ahmad T, Akashi M, Matsusaki M, Shin H (**2018**). One-Step Delivery of a Functional Multi-Layered Cell Sheet Using a Thermally Expandable Hydrogel with Controlled Presentation of Cell Adhesive Proteins. *Biofabrication,* 10 (2):025001.

135. Lessard JC, Coulombe PA (**2012**). Keratin 16-Null Mice Develop Palmoplantar Keratoderma, a Hallmark Feature of Pachyonychia Congenita and Related Disorders. *J Invest Dermatol,* 132 (5):1384-1391.

136. Liao JL, Zhong S, Wang SH, Liu JY, Chen J, He G, He B, Xu JQ, Liang ZH, Mei T, Wu S, Cao K, Zhou JD (**2017**). Preparation and Properties of a Novel Carbon Nanotubes/Poly(Vinyl Alcohol)/Epidermal Growth Factor Composite Biological Dressing. *Exp Ther Med,* 14 (3):2341-2348.

137. Lin YC, Grahovac T, Oh SJ, Ieraci M, Rubin JP, Marra KG (**2013**). Evaluation of a Multi-Layer Adipose-Derived Stem Cell Sheet in a Full-Thickness Wound Healing Model. *Acta Biomater,* 9 (2):5243-5250.

138. Liu GS, Yan X, Yan FF, Chen FX, Hao LY, Chen SJ, Lou T, Ning X, Long YZ (**2018a**). In Situ Electrospinning Iodine-Based Fibrous Meshes for Antibacterial Wound Dressing. *Nanoscale Res Lett,* 13 (1):309.

139. Liu R, Dai L, Si C, Zeng Z (**2018b**). Antibacterial and Hemostatic Hydrogel Via Nanocomposite from Cellulose Nanofibers. *Carbohydr Polym,* 195:63-70.

140. Lloyd C, Yu QC, Cheng J, Turksen K, Degenstein L, Hutton E, Fuchs E (**1995**). The Basal Keratin Network of Stratified Squamous Epithelia: Defining K15 Function in the Absence of K14. *J Cell Biol,* 129 (5):1329-1344.

141. Lopez-Garcia MD, Beebe DJ, Crone WC (**2010**). Mechanical Interactions of Mouse Mammary Gland Cells with Collagen in a Three-Dimensional Construct. *Annals of Biomedical Engineering,* 38 (8):2485-2498.

142. Lotz C, Schmid FF, Oechsle E, Monaghan MG, Walles H, Groeber-Becker F (**2017**). Cross-Linked Collagen Hydrogel Matrix Resisting Contraction to Facilitate Full-Thickness Skin Equivalents. *ACS Appl Mater Interfaces,* 9 (24):20417-20425.

143. Magnusson M, Papini RP, Rea SM, Reed CC, Wood FM (**2007**). Cultured Autologous Keratinocytes in Suspension Accelerate Epithelial Maturation in an in Vivo Wound Model as Measured by Surface Electrical Capacitance. *Plast Reconstr Surg,* 119 (2):495-499.

144. Mahjour SB, Fu X, Yang X, Fong J, Sefat F, Wang H (**2015**). Rapid Creation of Skin Substitutes from Human Skin Cells and Biomimetic Nanofibers for Acute Full-Thickness Wound Repair. *Burns,* 41 (8):1764-1774.

145. Marino D, Luginbuhl J, Scola S, Meuli M, Reichmann E (**2014**). Bioengineering Dermo-Epidermal Skin Grafts with Blood and Lymphatic Capillaries. *Science Translational Medicine,* 6 (221).

146. Marionnet C, Pierrard C, Vioux-Chagnoleau C, Sok J, Asselineau D, Bernerd F (**2006**). Interactions between Fibroblasts and Keratinocytes in Morphogenesis of Dermal Epidermal Junction in a Model of Reconstructed Skin. *Journal of Investigative Dermatology,* 126 (5):971-979.

147. Martinson M, Martinson N (**2016**). A Comparative Analysis of Skin Substitutes Used in the Management of Diabetic Foot Ulcers. *J Wound Care,* 25 (Sup10):S8-S17.

148. Mateos-Timoneda MA, Castano O, Planell JA, Engel E (**2014**). Effect of Structure, Topography and Chemistry on Fibroblast Adhesion and Morphology. *Journal of Materials Science-Materials in Medicine,* 25 (7):1781-1787.

149. Mazlyzam AL, Aminuddin BS, Fuzina NH, Norhayati MM, Fauziah O, Isa MR, Saim L, Ruszymah BHI (**2007**). Reconstruction of Living Bilayer Human Skin Equivalent Utilizing Human Fibrin as a Scaffold. *Burns,* 33 (3):355-363.

150. Melkun ET, Few JW (**2005**). The Use of Biosynthetic Skin Substitute (Biobrane) for Axillary Reconstruction after Surgical Excision for Hidradenitis Suppurativa. *Plast Reconstr Surg,* 115 (5):1385-1388.

151. Min JH, Yun IS, Lew DH, Roh TS, Lee WJ (**2014**). The Use of Matriderm and Autologous Skin Graft in the Treatment of Full Thickness Skin Defects. *Arch Plast Surg,* 41 (4):330-336.

152. Miron-Mendoza M, Lin X, Ma L, Ririe P, Petroll WM (**2012**). Individual Versus Collective Fibroblast Spreading and Migration: Regulation by Matrix Composition in 3d Culture. *Exp Eye Res,* 99:36-44.

153. Moll R, Divo M, Langbein L (**2008**). The Human Keratins: Biology and Pathology. *Histochem Cell Biol,* 129 (6):705-733.

154. Mongiat M, Andreuzzi E, Tarticchio G, Paulitti A (**2016**). Extracellular Matrix, a Hard Player in Angiogenesis. *Int J Mol Sci,* 17 (11):1822.

155. Moon JJ, West JL (**2008**). Vascularization of Engineered Tissues: Approaches to Promote Angiogenesis in Biomaterials. *Current Topics in Medicinal Chemistry,* 8 (4):300-310.

156. Moreno-Arotzena O, Meier JG, Del Amo C, Garcia-Aznar JM (**2015**). Characterization of Fibrin and Collagen Gels for Engineering Wound Healing Models. *Materials (Basel),* 8 (4):1636-1651.

157. Muller SA, van der Smissen A, von Feilitzsch M, Anderegg U, Kalkhof S, von Bergen M (**2012**). Quantitative Proteomics Reveals Altered Expression of Extracellular Matrix Related Proteins of Human Primary Dermal Fibroblasts in Response to Sulfated Hyaluronan and Collagen Applied as Artificial Extracellular Matrix. *J Mater Sci Mater Med,* 23 (12):3053-3065.

158. Nagase K, Yamato M, Kanazawa H, Okano T (**2018**). Poly(N-Isopropylacrylamide)-Based Thermoresponsive Surfaces Provide New Types of Biomedical Applications. *Biomaterials,* 153:27-48.

159. Nair RP, Joseph J, Harikrishnan VS, Krishnan VK, Krishnan L (**2014**). Contribution of Fibroblasts to the Mechanical Stability of in Vitro Engineered Dermal-Like Tissue through Extracellular Matrix Deposition. *Biores Open Access,* 3 (5):217-225.

160. Nathoo R, Howe N, Cohen G (**2014**). Skin Substitutes: An Overview of the Key Players in Wound Management. *The Journal of Clinical and Aesthetic Dermatology,* 7 (10):44-48.

161. Nguyen AT, Sathe SR, Yim EK (**2016**). From Nano to Micro: Topographical Scale and Its Impact on Cell Adhesion, Morphology and Contact Guidance. *J Phys Condens Matter,* 28 (18):183001.

162. Nishiyama T, Amano S, Tsunenaga M, Kadoya K, Takeda A, Adachi E, Burgeson RE (**2000**). The Importance of Laminin 5 in the Dermal-Epidermal Basement Membrane. *J Dermatol Sci,* 24 Suppl 1:S51-59.

163. O'Connor NE, Mulliken JB, Banks-Schlegel S, Kehinde O, Green H (**1981**). Grafting of Burns with Cultured Epithelium Prepared from Autologous Epidermal Cells. *Lancet,* 1 (8211):75-78.

164. Ohkawa K (**2015**). Nanofibers of Cellulose and Its Derivatives Fabricated Using Direct Electrospinning. *Molecules,* 20 (5):9139-9154.

165. Olczyk P, Mencner L, Komosinska-Vassev K (**2014**). The Role of the Extracellular Matrix Components in Cutaneous Wound Healing. *Biomed Res Int,* 2014:8.

166. Oostendorp C, Meyer S, Sobrio M, van Arendonk J, Reichmann E, Daamen WF, van Kuppevelt TH (**2017**). Evaluation of Cultured Human Dermal- and Dermo-Epidermal Substitutes Focusing on Extracellular Matrix Components: Comparison of Protein and Rna Analysis. *Burns,* 43 (3):520-530.

167. Otrock ZK, Mahfouz RAR, Makarm JA, Shamseddine AI (**2007**). Understanding the Biology of Angiogenesis: Review of the Most Important Molecular Mechanisms. *Blood Cells Molecules and Diseases,* 39 (2):212-220.

168. Pajorova J, Bacakova M, Musilkova J, Broz A, Hadraba D, Lopot F, Bacakova L (**2018**). Morphology of a Fibrin Nanocoating Influences Dermal Fibroblast Behavior. *Int J Nanomedicine,* 13:3367-3380.

169. Pajorova J, Skogberg A, Hadraba D, Broz A, Travnickova M, Zikmundova M, Honkanen M, Hannula M, Lahtinen P, Tomkova M, Bacakova L, Kallio P (**2020**). Cellulose Mesh with Charged Nanocellulose Coatings as a Promising Carrier of Skin and Stem Cells for Regenerative Applications. *Biomacromolecules,* 21 (12):4857-4870.

170. Pal P, Dadhich P, Srivas PK, Das B, Maulik D, Dhara S (**2017**). Bilayered Nanofibrous 3d Hierarchy as Skin Rudiment by Emulsion Electrospinning for Burn Wound Management. *Biomater Sci,* 5 (9):1786-1799.

171. Park HB, Yang JH, Chung KH (**2011**). Characterization of the Cytokine Profile of Platelet Rich Plasma (Prp) and Prp-Induced Cell Proliferation and Migration: Upregulation of Matrix Metalloproteinase-1 and -9 in Hacat Cells. *Korean J Hematol,* 46 (4):265-273.

172. Park JY, Kim JI, Lee IH (**2015**). Fabrication and Characterization of Antimicrobial Ethyl Cellulose Nanofibers Using Electrospinning Techniques. *J Nanosci Nanotechnol,* 15 (8):5672-5675.

173. Peng N, Wang Y, Ye Q, Liang L, An Y, Li Q, Chang C (**2016**). Biocompatible Cellulose-Based Superabsorbent Hydrogels with Antimicrobial Activity. *Carbohydr Polym,* 137:59-64.

174. Pilcher BK, Dumin JA, Sudbeck BD, Krane SM, Welgus HG, Parks WC (**1997**). The Activity of Collagenase-1 Is Required for Keratinocyte Migration on a Type I Collagen Matrix. *J Cell Biol,* 137 (6):1445-1457.

175. Polio SR, Smith ML (**2014**). Patterned Hydrogels for Simplified Measurement of Cell Traction Forces. *Methods Cell Biol,* 121:17-31.

176. Poschl E, Schlotzer-Schrehardt U, Brachvogel B, Saito K, Ninomiya Y, Mayer U (**2004**). Collagen Iv Is Essential for Basement Membrane Stability but Dispensable for

Initiation of Its Assembly During Early Development. *Development,* 131 (7):1619-1628.

177. Prakash TV, Chaudhary DA, Purushothaman S, K VS, Arvind KV (**2016**). Epidermal Grafting for Chronic Complex Wounds in India: A Case Series. *Cureus,* 8 (3):e516.

178. Prasad A, Clark RA (**2018**). Fibronectin Interaction with Growth Factors in the Context of General Ways Extracellular Matrix Molecules Regulate Growth Factor Signaling. *G Ital Dermatol Venereol,* 153 (3):361-374.

179. Ramms L, Fabris G, Windoffer R, Schwarz N, Springer R, Zhou C, Lazar J, Stiefel S, Hersch N, Schnakenberg U, Magin TM, Leube RE, Merkel R, Hoffmann B (**2013**). Keratins as the Main Component for the Mechanical Integrity of Keratinocytes. *Proc Natl Acad Sci U S A,* 110 (46):18513-18518.

180. Raveendran S, Rochani AK, Maekawa T, Kumar DS (**2017**). Smart Carriers and Nanohealers: A Nanomedical Insight on Natural Polymers. *Materials (Basel),* 10 (8).

181. Reed CR, Han L, Andrady A, Caballero M, Jack MC, Collins JB, Saba SC, Loboa EG, Cairns BA, van Aalst JA (**2009**). Composite Tissue Engineering on Polycaprolactone Nanofiber Scaffolds. *Ann Plast Surg,* 62 (5):505-512.

182. Rheinwald JG, Green H (**1975**). Serial Cultivation of Strains of Human Epidermal Keratinocytes: The Formation of Keratinizing Colonies from Single Cells. *Cell,* 6 (3):331-343.

183. Riedel T, Brynda E, Dyr JE, Houska M (**2009**). Controlled Preparation of Thin Fibrin Films Immobilized at Solid Surfaces. *Journal of Biomedical Materials Research Part A,* 88a (2):437-447.

184. Rockwood DN, Woodhouse KA, Fromstein JD, Chase DB, Rabolt JF (**2007**). Characterization of Biodegradable Polyurethane Microfibers for Tissue Engineering. *J Biomater Sci Polym Ed,* 18 (6):743-758.

185. Rodero MP, Khosrotehrani K (**2010**). Skin Wound Healing Modulation by Macrophages. *Int J Clin Exp Pathol,* 3 (7):643-653.

186. Ruoslahti E, Pierschbacher MD (**1987**). New Perspectives in Cell Adhesion: Rgd and Integrins. *Science,* 238 (4826):491-497.

187. Saarialho-Kere UK, Pentland AP, Birkedal-Hansen H, Parks WC, Welgus HG (**1994**). Distinct Populations of Basal Keratinocytes Express Stromelysin-1 and Stromelysin-2 in Chronic Wounds. *J Clin Invest,* 94 (1):79-88.

188. Sakai S, Ito S, Ogushi Y, Hashimoto I, Hosoda N, Sawae Y, Kawakami K (**2009**). Enzymatically Fabricated and Degradable Microcapsules for Production of Multicellular Spheroids with Well-Defined Diameters of Less Than 150 Mu M. *Biomaterials,* 30 (30):5937-5942.

189. Salo T, Makela M, Kylmaniemi M, Autio-Harmainen H, Larjava H (**1994**). Expression of Matrix Metalloproteinase-2 and -9 During Early Human Wound Healing. *Lab Invest,* 70 (2):176-182.

190. Savoji H, Godau B, Hassani MS, Akbari M (**2018**). Skin Tissue Substitutes and Biomaterial Risk Assessment and Testing. *Front Bioeng Biotechnol,* 6:86.

191. Sese N, Cole M, Tawil B (**2011**). Proliferation of Human Keratinocytes and Cocultured Human Keratinocytes and Fibroblasts in Three-Dimensional Fibrin Constructs. *Tissue Eng Part A,* 17 (3-4):429-437.

192. Sethi KK, Yannas IV, Mudera V, Eastwood M, McFarland C, Brown RA (**2002**). Evidence for Sequential Utilization of Fibronectin, Vitronectin, and Collagen During Fibroblast-Mediated Collagen Contraction. *Wound Repair and Regeneration,* 10 (6):397-408.

193. Shababdoust A, Ehsani M, Shokrollahi P, Zandi M (**2018**). Fabrication of Curcumin-Loaded Electrospun Nanofiberous Polyurethanes with Anti-Bacterial Activity. *Prog Biomater,* 7 (1):23-33.

194. Shang J, Theato P (**2018**). Smart Composite Hydrogel with Ph-, Ionic Strength- and Temperature-Induced Actuation. *Soft Matter*.

195. Shefa AA, Amirian J, Kang HJ, Bae SH, Jung HI, Choi HJ, Lee SY, Lee BT (**2017**). In Vitro and in Vivo Evaluation of Effectiveness of a Novel Tempo-Oxidized Cellulose Nanofiber-Silk Fibroin Scaffold in Wound Healing. *Carbohydr Polym,* 177:284-296.

196. Scharffetter-Kochanek K, Klein CE, Heinen G, Mauch C, Schaefer T, Adelmann-Grill BC, Goerz G, Fusenig NE, Krieg TM, Plewig G (**1992**). Migration of a Human Keratinocyte Cell Line (Hacat) to Interstitial Collagen Type I Is Mediated by the Alpha 2 Beta 1-Integrin Receptor. *J Invest Dermatol,* 98 (1):3-11.

197. Skardal A, Mack D, Atala A, Soker S (**2013**). Substrate Elasticity Controls Cell Proliferation, Surface Marker Expression and Motile Phenotype in Amniotic Fluid-Derived Stem Cells. *J Mech Behav Biomed Mater,* 17:307-316.

198. Skogberg A, Maki AJ, Mettanen M, Lahtinen P, Kallio P (**2017**). Cellulose Nanofiber Alignment Using Evaporation-Induced Droplet-Casting, and Cell Alignment on Aligned Nanocellulose Surfaces. *Biomacromolecules,* 18 (12):3936-3953.

199. Slevin M, Kumar S, Gaffney J (**2002**). Angiogenic Oligosaccharides of Hyaluronan Induce Multiple Signaling Pathways Affecting Vascular Endothelial Cell Mitogenic and Wound Healing Responses. *J Biol Chem,* 277 (43):41046-41059.

200. Smithmyer ME, Sawicki LA, Kloxin AM (**2014**). Hydrogel Scaffolds as in Vitro Models to Study Fibroblast Activation in Wound Healing and Disease. *Biomater Sci,* 2 (5):634-650.

201. Snyder RJ, Shimozaki K, Tallis A, Kerzner M, Reyzelman A, Lintzeris D, Bell D, Rutan RL, Rosenblum B (**2016**). A Prospective, Randomized, Multicenter, Controlled Evaluation of the Use of Dehydrated Amniotic Membrane Allograft Compared to Standard of Care for the Closure of Chronic Diabetic Foot Ulcer. *Wounds,* 28 (3):70-77.

202. Sottile J, Hocking DC (**2002**). Fibronectin Polymerization Regulates the Composition and Stability of Extracellular Matrix Fibrils and Cell-Matrix Adhesions. *Mol Biol Cell,* 13 (10):3546-3559.

203. Spiekstra SW, Breetveld M, Rustemeyer T, Scheper RJ, Gibbs S (**2007**). Wound-Healing Factors Secreted by Epidermal Keratinocytes and Dermal Fibroblasts in Skin Substitutes. *Wound Repair Regen,* 15 (5):708-717.

204. Sriram G, Bigliardi PL, Bigliardi-Qi M (**2015**). Fibroblast Heterogeneity and Its Implications for Engineering Organotypic Skin Models in Vitro. *Eur J Cell Biol,* 94 (11):483-512.

205. Staatz WD, Fok KF, Zutter MM, Adams SP, Rodriguez BA, Santoro SA (**1991**). Identification of a Tetrapeptide Recognition Sequence for the Alpha 2 Beta 1 Integrin in Collagen. *J Biol Chem,* 266 (12):7363-7367.

206. Stark H-J, Szabowski A, Fusenig NE, Maas-Szabowski N (**2004**). Organotypic Cocultures as Skin Equivalents: A Complex and Sophisticated in Vitro System. *Biological Procedures Online,* 6:55-60.

207. Stark HJ, Breitkreutz D, Limat A, Bowden P, Fusenig NE (**1987**). Keratins of the Human Hair Follicle: "Hyperproliferative" Keratins Consistently Expressed in Outer Root Sheath Cells in Vivo and in Vitro. *Differentiation,* 35 (3):236-248.

208. Still J, Glat P, Silverstein P, Griswold J, Mozingo D (**2003**). The Use of a Collagen Sponge/Living Cell Composite Material to Treat Donor Sites in Burn Patients. *Burns,* 29 (8):837-841.

209. Stunova A, Vistejnova L (**2018**). Dermal Fibroblasts-a Heterogeneous Population with Regulatory Function in Wound Healing. *Cytokine & Growth Factor Reviews,* 39:137-150.

210. Sun M, Jiang M, Cui J, Liu W, Yin L, Xu C, Wei Q, Yan X, Chen F (**2016a**). A Novel Approach for the Cryodesiccated Preservation of Tissue-Engineered Skin Substitutes with Trehalose. *Mater Sci Eng C Mater Biol Appl,* 60:60-66.

211. Sun W, Sun Y, Klar AS, Geutjes P, Reichmann E, Heerschap A, Oosterwijk E (**2016b**). Functional Analysis of Vascularized Collagen/Fibrin Templates by Mri in Vivo. *Tissue Eng Part C Methods,* 22 (8):747-755.

212. Swieringa F, Spronk HMH, Heemskerk JWM, van der Meijden PEJ (**2018**). Integrating Platelet and Coagulation Activation in Fibrin Clot Formation. *Res Pract Thromb Haemost,* 2 (3):450-460.

213. Syverud K (**2017**). Tissue Engineering Using Plant-Derived Cellulose Nanofibrils (Cnf) as Scaffold Material. In *Nanocelluloses: Their Preparation, Properties, and Applications*. *American Chemical Society*, 171-189.

214. Tausche AK, Skaria M, Bohlen L, Liebold K, Hafner J, Friedlein H, Meurer M, Goedkoop RJ, Wollina U, Salomon D, Hunziker T (**2003**). An Autologous Epidermal Equivalent Tissue-Engineered from Follicular Outer Root Sheath Keratinocytes Is as

Effective as Split-Thickness Skin Autograft in Recalcitrant Vascular Leg Ulcers. *Wound Repair Regen,* 11 (4):248-252.

215. Tavakoli S, Klar AS (**2020**). Advanced Hydrogels as Wound Dressings. *Biomolecules,* 10 (8).

216. Ter Horst B, Chouhan G, Moiemen NS, Grover LM (**2018**). Advances in Keratinocyte Delivery in Burn Wound Care. *Adv Drug Deliv Rev,* 123:18-32.

217. Tolg C, Telmer P, Turley E (**2014**). Specific Sizes of Hyaluronan Oligosaccharides Stimulate Fibroblast Migration and Excisional Wound Repair. *PLoS One,* 9 (2):e88479.

218. Tonnesen MG, Feng X, Clark RA (**2000**). Angiogenesis in Wound Healing. *J Investig Dermatol Symp Proc,* 5 (1):40-46.

219. Tracy LE, Minasian RA, Caterson EJ (**2016**). Extracellular Matrix and Dermal Fibroblast Function in the Healing Wound. *Adv Wound Care (New Rochelle),* 5 (3):119-136.

220. Travnickova M, Pajorova J, Zarubova J, Krocilova N, Molitor M, Bacakova L (**2020**). The Influence of Negative Pressure and of the Harvesting Site on the Characteristics of Human Adipose Tissue-Derived Stromal Cells from Lipoaspirates. *Stem Cells International,* 2020:1016231.

221. Tremblay PL, Hudon V, Berthod F, Germain L, Auger FA (**2005**). Inosculation of Tissue-Engineered Capillaries with the Host's Vasculature in a Reconstructed Skin Transplanted on Mice. *American Journal of Transplantation,* 5 (5):1002-1010.

222. Trovatti E, Tang H, Hajian A, Meng Q, Gandini A, Berglund LA, Zhou Q (**2018**). Enhancing Strength and Toughness of Cellulose Nanofibril Network Structures with an Adhesive Peptide. *Carbohydr Polym,* 181:256-263.

223. Tsao CT, Leung M, Chang JY, Zhang M (**2014**). A Simple Material Model to Generate Epidermal and Dermal Layers in Vitro for Skin Regeneration. *J Mater Chem B,* 2 (32):5256-5264.

224. Tuan TL, Keller LC, Sun D, Nimni ME, Cheung D (**1994**). Dermal Fibroblasts Activate Keratinocyte Outgrowth on Collagen Gels. *J Cell Sci,* 107 (Pt 8):2285-2289.

225. Tuan TL, Song A, Chang S, Younai S, Nimni ME (**1996**). In Vitro Fibroplasia: Matrix Contraction, Cell Growth, and Collagen Production of Fibroblasts Cultured in Fibrin Gels. *Exp Cell Res,* 223 (1):127-134.

226. Uccioli L, Giurato L, Ruotolo V, Ciavarella A, Grimaldi MS, Piaggesi A, Teobaldi I, Ricci L, Scionti L, Vermigli C, Seguro R, Mancini L, Ghirlanda G (**2011**). Two-Step Autologous Grafting Using Hyaff Scaffolds in Treating Difficult Diabetic Foot Ulcers: Results of a Multicenter, Randomized Controlled Clinical Trial with Long-Term Follow-Up. *Int J Low Extrem Wounds,* 10 (2):80-85.

227. Varkey M, Ding J, Tredget EE (**2014**). Superficial Dermal Fibroblasts Enhance Basement Membrane and Epidermal Barrier Formation in Tissue-Engineered Skin:

Implications for Treatment of Skin Basement Membrane Disorders. *Tissue Eng Part A,* 20 (3-4):540-552.

228. Vig K, Chaudhari A, Tripathi S, Dixit S, Sahu R, Pillai S, Dennis VA, Singh SR (**2017**). Advances in Skin Regeneration Using Tissue Engineering. *Int J Mol Sci,* 18 (4):789.

229. Vroman L, Adams AL, Fischer GC, Munoz PC (**1980**). Interaction of High Molecular-Weight Kininogen, Factor-Xii, and Fibrinogen in Plasma at Interfaces. *Blood,* 55 (1):156-159.

230. Wahl SM, Hunt DA, Wakefield LM, McCartney-Francis N, Wahl LM, Roberts AB, Sporn MB (**1987**). Transforming Growth Factor Type Beta Induces Monocyte Chemotaxis and Growth Factor Production. *Proc Natl Acad Sci U S A,* 84 (16):5788-5792.

231. Wang F, Zieman A, Coulombe PA (**2016**). Skin Keratins. *Methods Enzymol,* 568:303-350.

232. Wang J (**2018**). Neutrophils in Tissue Injury and Repair. *Cell Tissue Res,* 371 (3):531-539.

233. Wang X, Shen C, Li Z, Xu S, Li D (**2018**). Efficient Isolation and High Yield of Epidermal Cells from Foreskin Biopsies by Dynamic Trypsinization. *Burns,* 44 (5):1240-1250.

234. Wang XQ, Song F, Liu YK (**2017**). Hypertrophic Scar Regression Is Linked to the Occurrence of Endothelial Dysfunction. *PLoS One,* 12 (5):e0176681.

235. Wang ZQ, Xu QJ, Zhang NW, Du XM, Xu GZ, Yan XY (**2020**). Cd146, from a Melanoma Cell Adhesion Molecule to a Signaling Receptor. *Signal Transduction and Targeted Therapy,* 5 (1).

236. Webber J, Jenkins RH, Meran S, Phillips A, Steadman R (**2009a**). Modulation of Tgfbeta1-Dependent Myofibroblast Differentiation by Hyaluronan. *Am J Pathol,* 175 (1):148-160.

237. Webber J, Meran S, Steadman R, Phillips A (**2009b**). Hyaluronan Orchestrates Transforming Growth Factor-Beta1-Dependent Maintenance of Myofibroblast Phenotype. *J Biol Chem,* 284 (14):9083-9092.

238. Witte RP, Kao WJ (**2005**). Keratinocyte-Fibroblast Paracrine Interaction: The Effects of Substrate and Culture Condition. *Biomaterials,* 26 (17):3673-3682.

239. Wojtowicz AM, Oliveira S, Carlson MW, Zawadzka A, Rousseau CF, Baksh D (**2014**). The Importance of Both Fibroblasts and Keratinocytes in a Bilayered Living Cellular Construct Used in Wound Healing. *Wound Repair Regen,* 22 (2):246-255.

240. Wolberg AS (**2007**). Thrombin Generation and Fibrin Clot Structure. *Blood Reviews,* 21 (3):131-142.

241. Wu T, Farnood R, O'Kelly K, Chen B (**2014**). Mechanical Behavior of Transparent Nanofibrillar Cellulose-Chitosan Nanocomposite Films in Dry and Wet Conditions. *J Mech Behav Biomed Mater,* 32:279-286.

242. Wu YS, Chen SN (**2014**). Apoptotic Cell: Linkage of Inflammation and Wound Healing. *Front Pharmacol,* 5:1.

243. Wu Z, Fan L, Xu B, Lin Y, Zhang P, Wei X (**2015**). Use of Decellularized Scaffolds Combined with Hyaluronic Acid and Basic Fibroblast Growth Factor for Skin Tissue Engineering. *Tissue Eng Part A,* 21 (1-2):390-402.

244. Xie J, Bao M, Bruekers SMC, Huck WTS (**2017**). Collagen Gels with Different Fibrillar Microarchitectures Elicit Different Cellular Responses. *ACS Appl Mater Interfaces,* 9 (23):19630-19637.

245. Xie Z, Paras CB, Weng H, Punnakitikashem P, Su LC, Vu K, Tang L, Yang J, Nguyen KT (**2013**). Dual Growth Factor Releasing Multi-Functional Nanofibers for Wound Healing. *Acta Biomater,* 9 (12):9351-9359.

246. Xu X, Wang W, Kratz K, Fang L, Li Z, Kurtz A, Ma N, Lendlein A (**2014**). Controlling Major Cellular Processes of Human Mesenchymal Stem Cells Using Microwell Structures. *Adv Healthc Mater,* 3 (12):1991-2003.

247. Xue L, Greisler HP (**2002**). Angiogenic Effect of Fibroblast Growth Factor-1 and Vascular Endothelial Growth Factor and Their Synergism in a Novel in Vitro Quantitative Fibrin-Based 3-Dimensional Angiogenesis System. *Surgery,* 132 (2):259-267.

248. Xue M, Jackson CJ (**2015**). Extracellular Matrix Reorganization During Wound Healing and Its Impact on Abnormal Scarring. *Adv Wound Care (New Rochelle),* 4 (3):119-136.

249. Yamamoto M, Yanaga H, Nishina H, Watabe S, Mamba K (**2005**). Fibrin Stimulates the Proliferation of Human Keratinocytes through the Autocrine Mechanism of Transforming Growth Factor-Alpha and Epidermal Growth Factor Receptor. *Tohoku J Exp Med,* 207 (1):33-40.

250. Yang Y, Xia T, Zhi W, Wei L, Weng J, Zhang C, Li X (**2011**). Promotion of Skin Regeneration in Diabetic Rats by Electrospun Core-Sheath Fibers Loaded with Basic Fibroblast Growth Factor. *Biomaterials,* 32 (18):4243-4254.

251. Yari A, Teimourian S, Amidi F, Bakhtiyari M, Heidari F, Sajedi N, Veijouye SJ, Dodel M, Nobakht M (**2016**). The Role of Biodegradable Engineered Random Polycaprolactone Nanofiber Scaffolds Seeded with Nestin-Positive Hair Follicle Stem Cells for Tissue Engineering. *Adv Biomed Res,* 5:22.

252. Zelen CM, Serena TE, Gould L, Le L, Carter MJ, Keller J, Li WW (**2016**). Treatment of Chronic Diabetic Lower Extremity Ulcers with Advanced Therapies: A Prospective, Randomised, Controlled, Multi-Centre Comparative Study Examining Clinical Efficacy and Cost. *Int Wound J,* 13 (2):272-282.

253. Zhou T, Wang N, Xue Y, Ding T, Liu X, Mo X, Sun J (**2016**). Electrospun Tilapia Collagen Nanofibers Accelerating Wound Healing Via Inducing Keratinocytes Proliferation and Differentiation. *Colloids Surf B Biointerfaces,* 143:415-422.

254. Zikmundova M, Vereshaka M, Kolarova K, Pajorova J, Svorcik V, Bacakova L (**2020**). Effects of Bacterial Nanocellulose Loaded with Curcumin and Its Degradation Products on Human Dermal Fibroblasts. *Materials (Basel),* 13 (21).

255. Zimoch J, Padial JS, Klar AS, Vallmajo-Martin Q, Meuli M, Biedermann T, Wilson CJ, Rowan A, Reichmann E (**2018**). Polyisocyanopeptide Hydrogels: A Novel Thermo-Responsive Hydrogel Supporting Pre-Vascularization and the Development of Organotypic Structures. *Acta Biomater,* 70:129-139.

256. Zoppi N, Gardella R, De Paepe A, Barlati S, Colombi M (**2004**). Human Fibroblasts with Mutations in Col5a1 and Col3a1 Genes Do Not Organize Collagens and Fibronectin in the Extracellular Matrix, Down-Regulate Alpha2beta1 Integrin, and Recruit Alphavbeta3 Instead of Alpha5beta1 Integrin. *J Biol Chem,* 279 (18):18157-18168.

257. Zulkifli FH, Hussain FSJ, Zeyohannes SS, Rasad M, Yusuff MM (**2017**). A Facile Synthesis Method of Hydroxyethyl Cellulose-Silver Nanoparticle Scaffolds for Skin Tissue Engineering Applications. *Mater Sci Eng C Mater Biol Appl,* 79:151-160.

10 Publications

10.1 Publications Related to Dissertation Thesis

Bacakova M, Pajorova J, Stranska D, Hadraba D, Lopot F, Riedel T, Brynda E, Zaloudkova M, Bacakova L. Protein nanocoatings on synthetic polymeric nanofibrous membranes designed as carriers for skin cells. *Int J Nanomedicine* **2017**; 12:1143-1160. **IF = 6.4 (2020)**

Pajorova J, Bacakova M, Musilkova J, Broz A, Hadraba D, Lopot F, Bacakova L. Morphology of a fibrin nanocoating influences dermal fibroblast behavior. *Int J Nanomedicine* **2018**; 13:3367-3380. **IF = 6.4 (2020)**

Bacakova M, Pajorova J, Sopuch T, Bacakova L. Fibrin-Modified Cellulose as a Promising Dressing for Accelerated Wound Healing. *Materials (Basel)* **2018**; 11(11):2314. **IF = 3.623 (2020)**

Bacakova L, Zarubova J, Travnickova M, Musilkova J, Pajorova J, Slepicka P, Slepickova Kasalkova N, Svorcik V, Kolska Z, Motarjemi H, Molitor M. Stem cells: their source, potency and use in regenerative therapies with focus on adipose-derived stem cells - a review. *Biotechnol Adv* **2018**; 36(4):1111-1126. **IF = 14.227 (2020)**

Bacakova M#, Pajorova J#, Broz A, Hadraba D, Lopot F, Zavadakova A, Vistejnova L, Beno M, Kostic I, Jencova V, Bacakova L. A two-layer skin construct consisting of a collagen hydrogel reinforced by a fibrin-coated polylactide nanofibrous membrane. *Int J Nanomedicine* **2019**; 14:5033-5050. *#Contributed equally*. *Pavel Flachs award for the best publication in 2019 (Institute of Physiology CAS). **IF = 6.4 (2020)**

Bacakova L, Pajorova J, Bacakova M, Skogberg A, Kallio P, Kolarova K, Svorcik V. Versatile Application of Nanocellulose: From Industry to Skin Tissue Engineering and Wound Healing. *Nanomaterials (Basel)* **2019**; 9(2):164. **IF = 5.076 (2020)**

Travnickova M, Pajorova J, Zarubova J, Krocilova N, Molitor M, Bacakova L. The Influence of Negative Pressure and of the Harvesting Site on the Characteristics of Human Adipose Tissue-Derived Stromal Cells from Lipoaspirates. *Stem Cells Int* **2020**; 2020:1016231. **IF = 5.443 (2020)**

Pajorova J#, Skogberg A#, Hadraba D, Broz A, Travnickova M, Zikmundova M, Honkanen M, Hannula M, Lahtinen P, Tomkova M, Bacakova L, Kallio P. Cellulose mesh with charged

nanocellulose coatings as a promising carrier of skin and stem cells for regenerative applications. *Biomacromolecules* **2020**; 21(12):4857-70. *#Contributed equally*. *Pavel Flachs award for the best publication in 2020 (Institute of Physiology CAS). **IF = 6.988 (2020)**

10.2 Publications Non-Related to Dissertation Thesis

Przekora A, Vandrovcova M, Travnickova M, Pajorova J, Molitor M, Ginalska G, Bacakova L. Evaluation of the potential of chitosan/β-1,3-glucan/hydroxyapatite material as a scaffold for living bone graft production *in vitro* by comparison of ADSC and BMDSC behaviour on its surface. *Biomed Mater* **2017**; 12(1):015030. **IF = 3.715 (2020)**

Bacakova L, Pajorova J, Tomkova M, Matejka R, Broz A, Stepanovska J, Prazak S, Skogberg A, Siljander S, Kallio P. Applications of Nanocellulose/Nanocarbon Composites: Focus on Biotechnology and Medicine. *Nanomaterials (Basel)* **2020**; 10(2):196. **IF = 5.076 (2020)**

Zikmundova M, Vereshaka M, Kolarova K, Pajorova J, Svorcik V, Bacakova L. Effects of Bacterial Nanocellulose Loaded with Curcumin and Its Degradation Products on Human Dermal Fibroblasts. *Materials (Basel)* **2020**; 13(21):4759. **IF = 3.623 (2020)**

Book chapters:

Bacakova L, Bacakova M, Pajorova J, Kudlackova R, Stankova L, Filova E, Musilkova J, Potocky S and Kromka A. Nanofibrous Scaffolds as Promising Cell Carriers for Tissue Engineering, Nanofiber Research - Reaching New Heights. *InTech* **2016**; DOI: 10.5772/63707.

Bacakova L, Zikmundova M, Pajorova J, Broz A, Filova E, Blanquer A, Matejka R, Stepanovska J, Mikes P, Jencova V, Kostakova E, Sinica A. Nanofibrous Scaffolds for Skin Tissue Engineering and Wound Healing Based on Synthetic Polymers, Applications of Nanobiotechnology. *InTech* **2019**; DOI: 10.5772/intechopen.88744

Bacakova L, Pajorova J, Zikmundova M, Filova E, Mikes P, Jencova V, Kostakova E, Sinica A. Nanofibrous Scaffolds for Skin Tissue Engineering and Wound Healing Based on Nature-Derived Polymers, Current and Future Aspects of Nanomedicine. *InTech* **2019**; DOI: 10.5772/intechopen.88602

11 Conferences

11.1 International Conferences

Pajorova J *et al.*: Nanofibrous Polymer Membranes Modified with Fibrin and Collagen Structures as Carriers for Skin Cells. *4th International Conference on Tissue Science and Regenerative Medicine*, Rome, Italy, 27 – 29 July 2015. Poster presentation.

Pajorova J *et al.*: The potential application of fibrin-coated polylactide nanofibers in skin tissue engineering. *NanoInBio*, Guadeloupe, France, 31 May – 5 June 2016. Poster presentation.

Pajorova J *et al.*: Effect of fibrin-nanocoating of nanofibrous polymer membranes on the adhesion and proliferation of human dermal fibroblasts. *Conference on Biomaterials in Medicine and Veterinary Medicine*, Rytro, Poland, 13 – 16 October 2016. Poster and oral presentation.

Pajorova J *et al.*: Fibrin-coated Nanofibrous Polymer Membranes as Carriers for Skin Cells. *International Conference on Mechanics of Biomaterials and Tissues*, Waikoloa, Hawaii, USA, 10 – 14 December 2017. Poster presentation.

Pajorova J *et al.*: Morphology of a fibrin nanocoating influences dermal cell behavior. *Summer School GENE2SKIN*, Porto, Portugal, 6 – 8 June 2018. Poster presentation.

Pajorova J *et al.*: A full-thickness skin construct made of a collagen hydrogel strengthened by a fibrin-modified nanofibrous membrane. *18th European Burns Association Congress*, Helsinki, Finland, 4 – 7 September 2019. Poster presentation. **The best poster presentation award.*

11.2 Domestic Conferences

Pajorova J *et al.*: Nanofibrous polymer membranes modified with fibrin and collagen structures as carriers for skin cells. *PhD meeting in trest 2015*, Třešť, Czech Republic, 3 – 5 November 2015. Poster presentation. **The best poster presentation award.*

Bacakova L, Bacakova M, Pajorova J *et al.*: Skin Substitutes - Current state and future trends. *IX. Biomaterials and their surfaces*, Herbertov, Czech Republic, 20 – 23 September 2016. Oral presentation.

Pajorova J *et al.*: Potential applications of fibrin-modified nanofibrous membrane and adipose tissue-derived stem cells (ASCs) in skin tissue engineering. *V. International Conference – Stem Cells and Cell Therapy: From research to modern clinical application*, Černá Hora, Czech Republic, 5 – 6 October 2017. Oral presentation.

Pajorova *et al.*: Morphology of a fibrin nanocoating influences dermal cell behavior. Scientific conference 2.LF UK 2018, Praha, Czech Republic, 25 – 26 April 2018. Poster presentation. **The best poster presentation award.*

Pajorova J *et al.*: Nanocellulose in skin tissue engineering. *XI. Biomaterials and their surfaces*, Herbertov, Czech Republic, 18 – 21 September 2018. Oral presentation.

Pajorova *et al*.: Nanofibrous polymer membranes modified with fibrin and collagen structures as carriers for skin cells. *PhD meeting in Seč 2019*, Seč, Czech Republic, 29 – 31 October 2019. Poster presentation.

Pajorova *et al.*: Model kožní náhrady z kolagenního hydrogelu zpevněného fibrinem modifikovanou nanovlákennou membránou. *Česko-slovenský kongres: mezioborové přístupy v hojení ran,* Lednice, Czech Republic, 28 – 29 November 2019. Poster presentation.

12 Internship

November 2017, June and September 2019: Faculty of Biomedical Sciences and Engineering, Micro and Nanosystems Research Group, Tampere University, Finland, Prof. Pasi Kallio, Funding: Institute of Physiology CAS (Development of HR capabilities, internationalization, popularization and IP utilization) and Charles University (Mobility).

13 Appendix